Dissertation zur Erlangung des Doktorgrades
der Fakultät für Chemie und Pharmazie
der Ludwig-Maximilians-Universität München

β-Site Amyloid Precursor Protein Cleaving Enzyme 1 (BACE1)

Inhibition Impairs Synaptic Plasticity Via

Seizure Protein 6 (SZE6)

Kaichuan Zhu

aus

Qinhuangdao, Hebei, China

2018

Erklärung

Diese Dissertation wurde im Sinne von § 7 der Promotionsordnung vom 28 November 2011 von Herrn Prof Dr Jochen Herms betreut und von Herrn PD Dr Stylianos Michalakis von der Fakultät für Chemie und Pharmazie vertreten

Eidesstattliche Versicherung

Diese Dissertation wurde eigenständig und ohne unerlaubte Hilfe erarbeitet

München, 4.12 2017

ZHU, Kaichuan

……

Dissertation eingereicht am 4.12 2017

1 Gutachter: PD Dr Stylianos Michalakis ……

2 Gutacher: Prof Dr Jochen Herms ……

Mündliche Prüfung am 18.04.2018

Table of contents

List of Figures

List of Tables

Summary

Alzheimer's disease (AD) is the most prevalent neurodegenerative disorder among the elderly. Amyloid-β is thought to be one of the causative factors for AD, which is produced by BACE1 (Beta-secretase) initiated sequential proteolytic cleavage of APP. BACE1 inhibition is one of the promising therapeutic approaches for AD. Currently, several BACE1 inhibitors are undergoing Phase 2/3 clinical trials. However, prolonged BACE1 inhibition interferes structural and functional synaptic plasticity in mice, most likely due to the interrupted metabolism of BACE1 substrates. Seizure protein 6 (SEZ6) is predominantly cleaved by BACE1. Furthermore, *Sez6* null mice share some phenotype with BACE1-inhibited mice including reduced dendritic spine density in cortex and diminished performance in hippocampal-dependent behavioral tests.

In order to shed more light on the function of SEZ6, we analyzed the dendritic spine structure and synaptic plasticity in constitutive (*Sez6*$^{-/-}$*:GFP-M*) and conditional (*Sez6*$^{cKO/cKO}$*:SlickV*) Sez6 KO mice. *In vivo* two photon microscopy data showed that lack of SEZ6 induces a dose dependent alteration of dendritic spine density and morphology in adult mice. To rule out developmental deficits and identify which SEZ6 proteolytic fragments are involved we monitored spine density in *Sez6*$^{cKO/cKO}$*:SlickV* mice. The tamoxifen-inducible recombinase CreER^{T2} and eYFP are co-expressed in a small subset of neurons in SlickV mice. By applying tamoxifen, *Sez6* was knockout specifically in eYFP positive neurons in adult mice. It caused a small but significant spine density reduction. Electrophysiological field recordings in hippocampus CA1 region showed that SEZ6 is

involved in synaptic transmission and LTP mainly due to post-synaptic mechanism. To study the dendritic spine plasticity in *Sez6*$^{-/-}$*:GFP-M* mice, we repeatedly imaged the apical tufts of layer V pyramidal neurons in the cerebral cortex in both normal condition and environmental enrichment condition by intravital two-photon microscopy. *Sez6*$^{-/-}$ mice does not show alerted dendritic spine plasticity in base line condition, but they have deficits in conditions that boost spine plasticity like environmental enrichment.

Then, we investigated whether SEZ6 is involved in BACE1-inhibition-induced synaptic alteration. We applied a diet mixed with NB-360 to *Sez6*$^{-/-}$*:GFP-M* and *Sez6*$^{cKO/cKO}$*:SlickV* mice. NB-360 is a novel blood-brain barrier penetrable BACE1 inhibitor. Immunoblotting analysis showed that NB-360 strongly suppressed SEZ6 and APP cleavage similar to *Bace1* knockout. To study the impact of long-term pharmacological inhibition of BACE1 in *Sez6*$^{-/-}$*:GFP-M* mice, we repeatedly imaged the apical tufts of layer V pyramidal neurons in the cerebral cortex for 7 weeks using intravital two-photon microscopy. Although 3-week treatment of NB-360 caused a significant but reversible reduction of density of total dendritic spines, persistent spines (persisting $\geqslant$ 7 days) and new gained spines in control mice, the same treatment did not affect dendritic spine dynamics in *Sez6*$^{-/-}$*:GFP-M* mice. To rule out developmental deficits, we monitored spine dynamics upon NB-360 treatment in *Sez6*$^{cKO/cKO}$*:SlickV* mice. Chronic NB-360 treatment did not alter spine plasticity in the neurons lacking cell-autonomous SEZ6. Finally, electrophysiological field recordings in hippocampal CA1 region showed that LTP is reduced in chronic NB-360 treated WT mice and vehicle treated *Sez6*$^{-/-}$ mice, but NB-360 treatment did not interfere with LTP in *Sez6*$^{-/-}$ mice.

Our data suggest that SEZ6 has a pivotal role in maintaining normal dendritic spine structure and function. Furthermore, SEZ6 is involved in BACE1-inhibitor-induced structural and functional synaptic alterations.

INTRODUCTION

1. Alzheimer's disease

Alzheimer's disease (AD) is the most prevalent neurodegenerative disease. The first case of Alzheimer's disease was reported by German psychiatrist Dr. Alois Alzheimer in 1906 at the 37th meeting of the Society of Southwest German Psychiatrists (Caselli et al., 2006; Reiman, 2006; Selkoe, 2001). Alzheimer's disease is named after him. AD is the cause of 60% to 70% of cases of dementia (Prince et al., 2015). It is a progressive age-related disease which develops over several years. There is no effective medical treatment or preventive approach available for patients until now.

The typical clinical symptoms of AD are gradual loss of memory and cognitive ability. It is due to the destruction of nerve cells and neural connections which leads to atrophy of the cerebral cortex and hippocampus and an enlargement of ventricles (Götz et al., 2001; Hardy and Selkoe, 2002; Selkoe and Hardy, 2016; Serrano-Pozo et al., 2011). Three disease progression stages can generally be distinguished. This disease begins with mild cognitive impairment, like the episodic memory dysfunction, which is common in most Alzheimer's patients. In the middle stage, cognitive abilities such as orientation, language, problem solving, and spatial perception are reduced. In the severe stage, AD patients almost lost all cognitive abilities, and they are mentally and physically dependent on their caretaker (Jucker et al., 2006; Tarawneh and Holtzman, 2012).

Neuritic plaques and neurofibrillary tangles (NFTs) are the two typical neuropathological hallmarks of AD (Figure 1) (Hardy and Selkoe, 2002; Selkoe and Hardy, 2016). Neuritic plaques are formed by misfolded Amyloid-β peptide (Aβ). Aβ peptide is 36-43 amino acids long. The common theory is certain misfolding Aβ molecules served as seeds which induce misfolding of other Aβ molecules and oligomerize. These Aβ continually form Aβ fiber like a chain reaction akin to a prion infection (McLaurin et al., 2000; Takahashi et al., 2017; Wetzel et al., 2007). NFTs are formed by aggregated insoluble hyperphosphorylated tau protein. In physiological condition, Tau is a highly soluble microtubule-associated protein. In human, Tau proteins have six isoforms from 352-441 amino acids. All the six isoforms can be hyperphosphorylated and present in NFTs (Iqbal et al., 2016; Ma et al., 2017). Tangles are also found in numerous of other diseases known as tauopathies (Iqbal et al., 2016). Both Neuritic plaques and NFTs are visible in light microscopy using various staining techniques, e.g. silver, Congo red and Thioflavin S (Figure 1).

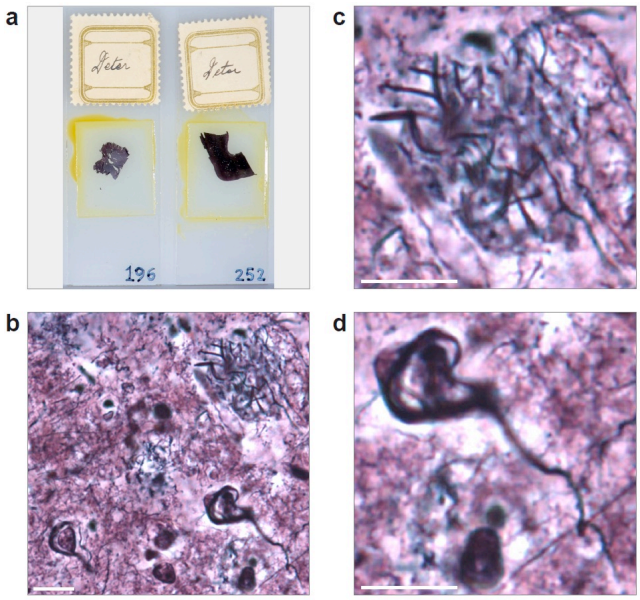

Figure 1: The histopathological characteristics of the first Alzheimer's patient

(A) The brain autopsies of the first Alzheimer's disease patient, Auguste Deter. Preserved in Center for Neuropathology and Prion Research at the Ludwig-Maximilians-University Munich. (B-D) Microimages of Bielschowsky's silver staining. (B) The over view image of two pathological hall mark of Alzheimer's disease. (C-D) Enlarged image of neuritic plaques and neurofibrillary tangles. (Kindly provide by Prof. Dr. h.c. Hans Kretzschmar and Dr. Burgold)

1.1. The amyloid cascade hypothesis

The exact cause for AD is not yet clear. In 1991, the amyloid cascade hypothesis synthesized the knowledges from histopathological and genetic studies and proposed that deposition of the Aβ peptide in the human brain is the initiative and crucial step leading to AD (Hardy and Allsop, 1991; Karran et al., 2011).

Aβ is the sequential proteolytic cleavage product of amyloid precursor protein (APP), a type-I trans-membrane protein. The N-terminus of APP is within the lumen/extracellular space and the C-terminus is within the cytosol. APP is proteolytically processed at several

different subcellular sites, for example Golgi apparatus and transport vesicles. APP can be processed by many secretases including α-secretase (A Disintegrin and metalloproteinase domain-containing protein 10, ADAM10), β-secretase (beta-site amyloid precursor protein cleaving enzyme 1, BACE1), γ-secretase complex and recently discovered η-secretase (e.g. membrane-type 5 matrix metalloproteinase, MT5-MMP) (Figure 2A). APP processing can be classified into non-amyloidogenic pathway (Figure 2B), amyloidogenic pathway (Figure 2C) and η-secretase pathway (Figure 2D-E) (Haass, 2004; Willem et al., 2015).

The non-amyloidogenic pathway is considered as the physiologically normal pathway which prevents Aβ generation (Haass et al., 1992, 1993). In this pathway, APP is first cleaved by α-secretase in the approximately middle of the Aβ region, releasing a large part of the ectodomain (sAPPα) into the lumen or extracellular space. The subsequent γ-secretase complex processing of the trans-membrane C-terminal fragment (CTFα or c83) generates nontoxic P3 fragment and APP intracellular fragment (AICD) (Figure 2B).

In the amyloidogenic processing of APP, which leads to generation of the toxic Aβ, is dependent on consecutive action of BACE1 and γ-secretase complex. Shedding by BACE1, APP generates another large part of the ectodomain (sAPPβ) and APP C-terminal fragment (CTFβ or c99). Then the γ-secretase complex performs intramembrane proteolysis within the biological membrane releasing Aβ and AICD. (Figure 2C).

The η-secretase pathway is reported recently as a new physiological APP processing pathway (Willem et al., 2015). The initiating enzyme of η-secretase pathway is

membrane-bound matrix metalloproteinases (e.g. MT5-MMP). CTF-η, the third type of large ectodomain fragment, is generated after MT5-MMP proteolysis. CTF-η is continually processed by α- and β-secretase and releasing Aη-α and Aη-β, respectively (Figure 2D-E).

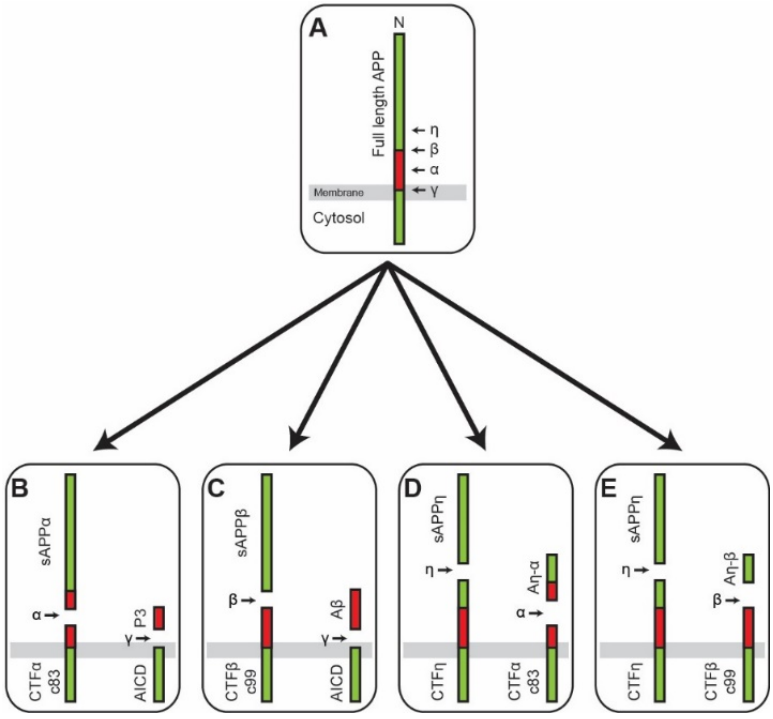

Figure 2: Schematic representation of amyloid precursor protein sequential cleavage

(A) APP is a type I trans-membrane protein. It can be processed by α-, β-, γ- and η-secretases. (B) In the non-amyloidogenic pathway, APP is first cleaved by α-secretases and released sAPPα into the extracellular space. The subsequent γ-secretase processing of the trans-membrane C-terminal fragment (CTFα, c83) generates nontoxic P3 fragment and APP intracellular fragment (AICD). (C) The amyloidogenic processing of APP is independent on β-secretases, resulting sAPPβ and CTFβ (c99). The toxic β-amyloid peptide (Aβ) is released by γ-secretases. (D-E) In the recent reported η-secretase pathway, APP is processed by η-secretase follow by α- and β-secretases and releasing Aη-α and Aη-β, respectively.

2. BACE1

BACE1 is a typical transmembrane aspartic protease with a luminal active site which sheds the ectodomain of membrane proteins (Yan et al., 1999). It is mainly expressed in the central nervous system (CNS), including the neocortex and hippocampus. BACE1 has more than 35 substrates, including APP, SEZ6, and CHL1 (Kuhn et al., 2012; Pigoni et al., 2016; Vassar et al., 1999; Yan et al., 1999; Zhou et al., 2012). Under physiological condition, BACE1 substrates are processed in acidic compartments, such as trans-Golgi network and endosome, where BACE1 displays its maximum proteolytic activity (Kalvodova et al., 2005; Vassar et al., 2014).

BACE1 is the sole enzyme for initiating Aβ generation, and it is the rate limiting enzyme of the amyloidogenic pathway (Ghosh and Osswald, 2014; Sinha and Lieberburg, 1999; Vassar, 2016; Vassar et al., 1999). Knockout of *Bace1* almost completely abolishes Aβ production in transgenic APP mouse models (Roberds et al., 2001; Vassar et al., 1999). The value of BACE1 as therapeutic target is further supported by the finding that the Icelandic mutation, $APP^{Ala673Thr}$, which suppresses APP cleavage by BACE1, results roughly in a 20-40% reduction of Aβ and protects against AD (Jonsson et al., 2012).

The transportation of BACE1 within neurites is via trafficking vesicles. For the anterograde axonal transport, BACE1 is co-transferred together with APP regulating by calsyntenin-1 and Rab11 (Buggia-Prévot et al., 2014; Steuble et al., 2012). Under physiological conditions, APP is cleaved by BACE1 in these vesicles (Del Prete et al., 2014). The retrograde trafficking of BACE1 is regulated by Vps35 in both axons and dendrites (Wang

et al., 2012). A recent report using fluorescence labeled technique demonstrated that BACE1 is located at both pre- and post-synaptic compartments within neurons (Das et al., 2016), indicating BACE1 has important function in the synapse. BACE1 also accumulates at amyloid plaque in axonal dystrophies in both AD mouse models and patients (Blazquez-Llorca et al., 2017; Kandalepas et al., 2013). It might directly facilitate the local generation of Aβ; hence further promoting the amyloid deposition.

2.1. BACE1 inhibitor

In the past decades, both academia and industry invested a lot of resources for developing BACE1 inhibitors. The 1st generation of BACE1 inhibitors are peptidomimetic molecules (Kandalepas and Vassar, 2014; Sinha et al., 1999). These peptide-based molecules mimic the β-site of APP and replaces it with a non-cleavable amide (Vassar, 2016). Although peptide-based BACE1 inhibitors strongly inhibit BACE1 *in vitro*, they do not have the properties to *in vivo* application, e.g. oral bioavailability, long serum half-life, or blood-brain barrier (BBB) penetrable. The 2nd generation of BACE1 inhibitors are developed based on the X-ray crystal structure of BACE1 (Durham and Shepherd, 2006; Hong et al., 2002). These inhibitors are small molecular weight chemical compounds which can be applied orally and are plasma membrane and BBB penetrable. However, the concentrations in the brain are still low (Vassar, 2014, 2016). The 3rd generation of BACE1 inhibitors exhibit satisfactory brain concentration and strong inhibition of BACE1 proteolytic activity. Several of the 3rd generation BACE1 inhibitors are in different phases of clinical trials. Some of these compounds showed promising results in phase 1 trials,

which did not show severe reveal adverse effects and very effectively reduce Aβ reduction in a dosage-dependent manner. Currently, at least 6 of them are being tested in phase 2/3 trials (Table 1).

Table 1: Ongoing BACE1 inhibitors in clinical trials

Compound	company	Clinical trial stage	NCT number	Dosages	Aβ Reduction #	Patient population	Expected completion years
CNP520	Novartis Amgen,	Phase 2/3	02565511 03131453	50mg 15/50mg	-60% (10mg) -80% (35mg)	Asymptomatic at-risk patients (APOE4)	2023 2024
AZD3293 (LY3314814)	Eli Lilly, AstraZeneca	Phase 2/3	02783573 02972658 02245737 03019549	20/50mg	-50% (15mg) -80% (50mg)	Early and mild AD	2021 2020 2019 2017
LY3202626	Eli Lilly	Phase 2	02791191		-50% (1mg)	Mild AD	2019
Elenbecestat (E2609)	Eisai, Biogen	Phase 2/3	02322021 03036280 02956486	50mg	-50% (5mg) -80% (50mg)	Early AD	2020 2020 2020
JNJ-54861911	Janssen	Phase 2/3	02569398 02406027	5/25mg 5/10/25mg	-50% (5mg) -80% (25mg)	Asymptomatic at-risk patients and Early AD	2023 2022
MK-8931	Merck	Phase 2/3 Phase 3	01739348 01953601	12/40/60mg 12/40mg	-32% (10mg) -80% (40mg)	Prodromal AD	2017* 2021

NCT numbers refer to the study codes in the ClinicalTrials.gov database

 # Data from pre-clinical human studies or phase 1 studies.

*** Terminated at April 2017**

2.2. BACE1 has physiological functions at the synapse

BACE1 has many physiological substrates, indicating it is involved in various functions. The knockout of *Bace1* leads to a number of physiological and behavioral deficits in mice, including increased astrogenesis and decreased number of mature neurons (Hu et al., 2013), impaired axon myelination during development (Hu et al., 2006), axon guidance errors in the olfactory bulb and hippocampus (Hitt et al., 2012; Rajapaksha et al., 2011), impaired remyelination in injured sciatic nerves in the adult mice (Hu et al., 2015), reduced number of muscle spindles resulting in a swaying walking pattern (Cheret et al., 2013), as well as decreased anxiety (Laird et al., 2005). Most likely, BACE1 is involved in these physiological functions via its substrates. In the last decade, more than 35 BACE1 substrates have been identified (Dislich et al., 2015; Kuhn et al., 2012; Zhou et al., 2012). Among those substrates, some of them are located at the synapse which are known to be of critical importance for synaptic function and plasticity (Table 2).

Table 2: BACE1 substrates involved in synaptic plasticity

BACE1 cleavage	Name	Localization	Phenotypes / Functions	Ref.
High	Seizure protein gene 6 (SEZ6)	Dendrite, Dendritic spine	Abnormal dendritic arborization, reduced dendritic spine density, synaptic transmission and LTP	(Gunnersen et al., 2007; Zhu et al., 2018)
	Amyloid precursor-like protein 1 (APLP1)	Pre- and post-synapse	Reduced synaptogenesis, dendritic spine density	(Schilling et al., 2017)
	Close homologue of L1 (CHL1)	Axon, Presynaptic boutons	Axon guidance defects	(Cao et al., 2012; Rajapaksha et al., 2011)
	Neuroligin 4 (NLGN4)	Glycinergic post-synapses	Affects synaptic transmission	(Hoon et al., 2011)
	Neuroligin 2 (NLGN2)	Inhibitory synapses	Affects synaptic transmission	(Nguyen et al., 2016)
	Contactin 2	Axon, Presynaptic boutons	Axon guidance defects	(Gautam et al., 2014)
	Amyloid precursor protein (APP)	Pre- and post-synapse	Increased primary dendrites, Impaired dendritic spine morphology, density and dynamic	(Weyer et al., 2014)
Low	Neuroligin 1 (NLGN1)	Dendritic spine of excitatory synapses	Reduced NMDAR-mediated synaptic transmission and LTP	(Jiang et al., 2017; Song et al., 1999)
?	Neuregulin 1 (NRG1)	Axon, Presynaptic boutons	Hyperactivity, hypomyelination, reduced dendritic spine density	(Hu et al., 2010; Savonenko et al., 2008)

2.2.1. BACE1 and synaptic structures

A synapse is a junction formed between two neurons, which transmits electrical or chemical signals from one to the other. The postsynaptic compartment of excitatory synapses, the dendritic spine, is a plastic structure that can change its shape within minutes or present over longer spans of weeks to months, which is termed structural plasticity (Fu and Zuo, 2011; Lendvai et al., 2000; Yang et al., 2009). Increased spine formation and stabilization is associated with learning and memory (Yang et al., 2009). Impairments of synaptic structure and plasticity is thought to be one of the most important mechanisms for memory loss in dementia (Herms and Dorostkar, 2016).

As mentioned above, BACE1 is located at pre-synaptic terminals, especially enriched in mossy fiber terminals (Hitt et al., 2012; Kandalepas et al., 2013). In *Bace1*$^{-/-}$ mice, the mossy fiber terminals have normal ultrastructure (Kandalepas et al., 2013), however the infrapyramidal bundle of mossy fibers is significantly shorter indicating a potential alteration in axonal outgrowth (Gautam et al., 2014; Hitt et al., 2012). The abnormal axonal growth might be due to reduced β-cleavage of contactin-2, a cell adhesion molecule, since contactin-2 plays an important role in regulating axon guidance and path finding (Furley et al., 1990; Gautam et al., 2014). Abnormal axonal growth cone collapse has been seen in both *Bace1*$^{-/-}$ or BACE1 inhibitor treated mice (Barão et al., 2015; Cao et al., 2012; Rajapaksha et al., 2011). The altered function of the neural cell adhesion molecule close homolog of L1 (CHL1) has been supposed to be involved in this process, too (Naus et al., 2004). Cleavage of CHL1 by BACE1 generates N-terminal fragment

(CHL1-NTFβ) (Kuhn et al., 2012), which is critical for growth cone collapse in thalamic neurons since CHL1-NTFβ interacts with semaphorin 3A (Sema3A) (Barão et al., 2015).

BACE1 is also located within dendritic spines. The density and plasticity of dendritic spines in *Bace1*$^{-/-}$ and *Bace1*$^{+/-}$ mice as well as WT mice treated with BACE1 inhibitors has been studied by various groups (Devi and Ohno, 2015; Filser et al., 2015; Sadleir et al., 2015; Zhu et al., 2018; Zou et al., 2016). The total spine density is significantly reduced in the CA1 region of *Bace1*$^{-/-}$ mice (Savonenko et al., 2008). Moreover, the proportion of mushroom spines is also significantly lower. This is concurrent with the reduction of PSD95 (post-synaptic density protein 95) density (Savonenko et al., 2008). These changes might be the consequences of an altered BACE1-dependent NRG1 (neuregulin-1) signaling. Indeed, NRG1 accumulation is known to cause a reduction in dendritic spine density by altering the interaction between ErbB4 (receptor tyrosine-protein kinase erbB-4) and PSD95 (Hu et al., 2006; Willem et al., 2006). Dendritic spine plasticity has not yet been studied in *Bace1*$^{-/-}$ mice. However, in adult *Bace1*$^{+/-}$ mice, there is no evidence showing that dendritic spine plasticity is impaired under enriched environment condition, a method for boosting spine turnover (Zou et al., 2016).

Given that the BACE1 protein level is highest during early postnatal development in mice (Willem et al., 2006), developmental deficit might cause certain structural changes at synapses indirectly. Especially, observations in constitutive knock-out mice are based on life-long absents of BACE1 protein in the brain were compensation may mask the effect of an acute loss of BACE1 function at the synapse. Therefore, it is necessary to validate

the effects of BACE1 inhibition during adulthood, as some side effects may limit its clinical application.

Several non-peptidic BACE1 inhibitors of different structures like SCH1682496 (Merck/Schering-Plough Pharmaceuticals, North Wales, Pennsylvania) (Stamford et al., 2012), LY2811376 (Eli Lilly and Company, Indianapolis, Indiana) (May et al., 2011) and β-Secretase Inhibitor IV (Stachel et al., 2004) have been developed within the last decade. All of these inhibitors strongly suppress Aβ production in mice (Filser et al., 2015; Kamikubo et al., 2017; May et al., 2011) and human (60). Using *in vivo* sequential microscopy, the effect of these inhibitors on individual dendritic spines has been studied in GFP-M mice. Administration of SCH1682496 (16 days, 100 mg/kg/day) or LY2811376 (16 days, 100 mg/kg/day) was found to reduce the overall density of dendritic spines, and lower the formation rate of new gained spines in GFP-M mice (Figure 3) (Filser et al., 2015). These impairments were not seen at lower doses (SCH1682496 or LY2811376, 30mg/kg/day) (Filser et al., 2015). Similar findings were obtained in cultured brain slices after β-Secretase inhibitor IV treatment (Kamikubo et al., 2017). The treatment was found to decrease the protein level of PSD95 during 3-17 days in vitro (DIV) (Kamikubo et al., 2017). Therefore, BACE1 proteolytic activity is important for maintaining the normal synaptic formation and maturation processes.

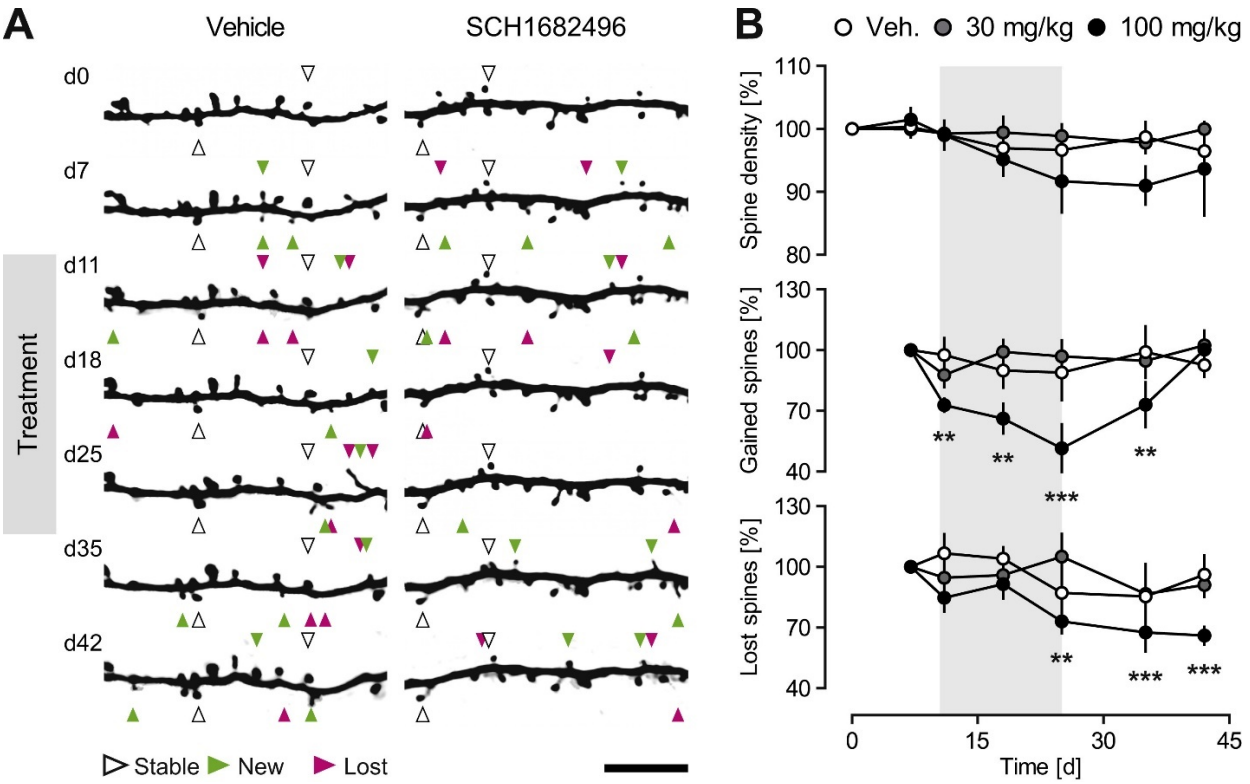

Figure 3: BACE1 inhibitor alters dendritic spine plasticity in adult GFP-M mice

(A) the layer V cortical neurons were labeled with eGFP in GFP-M mice. Their apical dendrites were imaged for 45 days. BACE1 inhibitor SCH1682496 was applied to mice from day 10 and over 16 days (every 12 hours). Two dosage, 30 mg/kg and 100mg/kg, were used. White arrowheads: stable spines. green arrowheads: new gained spines. magenta arrowheads: lost spines. Scale bar: 10 µm. (B) Quantification of relative spine density, new gained and lost spines. 4-5 animals per group,10 dendrites per animal. Error bars represent S.E.M. One-way analysis of variance. ** p<0.01; *** p<0.001; (Filser et al., 2015).

2.2.2. BACE1 and synaptic function

Structural alterations of synapses are considered as an indicator for functional changes. But how is BACE1 involved in neuronal function is not yet fully clear. *Bace1*$^{-/-}$ mice do not show any alterations in basal synaptic transmission under low stimulation intensity in

hippocampus CA1 (Figure 4A) (Filser et al., 2015; Laird et al., 2005). However, when using higher stimulation intensities, the slope of the stimulus-response response curve was significantly lower compared to controls (Filser et al., 2015). In line with knockout mouse model, various BACE1 inhibitors (SCH1682496 and LY2811376 and C3) were able to decrease the slope of the stimulus-response curve over a wide range of intensities in both mice and rat, indicating the weakening of synaptic transmission upon BACE1 inhibition (Filser et al., 2015; Kamikubo et al., 2017).

BACE1 regulates the surface expression of voltage-gated sodium channels, the key player for generating action potentials, by cleaving the β-subunits ($Na_V\beta2$) (Wong et al., 2005). However, controversy observations have been obtained in Bace1-/- mice: Hitt et al. reported that the expression level of $Na_V1.2$ is not altered in CA3 pyramidal neurons of *Bace1*$^{-/-}$ mice (Hitt et al., 2010). Hu et al. , however, showed that the expression level of $Na_V1.2$ is strongly increased (Hu et al., 2010). Using whole cell recordings, Dominguez et al. showed that Na+ current densities are lower in cortical pyramidal neurons of *Bace1*$^{-/-}$ mice (P23-30) (Dominguez et al., 2005), but Kim at al. reported that Na+ current densities in CA1 neurons is reduced in BACE1 overexpression mice (Kim et al., 2007). Hu et al. data support the notion that Na+ currents are significantly greater in hippocampal pyramidal neurons of *Bace1*$^{-/-}$ mice (P21-30) (Hu et al., 2010). These data suggest that BACE1 might affect neuronal activity by regulating the surface expression and function of voltage-gated sodium channels.

Hippocampal LTP (long-term potentiation) and LTD (depression) are the two commonly used paradigms of studying synaptic plasticity. Both LTP and LTD are activity-dependent strengthening or weakening in the efficacy of synapses, respectively (Lynch, 2004). These synaptic modifications are supposed to share the same cellular mechanisms that underlay learning and memory (Llinás et al., 1997; Nicoll, 2017). LTD seems not to be significantly altered in *Bace1*$^{-/-}$ mice: It is not altered in Schaffer collateral-CA1 pathway (Laird et al., 2005) and in mossy fiber-CA3 pathway a slight enlargement has been described (Wang et al., 2008). However, in LTP the situation is different: Using theta-burst stimulation (TBS) protocol, *Bace1*$^{-/-}$ mice show a slight but not significant LTP reduction in Schaffer collateral-CA1 pathway (Laird et al., 2005). This attenuation is more noticeable by using high frequency stimulation (HFS) protocol (Figure 4B) (Filser et al., 2015). The mossy fiber LTP is also impaired in *Bace1*$^{-/-}$ mice (Wang et al., 2014). Interestingly, activation of α7nAChR (α7 nicotinic acetylcholine receptor) by nicotine has been shown to restore LTP in *Bace1*$^{-/-}$ mice (Wang et al., 2010). Since α7nAChR is involved in NMDA receptor dependent hippocampal LTP by regulating astrocytic release of D-serine, the NMDA receptor co-agonist (Papouin et al., 2017), it would be interesting to study whether BACE1 regulates D-serine homeostasis. Impaired LTP also has been observed in chronic strong BACE1 inhibition in WT mouse (Filser et al., 2015; Zhu et al., 2018). Even pre-exposure to a single oral dose of SCH1682496 attenuates LTP (Willem et al., 2015). Intriguingly, LTP attenuation after BACE1 inhibition is clearly dose depended (Figure 4B) (Filser et al., 2015). Moreover, *Bace1*$^{+/-}$ mice have a normal Schaffer collateral-CA1 LTP (Giusti-Rodríguez et al., 2011; Wang et al., 2014). This indicates that synaptic deficits can be avoided if the dosage of BACE1 inhibitor does not reduce its

function by more than 50%. Consistent with reduced LTP, *Bace1*$^{-/-}$ and BACE1 inhibited mice, show deficits in hippocampus-dependent cognitive and emotional memory tests, but *Bace1*$^{+/-}$ mice behave normally (Dominguez et al., 2005; Filser et al., 2015; Kimura et al., 2010; Ohno et al., 2004, 2007; Savonenko et al., 2008; Weber et al., 2017).

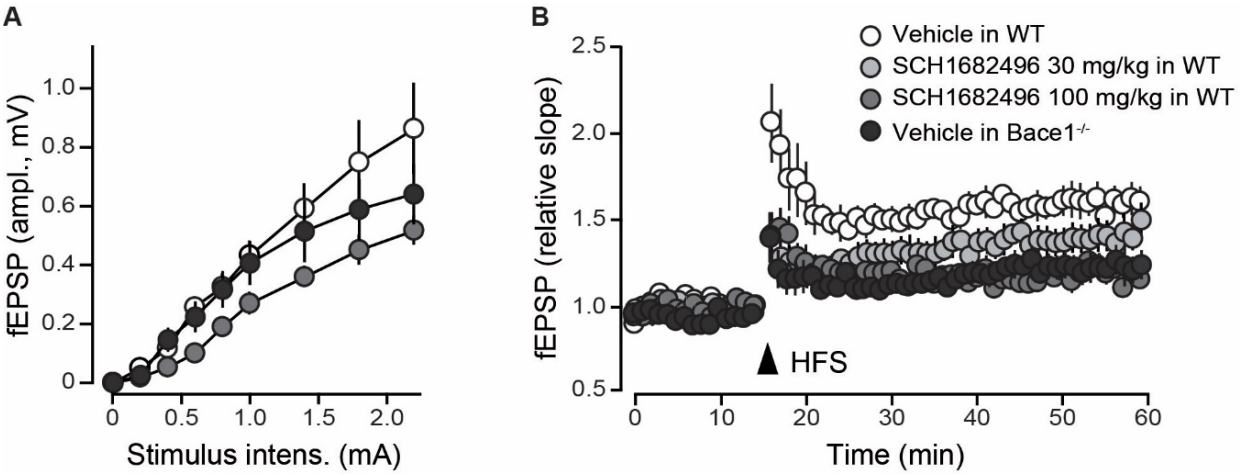

Figure 4: BACE1 inhibitor SCH1682496 attenuates synaptic transmission and long-term potentiation in CA1 neurons

(A) stimulus-response relationship graphs from WT mice treated with vehicle or 100 mg/kg of SCH1682496 and vehicle treated *Bace1*$^{-/-}$ mice. (B) Summary plots of fEPSP slope changes during baseline recording and after induction of long-term potentiation from WT mice treated with vehicle, 30 or 100 mg/kg of SCH1682496. This figure is adapted from Filser et al. (2015).

Paired-pulse facilitation (PPF) is a sensitive measurement of pre-synaptic vesicular release probability (Manabe et al., 1993). This approach was applied to understand how BACE1 affects synaptic transmission and LTP. Although the ultrastructure of mossy fiber terminals is normal in *Bace1*$^{-/-}$ mice, it has a significant increased PPF ratio mossy fibers-CA3 pathway (Kandalepas et al., 2013; Wang et al., 2008). The increased PPF occurs specifically at synapses of mossy fiber-CA3 pyramidal neuron. The PPF at mossy fiber-

CA3 interneurons synapses is normal (Wang et al., 2014). A significantly enlarged PPF ratio is also seen in Schaffer collateral-CA1 pathway (Laird et al., 2005). PPF ratio remains normal in *Bace1*$^{+/-}$ mice (Giusti-Rodríguez et al., 2011; Wang et al., 2014). These results indicate that complete knockout of *Bace1* induces a deficit in pre-synaptic function. These results agree with the fact that expression of post-synaptic marker PSD-95, but not pre-synaptic marker synaptophysin, changes upon the treatment with the BACE-inhibitor IV (Kamikubo et al., 2017).

The functions of BACE1 in maintaining dendritic spine structure, synaptic transmission, as well as both short-term and long-term plasticity cannot be ignored (Table 3). However, all on-target side effects, which are seen in *Bace1*$^{-/-}$ and mice treated with high dose of BACE1 inhibitor, are largely prevented in *Bace1*$^{+/-}$ mice (50% reduction in BACE1 protein level) or low dose treatment. Therefore, the careful adjustment of the dosage of certain BACE1 inhibitor might be crucial for the success of these compounds in the treatment of AD.

Table 3: Consequences of genetically knockout *Bace1* and pharmacologically inhibits BACE1 on synapses

		Bace1$^{-/-}$	*Bace1*$^{+/-}$	BACE1 inhibition	Ref.
Synaptic structure	**Pre-synaptic terminals**	Normal in mossy fiber terminals			(Kandalepas et al., 2013)
	Spine Density	Reduced in CA1		Reduced in cortical L5 pyramidal neurons	(Filser et al., 2015; Savonenko et al., 2008; Zhu et al., 2018)
	Spine Plasticity		Normal adaptive plasticity in cortical L5 neurons	Impaired in cortical L5 pyramidal neurons	(Filser et al., 2015; Zhu et al., 2018; Zou et al., 2016)
Synaptic function	**Basal synaptic transmission**	Reduced in CA1	Normal in CA1	Reduced in CA1	(Filser et al., 2015; Giusti-Rodríguez et al., 2011; Kamikubo et al., 2017)
	Pre-synaptic function	Increased in CA1 & CA3	Normal in CA1 & CA3	Normal in CA1	(Giusti-Rodríguez et al., 2011; Kandalepas et al., 2013; Wang et al., 2008, 2014; Zhu et al., 2018)
	LTP	Reduced in CA1 & CA3	Normal in CA1 & CA3	Reduced in CA1	(Filser et al., 2015; Giusti-Rodríguez et al., 2011; Kamikubo et al., 2017; Wang et al., 2014; Zhu et al., 2018)
	LTD	Normal in CA1; Slight deficits in CA3			(Laird et al., 2005; Wang et al., 2008)

2.3. Long-term inhibition of BACE1 in AD mouse models

The effects of knocking out *Bace1* in AD mouse model are promising. Homozygous knockout of *Bace1* mice almost completely abolishes the generation of toxic Aβ peptides and amyloid plaques formation in various AD mice models (McConlogue et al., 2007; Roberds et al., 2001; Sadleir et al., 2015). Even partially reduction of BACE1 protein in AD mice model (*5XFAD:Bace1*$^{+/-}$) could significantly reduce the Aβ production and plaque load in female animals (Devi and Ohno, 2015; Sadleir et al., 2015).

2.3.1. BACE1 inhibition on Aβ induced impaired spine plasticity

Amyloid plaque deposition is the main pathological hallmark of Alzheimer's disease (Hardy and Selkoe, 2002). During the formation of amyloid plaques, dendritic spine density reduces in vicinity of Aβ deposition in various of AD mouse models, including APP/PS1, Tg2576 and App^{NL-G-F} mice (Bittner et al., 2012; Dorostkar et al., 2014; Saito et al., 2014). In areas in far distance to plaques the density of dendritic spines is not changed (Bittner et al., 2012; Dorostkar et al., 2014). The reduced spine density is mainly due to loss of spine (Bittner et al., 2012). It might due to strongly increased synaptic pruning via over activated microglia induced by complement protein-related pathway (Hong et al., 2016a). Aβ recruits complement C1q complex and C3 to synapses, and C3 mediates synapse elimination by phagocytic glia cells (Hong et al., 2016a). It is reasonable to speculate that lowering Aβ by BACE1 inhibition could rescue spine loss at plaques in AD mouse models.

2.3.2. Functional effect of BACE1 inhibition on AD pathophysiology

One of the typical electrophysiological consequences of accumulated Aβ is impaired synaptic plasticity in a dose dependent manner (Puzzo et al., 2008; Rammes et al., 2017). PPF is normal in APP/PS1 mice and APP^{V717I} transgenic mice(Chong et al., 2011; Gengler et al., 2010; Viana da Silva et al., 2016), and slightly increased in 3xTgAD mice (Davis et al., 2014). Several AD mouse models display an attenuated hippocampal LTP alteration started from 6-12 month of age (Gengler et al., 2010; Kimura and Ohno, 2009; Ma et al., 2013; Oddo et al., 2003; Roder et al., 2003; Volianskis et al., 2010). Although half reduction of BACE1 protein level in 5XFAD mice did not rescue the basal synaptic transmission deficits, it rescues the LTP deficit (Kimura et al., 2010). Hippocampus-dependent fear conditioning task further confirmed that *5XFAD:Bace1*$^{+/-}$ mice are rescued completely back to wild-type levels (Kimura et al., 2010). Similar effects are reproducible using BACE1 inhibitor. Application of BACE1 inhibitor LY2886721 over 3-days (0.2 nmol/day, Eli Lilly and Company, Indianapolis, Indiana) rescues the *in vivo* LTP reduction in McGill-Thy1-APP-TG rats (Qi et al., 2014).

3. Seizure protein 6

SEZ6 (Seizure protein 6), also known as brain specific receptor-like protein C, is first reported by Shimizu-Nishikawa and colleagues (Shimizu-Nishikawa et al., 1995a). The *Sez6* mRNA expression is increased in cultured mice cortical neurons after acute Pentylenetetrazol (PTZ) treatment induced bursting activity (Shimizu-Nishikawa et al., 1995a, 1995b). In mice, knockout of *Sez6* does not show increased or decreased

sensitivity to PTZ induced clonic seizure (Gunnersen et al., 2007). Further study demonstrated that the expression of SEZ6 is regulated by neuronal activity (Rampon et al., 2000).

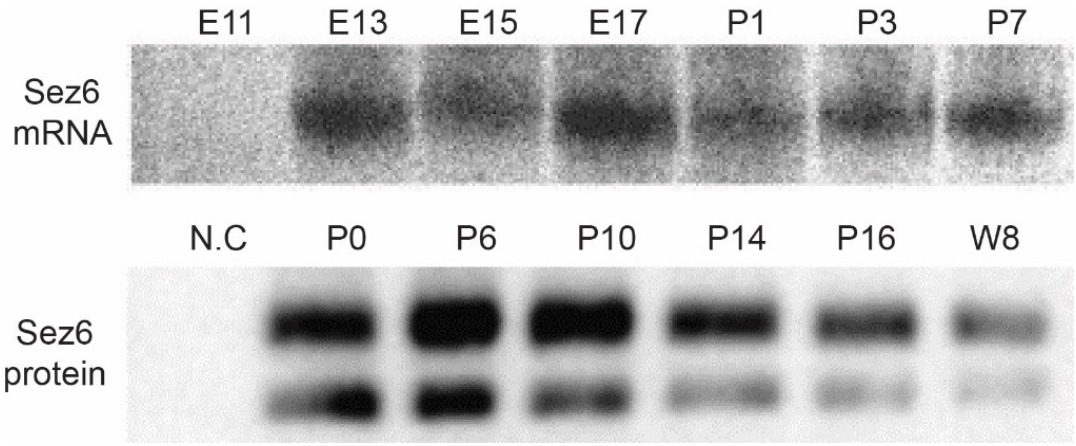

Figure 5: SEZ6 expression level in different age

Upper: SEZ6 mRNA is about 4 Kb, it is detectable from embryonic day 13 in mouse neocortex. Lower: SEZ6 protein level. (Adapted from Kim et al., 2002 and Osaki et al., 2011)

SEZ6 is a typical type I trans-membrane protein expressed exclusively in cortical and hippocampal pyramidal neurons. The expression of SEZ6 starts from embryonic day 13 and its protein level decreased during postnatal development (Figure 5) (Kim et al., 2002). SEZ6 is expressed prominently in deep cortical layers, hippocampal CA1 and the striatum (Figure 6) (Osaki et al., 2011). In young mice, SEZ6 is located in the somatodendritic compartment, specifically in the dendritic plasma membrane, synaptosomes and recycling endosomes (Carrodus et al., 2014; Gunnersen et al., 2007; Mitsui et al., 2013;

Shimizu-Nishikawa et al., 1995b). In adult mice, SEZ6 is mainly detecable in the soma of pyamidal neurons.

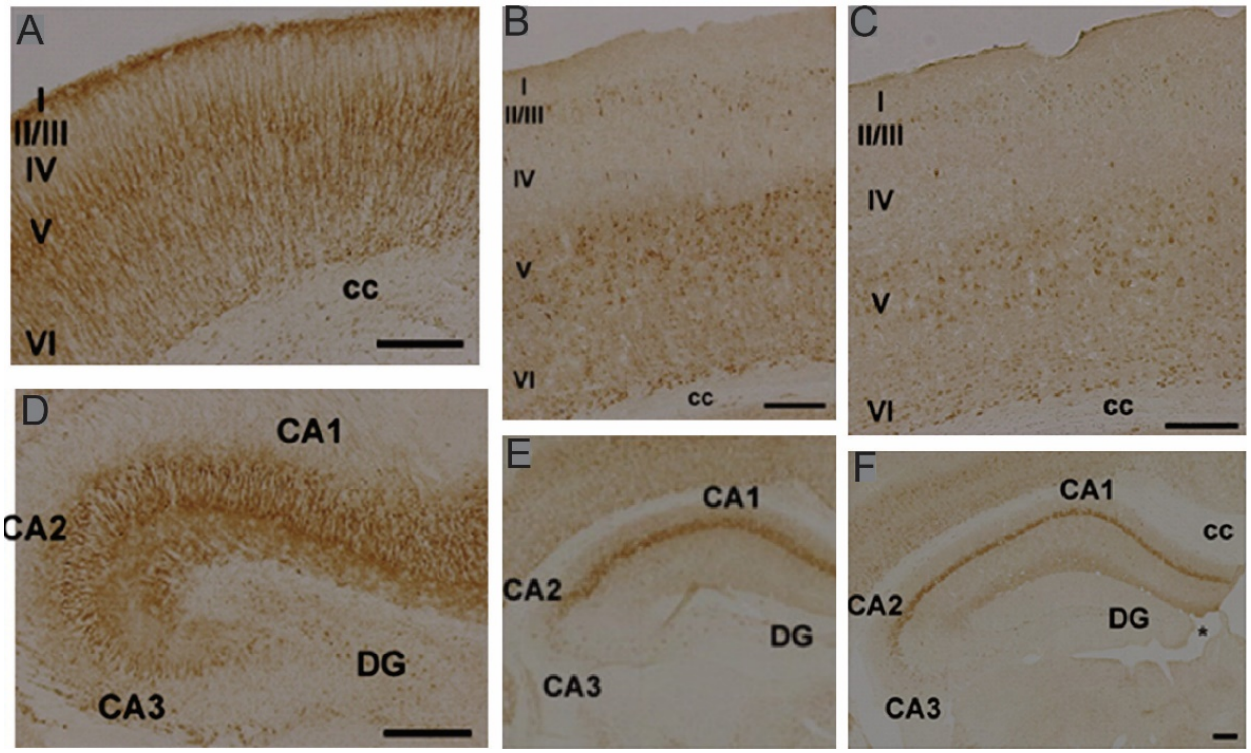

Figure 6: SEZ6 distribution in mouse cortex and hippocampus

SEZ6 is expressed by neurons. SEZ6 locates in both neurites and soma in young mice. In adult mice, SEZ6 is mainly located in the soma of neurons. (A-C) Cerebral cortex; (D-F) Hippocampus; (A, D) P0; (B, E) P14; (C, F) Adult. I, II/III, IV, V, VI: Cortex layer I, II/III, IV, V, VI; cc: corpus callosum; CA1: Cornu Ammonis 1; CA2: Cornu Ammonis 2; CA3: Cornu Ammonis 3; DG: dentate gyrus. Bar, 200 μm. (Adapted from Osaki et al., 2011).

3.1. The structural of SEZ6

The SEZ6 ectodomain has several predicted sub-domains, including 3 CUB (complement C3b/C4b binding site) domains and 5 SCR (Short Consensus Repeat) domains (Figure

7). These sub-domains are commonly known as protein-protein interaction domains which are also found in a variety of cell surface receptors. SCR domain is also known as complement control protein module, it exists in a wide variety of complement and adhesion proteins, for example complement protein C2 (Krishnan et al., 2009). CUB domains are involved in a diverse range of functions, including complement activation. These domains imply that SEZ6 might interact with other extracellular or cell-surface proteins, and it might have a functional link with complement proteins.

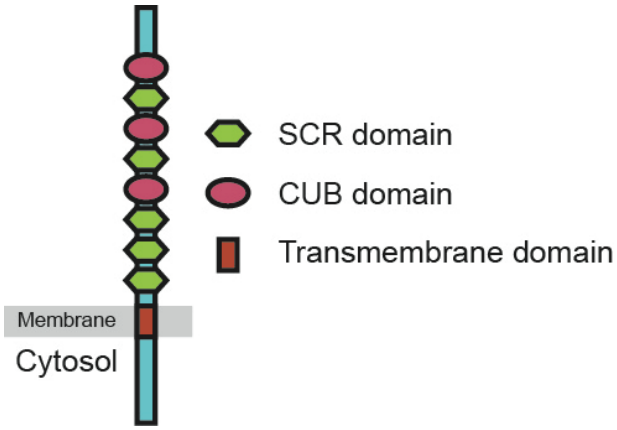

Figure 7: Schematic diagram of microdomains of SEZ6

SEZ6 has 3 CUB (Complement C1r/C1s, Uegf, Bmp1) domains and 5 SCR (Short Consensus Repeats) domains.

3.2. Proteolytic processing of SEZ6

The full length SEZ6 is exclusively and initially cleaved by BACE1 (Kuhn et al., 2012; Pigoni et al., 2016). Similar to the other substrates, BACE1 cuts SEZ6 at the juxtamembrane domain between leucine-906 and aspartate-907 (Pigoni et al., 2016),

generating a secreted soluble SEZ6 (sSEZ6) fragment and SEZ6 C-terminal transmembrane fragment (SEZ6-CTF) (Kuhn et al., 2012; Pigoni et al., 2016). Like other substrates, e.g. contactin-2 and CHL1 (close homolog of L1), BACE1 is a negative regulator of SEZ6 cell surface level in neurons, indicating BACE1 may be deeply involved in the regulation of SEZ6 functions. Then, SEZ6-CTF subsequently cleaved by γ-secretase, which leads to release of another SEZ6 intracellular domain (SEZ6-ICD) (Pigoni et al., 2016). The sSEZ6 is secreted to extracellular matrix, because it is detectable in medium and CSF (cerebrospinal fluid) of murine and human (Khoonsari et al., 2016; Pigoni et al., 2016).

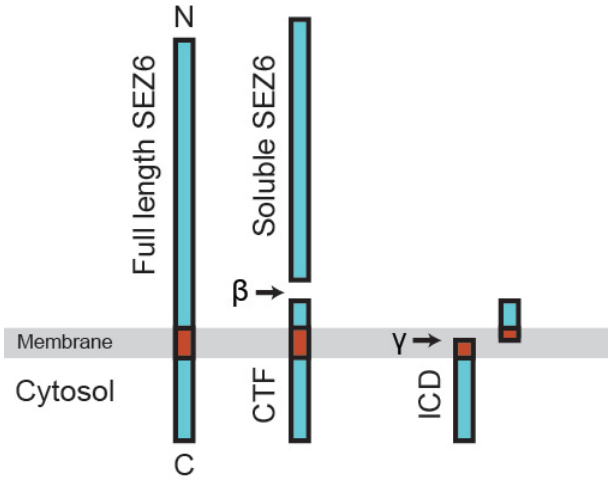

Figure 8: Schematic diagram of processing of SEZ6 by BACE1 and γ-secreatase

SEZ6 is a type I trans-membrane protein. SEZ6 is cleaved by BACE1, generating soluble SEZ6 and its c-terminal fragments (SEZ6-CTF). γ-secretase subsequently cuts SEZ6-CTF releasing SEZ6 intracellular domain (SEZ6-ICD).

3.3. Function of SEZ6

SEZ6 has important roles in dendritic development, regulating excitatory synaptic connectivity, motor coordination and spatial memory. Knockout *Sez6* induces some specific deficits in mice. First, knock out *Sez6* induces morphological changes in neurons. *Sez6*$^{-/-}$ mice show an increased numbers of short neurites but decreased total neurite length (Gunnersen et al., 2007). Results from primary cultured cortical neurons showed that full length SEZ6 and soluble SEZ6 have opposite function in regulating neurites outgrowth. sSEZ6 strongly increased neurites number, whereas full length SEZ6 slightly but significantly decreased neurites number (Gunnersen et al., 2007). Then, the dendritic spine density and reduced PSD95 puncta are reduced in somatosensory cortex of 5- to 7-week-old *Sez6*$^{-/-}$ mice (Gunnersen et al., 2007). This reduction impairs the connectivity between pyramidal neurons from layer II/III to layer V (Gunnersen et al., 2007). Finally, these deficits lead to an altered behavior in many tests. For example: 1) *Sez6*$^{-/-}$ mice cover less distance in locomotor tests; 2) *Sez6*$^{-/-}$ mice spend more time on the open arms of the plus maze and in the novel arm of the Y-maze compared with their WT counterparts; 3) in the Morris water maze test, *Sez6*$^{-/-}$ mice perform as normal as WT in spatial learning of the hidden platform position, but did not display a preference for the target quadrant in probe trials (Gunnersen et al., 2007).

Two independent groups reported that *Sez6* genetically links to febrile seizures and epilepsy in human (Mulley et al., 2011; Yu et al., 2007). Furthermore, using whole-exome sequencing, mutated Sez6 may be one of the candidates to be involved in the etiology of

severe intellectual disability and childhood onset schizophrenia, two severe neurodevelopmental disorders of unknown etiology. Three amino acids in SEZ6 (Thr229, Thr230 and Thr231) are deleted in childhood onset schizophrenia patients (Ambalavanan et al., 2016). One missense mutation is identified in SEZ6 (Arg657Gln) from severe intellectual disability patients (Gilissen et al., 2014). Both diseases are diagnosed in children, suggesting SEZ6 may have important function in neuronal development.

MATERIAL AND METHODS

1. Animals and housing conditions

In these experiments, the used mice lines are listed in Table 4. All mice were hold under pathogen-free conditions in the animal facility of ZNP (Zentrum für Neuropathologie und Prionforschung) of the LMU (Ludwig-Maximilians-Universität München). The room temperature was kept at 21 ± 1°C. Mice were group housed up to a maximum of 5 mice per cage. All animals had access to food and water ad libitum and were maintained on a 12h light: 12h dark cycle. Health condition of each animal was checked every day with recorded body weight. All animal experimental procedures and protocols were followed the regulations of LMU and approved by the government of Upper.

Table 4: list of mice line

Mouse line		Origin	Ref.
C57BL/6J		Charles River Laboratories (Sulzfeld, Germany)	
***Bace1*$^{-/-}$**	B6.129-Bace1^{tm1}Pcw/J	Jackson Laboratory (Bar Harbor, Maine)	(Cai et al., 2001)
***APP*$^{-/-}$**	B6.129S7-App^{tm1}Dbo/J	Prof. Dr. Ulrike C. Müller (University of Heidelberg)	(Zheng et al., 1995)
SlickV	B6;SJL-Tg(Thy1-cre/ERT2,-EYFP)VGfng/J	Jackson Laboratory (Bar Harbor, Maine)	(Young et al., 2008)
GFP-M	Tg(Thy1-eGFP)MJrs	Jackson Laboratory (Bar Harbor, Maine)	(Feng et al., 2000)
***Sez6*$^{-/-}$**	Sez6-tm1.1Sest	Dr. Jenny Gunnersen (University of Melbourne)	(Gunnersen et al., 2007)
***Sez6*$^{LoxP/LoxP}$**		Dr. Jenny Gunnersen (University of Melbourne)	(Gunnersen et al., 2007)
Sez6*$^{-/-}$: *GFP-M		In house (ZNP)	
Sez6*$^{LoxP/LoxP}$: *SlickV		In house (ZNP)	

2. Chemical compound and administration

BACE1 inhibitor NB-360 was kindly provided by Dr. Ulf Neumann and Dr. Derya R. Shimshek (Novartis Institutes for BioMedical Research; Basel, Switzerland) (Neumann et al., 2015). The structural formula of NB-360 is showed in Figure 9. NB-360 was mixed in mice food in the final concentration of 250 mg/kg.

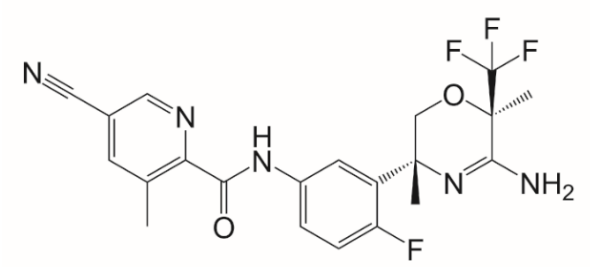

Figure 9: Structural formula of NB-360

Tamoxifen (Sigma-Aldrich) was used to induce single cell genetic modification in *Sez6*$^{LoxP/LoxP}$*:SlickV* mice. Tamoxifen was dissolved in a mixture of ethanol and corn oil (1:10 ethanol: corn oil) at the final concentration of 20 mg/ml. The application of tamoxifen was performed by oral gavage. The tamoxifen was given to mice at 0.25 mg per body weight (Ochs et al., 2015). The structural formula of tamoxifen is showed in Figure 10.

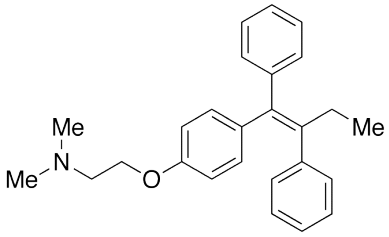

Figure 10: Structural formula of tamoxifen

3. Genotyping

The Genotypes of all mice lines were determined by polymerase chain reaction (PCR). A small piece of tissue was obtained from each mouse. Invisorb® DNA Tissue HTS 96 Kit/C (Stratec molecular) was used for DNA extraction. In brief, 400 µl of Lysis Buffer G was incubated with mouse tissue overnight under 52°C shaking condition, follow by 1700g centrifugation for 10 mins. The supernatant was transferred into collection plate and mix with 200 µl binding buffer A, follow by 1700 g centrifugation for 5 mins. After discarded the filtrated, the pellet was washed in 550 µl washing buffer, followed by twice 5 mins centrifugation at 1700 g. Finally, 100 µl of warmed (52°C) elution buffer was used to collects the DNA extraction.

The extracted DNA was used for PCR to identify the genotypes of each animal. The primers are listed in Table 5. The formulation of PCR solution is listed in Table 6. The PCR solution was placed in a thermocycler. The PCR program is listed in Table 7. PCR products were analyzed by gel electrophoresis. The samples were loaded to 1.5% agarose gel with SYBR® gold nucleic acid gel stain. The agarose gel was immerged into TAE running buffer. DNA migration was driven by 120-195 V electric fields for 60-90 minutes. A photograph of the gel was taken under UV light source for documentation.

Table 5: Primers for Genotypes

	Primer	Sequence
***Bace1*$^{-/-}$**	Forward	CGGGAA ATGGAA AGGCTACTCC
	Reverse	TGGATGTGGAATGTGTGCGAG AGGCAGCTTTGTGGAGATGGTG
***APP*$^{-/-}$**	Forward	GAGACGAGGACGCTCAGTCCTAGGG
	Reverse	ATCACCTGGTTCTAATCAGAGGCCC
SlickV	Forward	TCTGAGTGGCAAAGGACCTTAGG
	Reverse	CGCTGAACTTGTGGCCGTTTACG
GFP-M	Forward	TCTGAGTGGCAAAGGACCTTAG
	Reverse	TGAACTTGTGGCCGTTTACG
***Sez6*$^{-/-}$**	Forward	CGTATGGCATCTGTGACCTG GTAACCTTCGGGCTCCATCCTC
	Reverse	GAACTTCCATTGCTAGGAAACAGAC
***Sez6*$^{LoxP/LoxP}$**	Forward	CGTATGGCATCTGTGACCTG GTAACCTTCGGGCTCCATCCTC
	Reverse	GAACTTCCATTGCTAGGAAACAGAC

Table 6: PCR solution

Items	Volume
Onetaq hotstart quickload	12.5 µl
Forward primer	0.5 µl
Reverse primer	0.5 µl
Template DNA	0.5 µl
Distilled water	10 µl

Table 7: PCR program

Step	Temperature (°C)	Time (s)
1	94	180
2	94	30
3	60	60
4	68	20
5	68	120
6	10	∞
Step 2-4: repeat for 35 times.		

4. Protein Extraction and Immunoblotting

Mouse brains were harvested and separated to left and right cerebral hemispheres. Both hemispheres were snap freezing by liquid nitrogen and stored at -80°C. The membrane protein and soluble protein were extracted from brain tissues and separated using DEA buffer (50 mM NaCl, 0.2% diethylamine, pH = 10) and RIPA buffer (20 mM Tris-HCl, pH = 7.5, 150 mM NaCl, 1 mM EDTA, 1 mM EGTA, 1% NP-40, 0.5% sodium deoxycholate, 0.05% Triton X-100) with freshly supplemented protease inhibitors (P8340, Sigma-Aldrich). Using the BCA method, concentrations of total protein were measured.

Protein samples were mixed with Laemmli sample buffer supplemented with 2-mercaptoethanol and separated by SDS-PAGE. The electrophoresis of SEZ6 were performed in Tris-glycine gels with Tris-buffer (25 mM Tris, 190 mM glycine) and transferred onto polyvinylidene difluoride membranes (Amersham Hybond P 0.45 PVDF, GE Healthcare Life Science). APP C-terminal fragment (APP-CTF) was separated using Tricine Protein Gels (10-20%, Novex, Thermo Fisher Scientific) in Tris-tricine buffer (Novex, Thermo Fisher Scientific), followed by transferred onto nitrocellulose membranes (GE Healthcare Life Science). Both nitrocellulose and PVDF membranes were incubated for 1 h at room temperature with I-Block solution (0.2% I-BlockTM Thermo Fisher Scientific, 0.1% Tween 20 in PBS). Followed by overnight incubation with primary antibodies respectively (anti-SEZ6 antibody was provided by Dr. Gunnersen; anti-sAPPβ antibody: 18957 IBL; anti-β-CTF antibody: Y188, Abcam; in diluted I-Block solution) at 4°C. After 3 times washing by TBS-T buffer (140 mM NaCl, 2.68 mM KCl, 24.76 mM Tris,

0.3% Triton X-100, pH = 7.6), membranes were incubated with HRP-conjugated secondary antibody. Bound antibodies were visualized by using enhanced chemiluminescence (Thermo Fisher Scientific). Immunoblotting were performed on a LAS-4000 image reader and Multi-Gauge V 3.0 software were used for quantification analysis.

5. Cranial window implantation

Both genders were used in this experiment. At 2-month of age, the cranial window implantation surgery was performed. The surgery protocol was reported previously (Fuhrmann et al., 2007; Holtmaat et al., 2009). In brief, after anesthesia by intraperitoneal injection of the mixture of ketamine (130 mg/kg b.w. WDT/Bayer Health Care) and xylazine (10 mg/kg b.w. WDT/Bayer Health Care), mouse was fixed on the stereotaxic surgical setup (Figure 11A). Dexamethasone (6 mg/kg b.w. of Sigma) was applied by intraperitoneal injection to prevent development of cerebral edema. The mouse skull was exposed and cleaned by scalpel, then the piece of skull which was marked (Figure 11B). After carefully taking out the skull, the mice cerebral cortex was exposed (Figure 11C&D). A piece of coverslip was quickly fixed on top of cortex together with a metal bar by dental cement (Figure 11E). After surgery, the mice were put in a warm box for palinesthesia (Figure 11F). They received Carprofen (7.5 mg/kg b.w. Pfizer) and Cefotaxime (5 mg/kg b.w. Pharmore). The mice were singly housed for the 4-week recovery period with continuous postoperative observation.

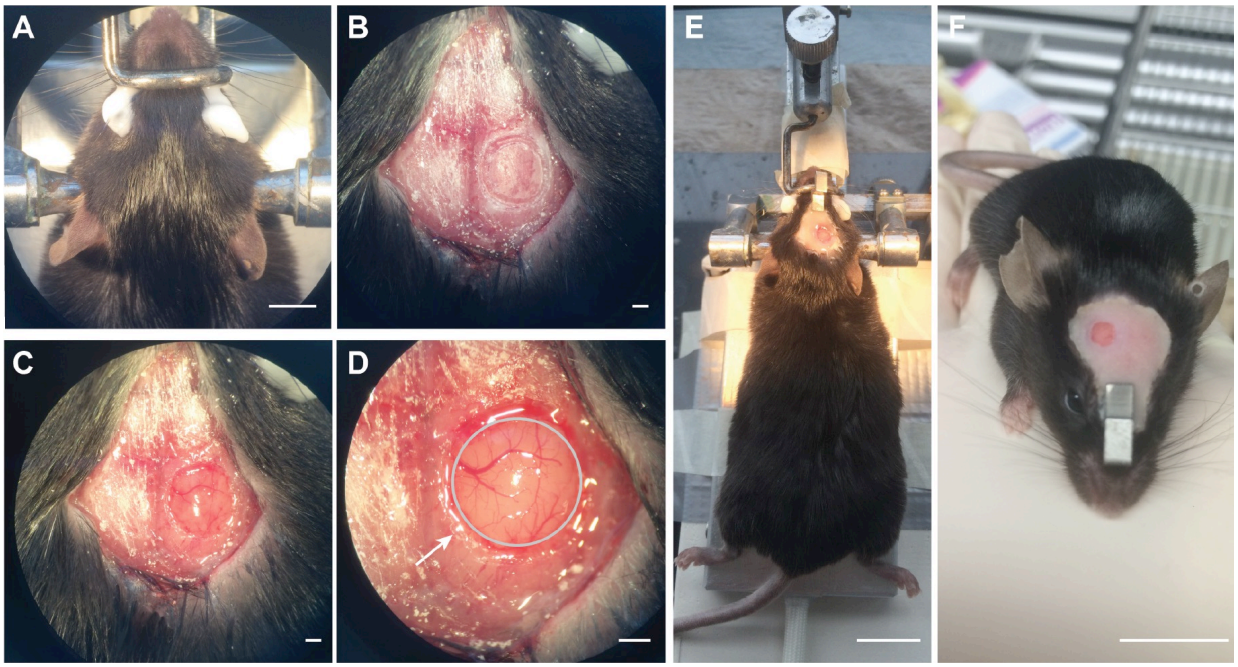

Figure 11: mouse cranial window implantation surgery

(A) A mouse was anesthetized and fixed on stereotaxic setup. (B) The skull was exposed, and a 4-mm diameter circle was marked. (C) A piece of the skull has been removed. (D) A 4-mm diameter cranial window. (E) The cranial window was covered by coverslip which is fixed to skull by dental cement. (F) After a few days of recovery, the mouse was healthy. C-D Scale bars: 1 mm. A, E & F Scale bars: 20 mm. (Kindly provide by Dr. Rodrigues)

6. Two-Photon in vivo imaging

Our main focused region is the layer V pyramidal neurons in the cerebral cortex. The apical dendrites of these neurons are labeled by eGFP and eYFP in GFP-M and SlickV mice respectively. Using LSM 7MP microscope (Carl Zeiss), we repeatedly imaged these apical dendrites. In general, mouse with cranial window was anaesthetized by isoflurane (1% in 95% O2, 5% CO2) and fixed under the microscope. Their body temperature was maintained by self-regulating heating pad (Fine Science Tools GmbH) and each image session was lasted less than 90 mins. All images were acquired through a water-

immersion objective (20x, NA=1.0; Carl Zeiss) with 920 nm wavelength femtosecond laser which is generated from Mai Tai DeepSee laser generator (Spectra Physics). Two types of images were acquired from each animal: (1) overview images which is 424 × 424 pixel per image frame (0.83 μm/pixel) with 3 μm axial resolution; (2) dendritic images which is 512 × 256 pixels per image frame (0.138 μm/pixel) with 1 μm axial resolution.

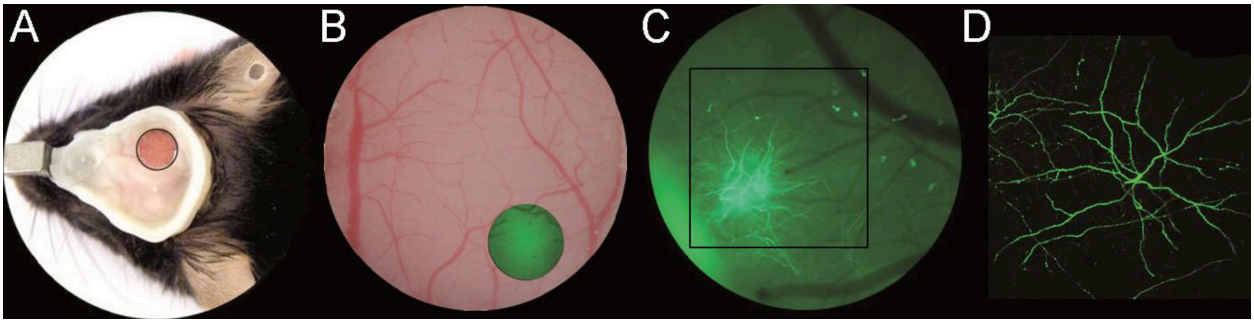

Figure 12: Two-Photon imaging

(A) A photograph of the mouse head with cranial window. The metal bar is used to fix the mouse under the 2P microscope. (B) Stereomicroscopic image of the brain surface. (C) Wide-field and (D) 2-photon micrograph of the apical dendrites of layer V pyramidal neurons in cortex of GFP-M mouse. (Kindly provide by Finn Peters)

7. Immunohistochemistry and confocal imaging

Mouse was deeply anesthetized by intraperitoneal injection of mixture of ketamine (130 mg/kg b.w. WDT/Bayer Health Care) and xylazine (10 mg/kg b.w. WDT/Bayer Health Care). Then the animal was placed on the perfusion stage and exposed the peritoneal cavity. After exposure of hart, a 25-gauge needle, which is attached to a peristaltic pump via silicon tubing, was incised into the left ventricle. After turning on peristaltic pump at a rate of 7 ml/min, an incision on right atrium was quickly made to allow drainage. 15 ml of phosphate-buffered saline (PBS) followed by 10 ml of 4% formalin solution was used for

each animal. Then the mouse brains were dissected with post-fixation for 24 hours in 4% formalin. The fixed brains were sliced by vibratome (VT1000S, Leica) into 50 μm coronal sections. The immunohistochemistry protocol is list in Table 8.

Table 8: immunohistochemistry protocol.

Step	Solution	Company	Time
Permeabilization	1% Triton X-100	Sigma-Aldrich	2-hours
Blocking	10% normal goat serum	Sigma-Aldrich	2-hours
Antibody	1:500 anti-GFP Alexa 488	Thermo Fisher	4-hours
Washing	PBS	Sigma-Aldrich	5 × 10 min
Mounting	Fluorescence conserving media	Dako	

8. Hippocampal slice preparation and electrophysiological recordings

After treated with BACE1 inhibitor or EE, WT and *Sez6*$^{-/-}$ mice were anesthetized with isoflurane (1% in 95% O2, 5% CO2). Then they were euthanatized by cervical dislocation. Their brains were quickly harvest and transferred into ice-cold carbogenated (95% of O2 and 5% of CO2) cutting solution (Table 9). Then 350 μm sagittal sections were performed to fresh obtained mouse brain by vibratome (VT1200S, Leica). The brain slices rest in 35°C artificial cerebrospinal fluid (aCSF) (Table 9) for 30 mins and another 60 mins at room temperature (21 - 22°C).

We tested field excitatory postsynaptic potentials (fEPSPs) in Schaffer collaterals-CA1 synapse. The recording electrodes were homemade glass microelectrode (1-3 MΩ) produced by P-97 puller (Sutter Instrument). After filled with aCSF, the recording electrodes was placed in the CA1 stratum radiatum. Two platinum/iridium concentric

stimulation electrodes (PI2CEA3, Life Science) were placed at both side of recording electrodes (Figure 13). The field potentials were amplified 100× using an EXT-10C amplifier (National Instruments) and digitized with BNC-2090A (National Instruments).

Table 9: Solutions for hippocampal slice preparation and electrophysiological recordings

Chemical compound	Cutting solution	Artificial cerebrospinal fluid
NaCl	125 mM	125 mM
KCl	2.5 mM	2.5 mM
NaH_2PO_4	1.25 mM	1.25 mM
$NaHCO_3$	25 mM	25 mM
$MgCl_2$	6 mM	1 mM
$CaCl_2$	0.5 mM	2 mM
D-glucose	25 mM	25 mM

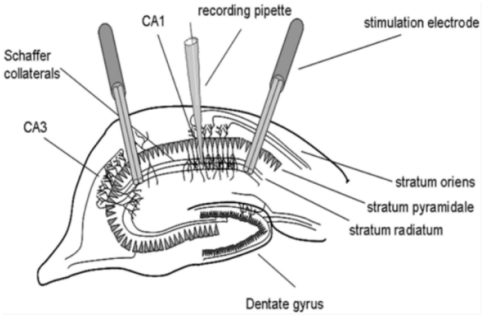

Figure 13: Schematic drawing of mouse hippocampal slices

Schaffer collaterals-CA1 pathway is axons projection from CA3 to CA1. The stimulation is performed in an antegrade or retrograde manner by two stimulation electrodes that were positioned in the stratum radiatum. CA1: Cornu Ammonis 1; CA3: Cornu Ammonis 3. (Kratzer et al., 2012).

For paired pulse facilitation (PPF), two stimulations with interval 50, 75, 100, 150, 200, 400, 800 and 1200ms were given to hippocampus slices. For Input-output curves, the stimulation intensity was increased stepwise from 0 v to 30 v. For the long-term potentiation (LTP), the stimulation intensities were adjusted to 50% of maximum

amplitude, and the stimulation frequency of each stimulation electrodes was set to every 15 s (0.033 Hz). Once reaching stable stimulation-response states, the Schaffer-collaterals were tetanized by 1 second of high frequency stimulation (HFS, 100Hz). Follow by 60 mins continuously recordings. Data were analyzed using the WinLTP 2.10 program.

9. Environmental enrichment

Environmental enrichment (EE) housing condition is a group (3-6) of mice in 48cm × 48cm × 48cm cage with 2 running wheels, one ladder, one tunnel and multiple hanging toys which were changed or reposition 3 times per week (Figure 14). Same gender mice from same litter were placed into EE housing conditions from 2-month-old or 3-month-old for 6-7 weeks. Both genders of animals were use in this experiment. The aggressive mice were removed from EE housing. Standard cages were 30 × 15 × 20 cm without wheels or toys.

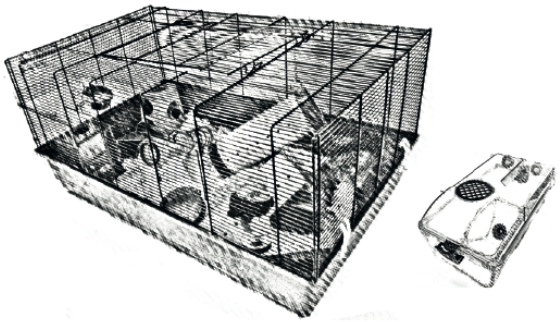

Figure 14: Environmental enrichment housing condition

Photograph of Environmental enrichment housing condition (left) and standard housing (right) (Zou et al., 2016).

10. Images, data processing and statistics

Dendritic spines were counted manually. For confocal micrographs, CA1 were counted in z-stacks by manually scrolling through the images. Because the z-plane resolution was low in two-photon micrographs, the dendritic spines of cortical neurons were restricted to laterally protruding spines. The dendritic spines dynamic analysis protocol was described before (Holtmaat et al., 2009). In brief, dendritic spines without changing location between consecutive imaging sessions (acceptable range < 1 μm) were defined as persistent spines. Newly emerged spines were defined as gained spine. Spines which were disappeared were defined as lost spines. For GFP-M mice, 8-10 dendrites were analyzed per mouse; for SlickV mice, 2-6 dendrites were analyzed per mouse.

GraphPad Prism (GraphPad Software, USA) was used for Statistical analyses. Data were presented as mean ± SEM. Statistical significances were determined by comparing means of different groups using two-tailed Student's *t*-text, one-way or two-way ANOVA, as specified in the figure legends. Bonferroni post-hoc tests were used to compare the different groups.

RESULTS

Part 1

SEZ6 and dendritic spine plasticity

1. SEZ6 and dendritic plasticity under basal condition

1.1. SEZ6 regulates dendritic spine density and morphology

To study the function of SEZ6 on dendritic spine density and plasticity, we first analyzed the dendritic spine densities of adult *Sez6*$^{-/-}$*:GFP-M* and *Sez6*$^{+/-}$*:GFP-M* mice. *Sez6*$^{+/+}$*:GFP-M* mice were served as control. We imaged layer I dendritic tufts of cortical layer V pyramidal neurons in these mice using *in vivo* two-photon microscopy. In line with previses report, the dendritic spine densities of *Sez6*$^{-/-}$ mice were reduced (Figure 15A) (Gunnersen et al., 2007). Furthermore, we demonstrated that SEZ6 was involved in dendritic spine density reduction in a dose dependent manner (Figure 15A).

Then, we classified all the spines into 3 categories (e.g. stubby, thin and mushroom spines) based on their morphology (Harris and Kater, 1994; Harris et al., 1992). We also calculated the number of dendritic filopodia (Figure 15B). Dendritic filopodia are hair-like transient structures which do not have bulbous head as dendritic spines. These structures may receive synaptic input. The newly formed spine is likely developed along the filopodia (Fiala et al., 1998; Hayashi and Majewska, 2005). As shown in Figure 15B, all of 3 types

of spines are significantly reduced in *Sez6*$^{-/-}$*:GFP-M* mice. The densities of filopodia were normal in both *Sez6*$^{-/-}$*:GFP-M* and *Sez6*$^{+/-}$*:GFP-M* mice, suggesting the formation rate of new gain spine may not affected (Figure 15B).

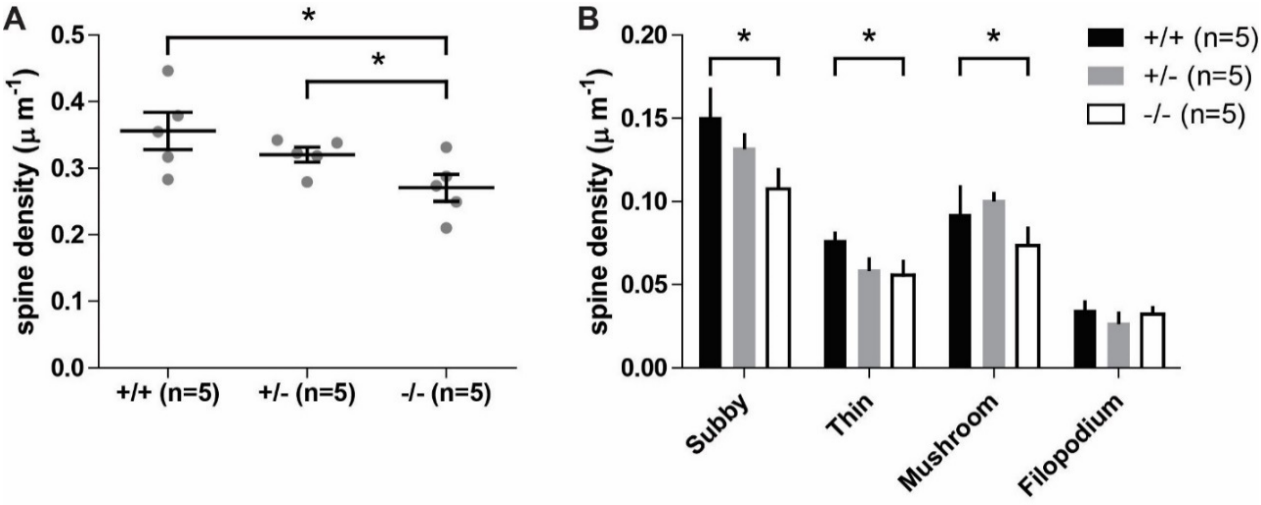

Figure 15: Dendritic spine density and morphology is altered in *Sez6*$^{-/-}$ mice

(A) Lack of SEZ6 alters dendritic spine density in apical dendrites of layer V pyramidal neurons in a dose depended manner. (B) Quantification of dendritic spine sub-type shows that stubby, thin and mushroom spines are reduced in *Sez6*$^{-/-}$ mice. The density of dendritic filopodia is normal. Animals per group: n=5. Two-tail Student's t-test, $p<0.05$ (*). Error bars represent S.E.M.

1.2. Knockout of *Sez6* in adult mice decreases dendritic spine density

The expression level of SEZ6 is high during early development, indicating it has important function for neuronal development. To exclude developmental deficits, as well as further study the impact of lack of SEZ6 in mature neurons, we used the conditional *Sez6* knockout mice, *Sez6*$^{LoxP/LoxP}$*:SlickV* mice. In *Sez6*$^{LoxP/LoxP}$ mice, *Sez6* exon 1 was inserted

with two flanked *LoxP* sequences (Figure 16A) (Gunnersen et al., 2007), which can be cleaved by activated Cre DNA-recombinase. *SlickV* mice express a modified Cre recombinase, CreER^{T2}, in a small subset of enhanced yellow fluorescent protein (eYFP) positive neurons in cortex and hippocampus (Figure 16A,B) (Young et al., 2008). CreER^{T2} is a ligand-dependent Cre recombinases which is only activated (nuclear translocated) by administration of tamoxifen to the animal (Feil et al., 2009; Ochs et al., 2015). Any alteration on eYFP and CreER(T2) positive neurons are mainly due to the cell autonomous knockout of *Sez6*. This cell specific gene editing occurs only in a small subset of neurons, the majority of neighboring eYFP and CreER(T2) negative neurons are not affected by tamoxifen treatment (Feil et al., 2009; Ochs et al., 2015; Young et al., 2008).

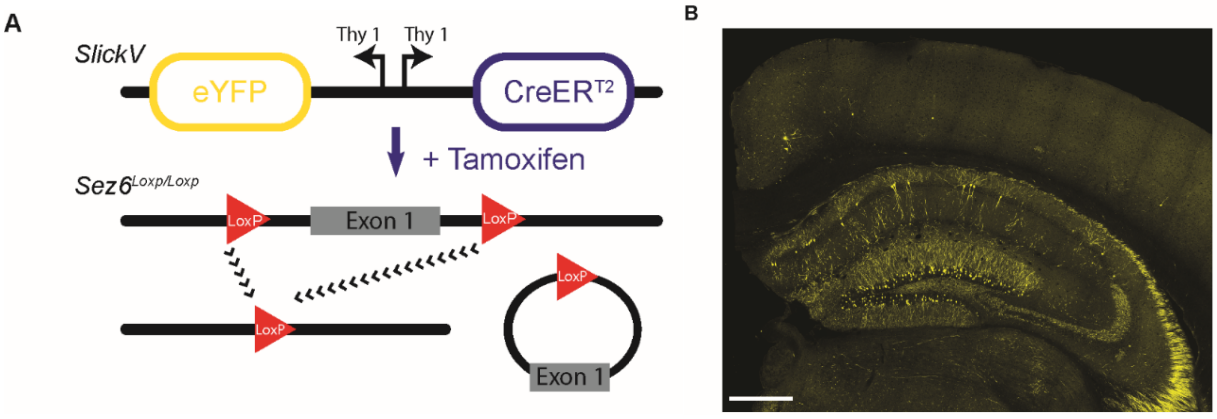

Figure 16: *Sez6$^{LoxP/LoxP}$:SlickV* mice

(A) Schematic diagram of tamoxifen activated CreER(T2) gene recombinases induced *Sez6* knockout in *Sez6$^{LoxP/LoxP}$:SlickV* mice. (B) Enhanced yellow fluorescent protein (eYFP) expression pattern in *Sez6$^{LoxP/LoxP}$:SliceV* mice.

By applying tamoxifen to *Sez6*$^{LoxP/LoxP}$*:SlickV* mice, we generated *Sez6*$^{cKO/cKO}$*:SlickV* mice. We performed *in vivo* two-photon microscopy to layer I dendritic tufts of cerebral cortex layer V pyramidal neurons in adult *Sez6*$^{cKO/cKO}$*:SlickV* mice (Figure 17A). As shown in Figure 17B, the dendritic spine densities of cortical layer V neurons are significantly reduced (Figure 17B). Then we investigated apical and basal dendrites of hippocampal CA1 eYFP and CreER^{T2} positive neurons after tamoxifen application using confocal microscopy (Figure 17C). Compared to vehicle control, the spine densities of both apical and basal dendrites showed a notable reduction in *Sez6*$^{cKO/cKO}$*:SlickV* mice (Figure 17D). As mention before, alteration in the extracellular environment is unlikely because the gene editing occurs only in a very small neuronal population. Therefore, we concluded that lack of SEZ6 induced dendritic spine deficits in a cell autonomous manner.

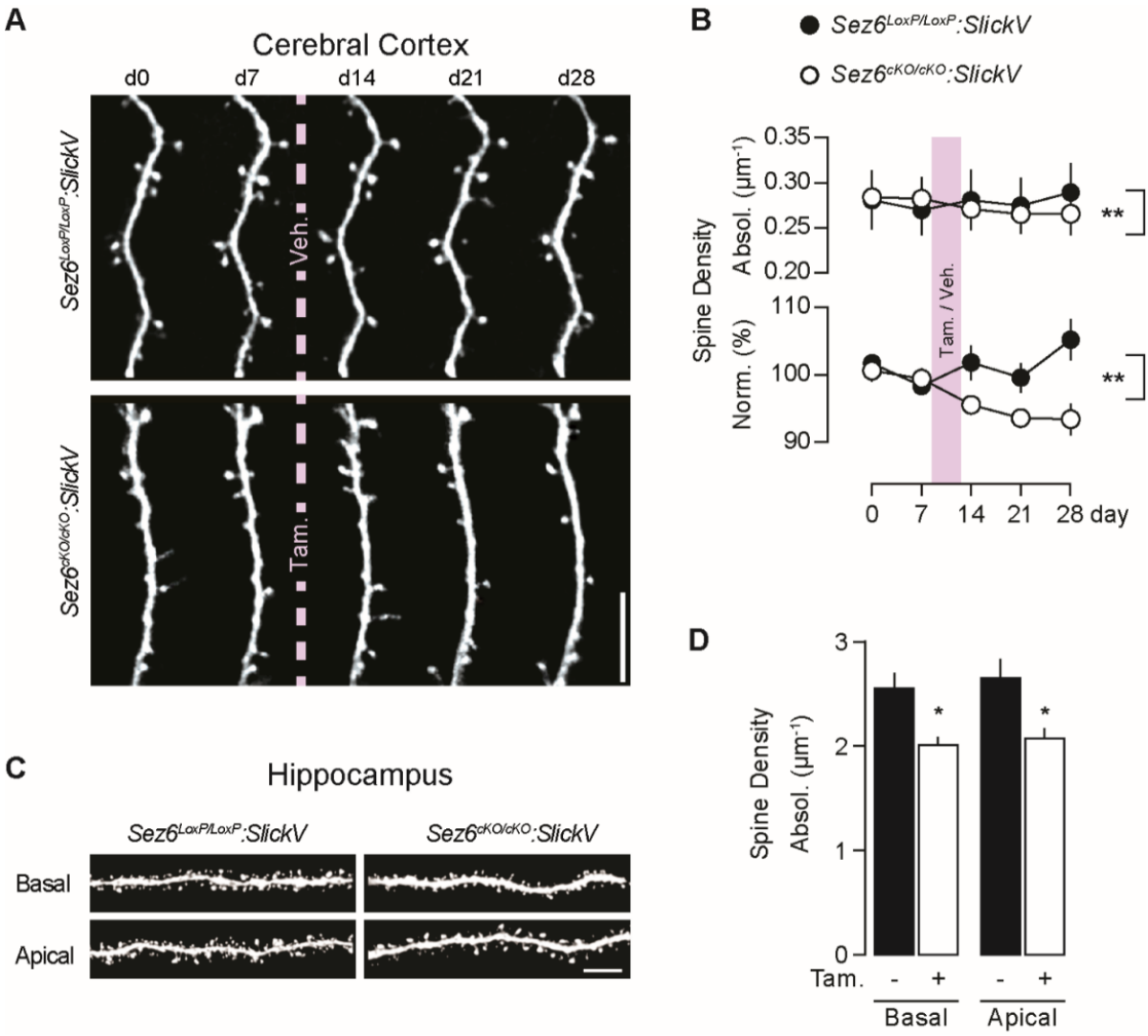

Figure 17: Knockout of *Sez6* impairs dendritic spine density in adult mice

(A) The apical dendrites from layer V cortical neurons were labeled by enhanced yellow fluorescent protein (eYFP). Micrographs of dendrites are acquired by sequential imaging by in vivo two-photon microscopy. Tamoxifen (0.25 mg/g b.w. in a mixture of 1:10 ethanol: corn oil) or vehicle treatment started at day 8 and continued for 5 days (highlighted in pink). Scale bar: 10µm. (B) Knockout of Sez6 impairs dendritic spine density in mature layer V cortical neurons. Top: absolute values; two-way ANOVA $F(4,40)=4.21$, interaction $p<0.01$, Genotype $p<0.001$, Days $p<0.001$. Bottom: The absolute values were normalized to the average of the first two timepoints. Two-way ANOVA $F(4,40)= 4.69$, interaction $p<0.01$, Genotype $p<0.01$, Days $p=0.11$. Tam: tamoxifen; Veh: vehicle. Animals per group: n=6. $p<0.01$(**). Error bars represent S.E.M. (C) The apical and basal dendrites of CA1 pyramidal neurons from *Sez6-cKO* mice and control were imaged by confocal microscopy. Scale bar: 5µm. (D) the dendritic spine density is reduced in *Sez6-cKO* CA1 neurons. Animals per group: n=3. Two-tail Student's *t*-test, $p<0.05$(*). Error bars represent S.E.M.

1.3. *Sez6*$^{-/-}$ mice have normal spine plasticity under base line condition

Dendritic spine plasticity is another important physiological feature. Therefore, it is reasonable to speculate that the dendritic spine plasticity might also regulated by SEZ6. To test this hypothesis, we repeatedly imaged *Sez6*$^{-/-}$*:GFP-M* and *Sez6*$^{+/-}$*:GFP-M* mice every 7 days over 4 weeks using *in vivo* two-photon microscopy. Then we analyzed the total dendritic spine density (Figure 18A), the fractions of new gained spines (Figure 18B) and lost spines (Figure 18C), as well as the spine turn-over rate (TOR) (Figure 18D). To our surprise, the fractions of new gained spines and lost spines, as well as spine TOR did not show obvious difference in both *Sez6*$^{+/-}$*:GFP-M* and *Sez6*$^{-/-}$*:GFP-M* mice compare with WT controls (Figure 18B-D). These results demonstrated that SEZ6 has important function in regulating dendritic spine density, but the spine plasticity remains unaffected.

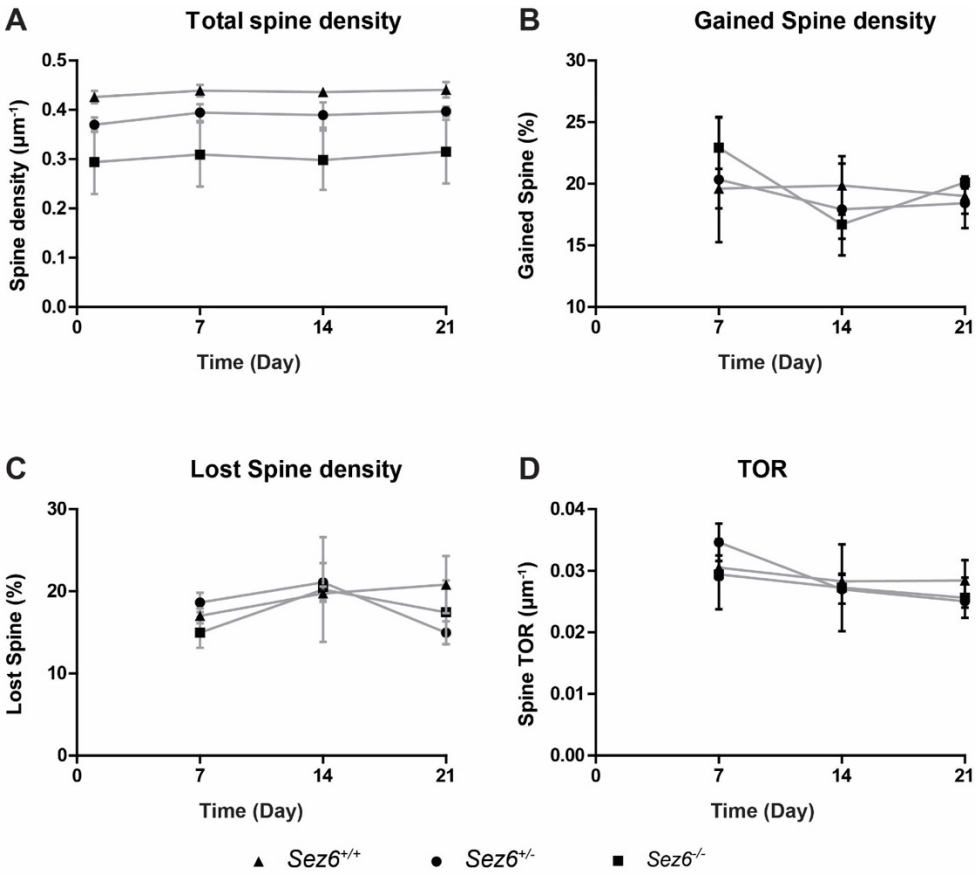

Figure 18: Dendritic spine plasticity is normal in *Sez6*$^{-/-}$ mice

(A) Quantitative analysis of the dendritic spine density over time in *Sez6*$^{-/-}$*:GFP-M*, *Sez6*$^{+/-}$*:GFP-M* and *Sez6*$^{+/+}$*:GFP-M* mice. Two-way ANOVA F(4,12)=0.32, interaction p=0.92, Genotype p=0.12, Days p<0.01; (B) Quantitative analysis of the new gained spines. Two-way ANOVA F(4,12)=0.97, interaction p=0.46, Genotype p=0.97, Days p=0.16; (C) Quantitative analysis of the lost spines. Two-way ANOVA F(4,12)=0.63, interaction p=0.65, Genotype p=0.83, Days p=0.34. (D) Quantitative analysis of the spines turn-over rate (TOR). Two-way ANOVA F(4,12)=0.68, interaction p=0.62, Genotype p=0.91, Days p=0.07. Error bars represent S.E.M.

1.4. *Sez6* knockout mice have impaired synaptic plasticity

Next, we investigated the role of SEZ6 in functional synaptic plasticity in hippocampal Schaffer collaterals-CA1 pathway by analysing PPF (paired-pulse facilitation), stimulus-response relationship and LTP (long-term potentiation) (Figure 19).

In the PPF test, we used stimulation intervals from 35 ms to 1200 ms. The results showed that *Sez6*$^{-/-}$ brain slices only have a minor elevation at 35 ms stimulation interval. For the longer intervals, *Sez6*$^{-/-}$ brain slices do not have differences compared to WT controls, suggesting SEZ6 is not involved into pre-synaptic plasticity (Figure 19A).

Then, we investigated the stimulus-response relationship by gradually increased stimulation intensity. *Sez6*$^{-/-}$ brain slices showed a significant reduction in synaptic transmission (Figure 19B).

Finally, we performed LTP measurement. After 10 minutes of baseline recordings, the Schaffer collaterals were tetanized by high-frequency stimulation (HFS; 100 pulses/s), followed by a continuous recording for 50 minutes. HFS caused a pronounced post-tetanic potentiation in WT mice, but the magnitude of LTP in *Sez6*$^{-/-}$ brain slices were significantly reduced (Figure 19C, D). Our findings suggest that SEZ6 regulates synaptic transmission and LTP mainly in the post-synaptic compartments.

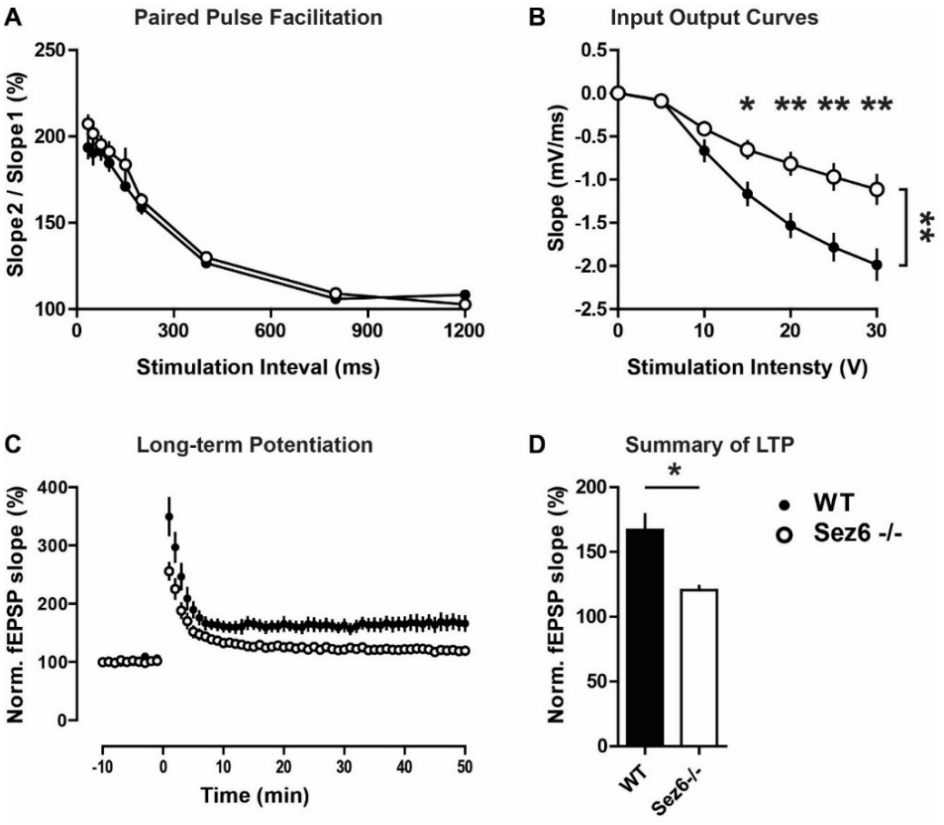

Figure 19: SEZ6 regulates synaptic plasticity

SEZ6 is involved in synaptic function. (A) The Paired-pulse ratio in hippocampal slices of *Sez6*$^{-/-}$ brain slices have no different compare to WT control. Two-way ANOVA $F(8,104)=1.46$, interaction $p=0.18$, Genotype $p=0.20$, Days $p<0.001$. (B) Sez6-/- mice have a significant reduction in stimulus-response relationship test. Two-way ANOVA $F(6,114)=11.02$, interaction $p<0.001$, Genotype $p<0.001$, Days $p<0.01$. Bonferroni post-test $p<0.05$ (*); $p<0.01$(**). (C) Representative traces of evoked field excitatory postsynaptic potential (fEPSP) acquired from *Sez6*$^{-/-}$ brain slices. LTP was induced by high-frequency stimulation (HFS) at Schaffer collaterals. *Sez6*$^{-/-}$ brain slices presented a notable impairment in LTP. (D) Summary graph of LTP magnitudes calculated 40 to 50 minutes after HFS from graphs in panels (C). Two-tail Student's t-test, $p<0.05$(*). Animals per group: n=7-9. Error bars represent S.E.M.

2. Adaptive plasticity of dendritic spine is impaired in *Sez6*$^{-/-}$ mice

2.1. Environmental enrichment does not alter spine plasticity in *Sez6*$^{-/-}$ mice

Environmental enrichment (EE) is a combination of enriched social interactions and housing conditions, including enhanced opportunities for cognitive, sensory, and motor stimulation. EE provides a larger number of learning opportunities than standard housing conditions (Leuner and Gould, 2010; van Praag et al., 2000). Increased environmental complexity has been shown to have a beneficial effect on many aspects of brain structure, including increased neurogenesis, synaptogenesis and a strongly increase in dendritic spine dynamics (Barnea and Nottebohm, 1994; Globus et al., 1973; Jung and Herms, 2014). Although spine density is reduced in *Sez6*$^{-/-}$ mice, the spine dynamics is normal under base line condition. Interestingly SEZ6 is upregulated under EE condition (Rampon et al., 2000), suggesting SEZ6 may be involved in adaptive synaptic alterations within the adult mouse brain. To investigate whether lack of SEZ6 has a functional consequence in neural circuit remodeling in the adult brain, we applied EE stimulation to *Sez6*$^{-/-}$*:GFP-M* mice. WT (*Sez6*$^{+/+}$*:GFP-M*) mice served as control. After two imaging timepoint, both *Sez6*$^{-/-}$*:GFP-M* and WT mice were exposed to EE over 6 weeks. The spine densities and dynamics were continuity monitored using *in vivo* two-photon microscopy.

In agreement with earlier reports (Jung and Herms, 2014; Zou et al., 2016) a steady increased of both mean and normalized spine densities were seen in WT mice under EE condition (Figure 20A&B filled circles). In sharp contrast, both mean and normalized spine densities were not altered by EE in *Sez6*$^{-/-}$*:GFP-M* mice (Figure 20A&B open circles). This

increased spine density in WT mice is mainly due to an enhanced fraction of new gained spines and stable spines (Figure 20C&D filled circles). There is a notable increase in new gained spine in WT mice at first timepoint after EE, which remains unaffected in *Sez6*$^{-/-}$ *:GFP-M* mice (Figure 20C). The number of lost spines is not altered in both knockout and WT mice (Figure 20E). The survival of pre-existing spine is a bit lower in *Sez6*$^{-/-}$*:GFP-M* mice compare to WT control, but it does not reach to statistical significant (Figure 20F). Collectively, these data demonstrate an essential role of SEZ6 in regulating adaptive remodeling in the adult mice brain.

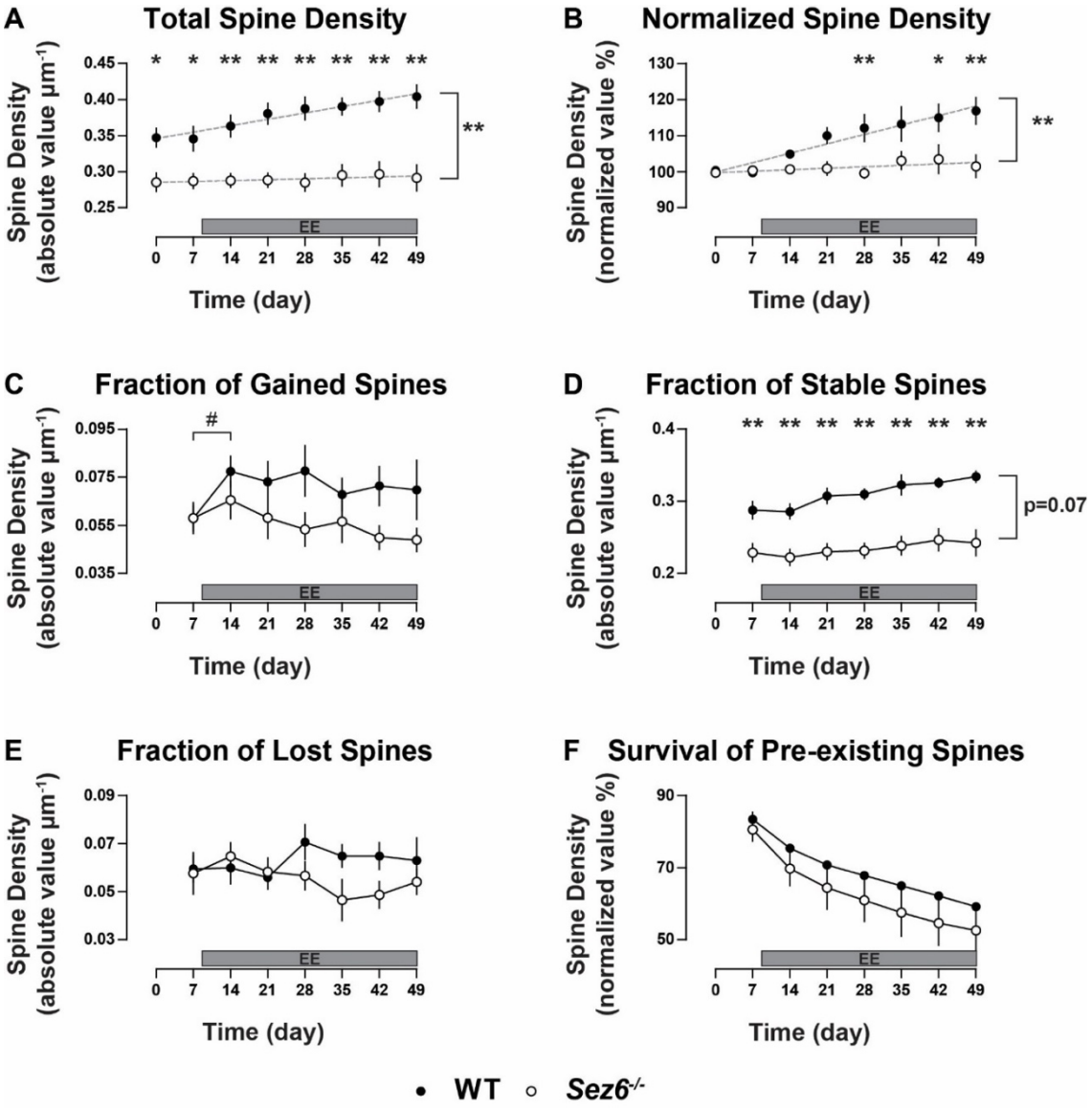

Figure 20: Dendritic spines adaptive plasticity is impaired in *Sez6*$^{-/-}$ mice

Adaptive plasticity of dendritic spines is impaired in *Sez6*$^{-/-}$ mice. Weekly imaging of GFP-labeled apical dendrites of layer V pyramidal neurons was performed since day 0. Enriched environment (EE) stimulation stars from day 8. Quantifications of mean (A) Two-way ANOVA $F(7,49)=5.58$, interaction $p<0.001$) and relative (B) $F(7,49)=4.10$, interaction $p<0.01$) spine density, fraction of new gained spine (C) Two-tail Student's t-test, WT d7 Vs. d14, $p=0.05$ (#); Sez6-/- d7 Vs. d14 $p=0.48$), stable spine (D; ANOVA $F(6,42)=2.07$, interaction $p=0.07$), lost spines (E) $F(6,42)=2.44$, interaction $p<0.05$) and survival of pre-existing spine (F). Bonferroni post-test $p<0.05$ (*); $p<0.01$(**). Error bars represent S.E.M.

2.2. Hippocampal synaptic plasticity is not affected by environmental enrichment in *Sez6*$^{-/-}$ mice

We have shown that the activity-induced structural spine plasticity is disturbed in *Sez6*$^{-/-}$ mice. To further examine if damaged spine plasticity on dendrites has functional consequences, we housed *Sez6*$^{-/-}$ mice and their WT littermates under EE condition over 6 weeks and monitored the LTP on hippocampal Schaffer collaterals-CA1 pathway. EE enhanced hippocampal-CA1 LTP in WT control mice (Cui et al., 2006; Huang et al., 2007; Kempermann et al., 1997; van Praag et al., 2000). But LTP did not increase due to enriched environment in *Sez6*$^{-/-}$ mice.

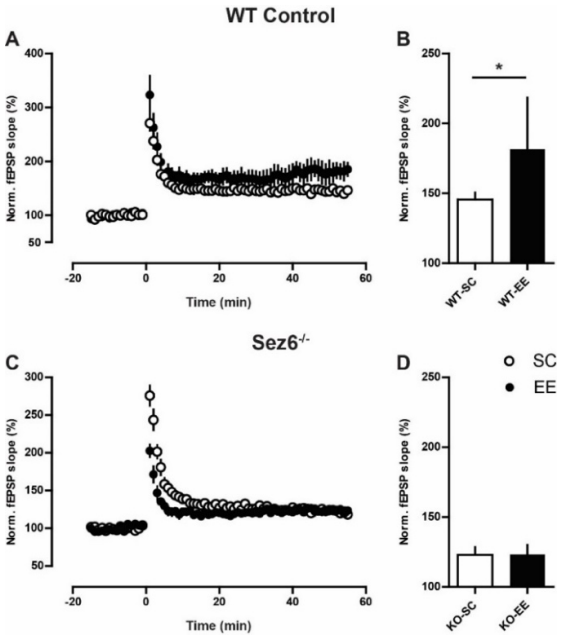

Figure 21: SEZ6 is a key factor underlineing environmental enrichment induced LTP increase

(A) Prolonged exposure to an enriched environment (EE) enhances hippocampal LTP in WT mice. (B) Quantifications of (A). (C) Prolonged exposure to an EE does not alter hippocampal LTP in *Sez6*$^{-/-}$ mice. (D) Quantifications of (C). Two-tail Student's t-test, $p<0.05$ (*). Error bars represent S.E.M.

Part 2

BACE1 Inhibition Impairs Synaptic Plasticity via SZE6

1. NB-360 strongly suppresses proteolytic activity of BACE1

NB-360 is a novel 3rd generation BACE1 inhibitor developed by Novartis Pharma AG (Basel, Switzerland). NB-360 has small molecule weight, and does cross the blood-brain-barrier efficiently (the molecular structure is illustrated at Figure 9) (Neumann et al., 2015). In this study, NB-360 was mixed in the mouse food pellets. The advantage of this approach is minimizing the stress to experimental animals caused by repeated drug administration. It might also reach to a more stable inhibitory effect because mice consistently consume these food pellets. By monitoring the weight of the food, we calculated that each mouse consumed 4.6 ± 0.1 g food pellets per day (N = 44) in average which is corresponding to a daily oral dose of 20 μM/kg/day. The body weight and health conditions are monitored on daily basis. During and after NB-360 treatment, we did not observe any impairment, expect hair depigmentation alteration (Figure 22). It is due to that NB-360 inhibits BACE2 which has been reported important for melanogenesis (Filser et al., 2015; Neumann et al., 2015; Rochin et al., 2013; Shimshek et al., 2016).

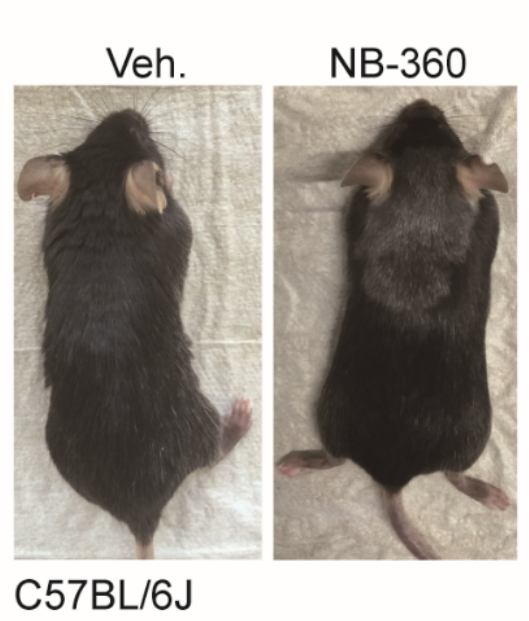

Figure 22: Chronic treatment of NB-360 induces hair depigmentation in mice

Mice was treated with NB-360 (right) or vehicle (left) for 21 days. NB-360 caused hair depigmentation in mice.

We first verified the inhibitory effect of NB-360. After administration of NB-360 or vehicle over 3 weeks, the mice cerebrums were harvested. The samples were homogenized and separated to soluble fractions and membrane extracts for immunoblotting. We analysed the protein levels of known BACE1 substrates: flSez6 (full length Sez6) and its cleavage product sSez6 (soluble Sez6), as well as the cleavage product of APP, sAPPβ (soluble APP beta) and β-CTF (C-terminal fragment of APP) (Kuhn et al., 2012; Pigoni et al., 2016). Samples from *Bace1*$^{-/-}$ (*Bace1* knockout) mice served as positive controls. Samples from *APP*$^{-/-}$ (*APP* knockout) mice were used for verifying the specificity of sAPPβ and β-CTF antibodies (Figure 23). The signal intensity of each immunoblot was analysed

using the Multi-Gauge software and normalized to the value of control (C57BL/6 vehicle) group. The results showed that after NB-360 treatment flSez6 was significantly increased, whereas the cleavage products sSez6, sAPPβ and β-CTF were significantly decreased. *Bace1*$^{-/-}$ vehicle condition showed similar results. In summary, we confirmed that NB-360 is a potent BACE1 inhibitor.

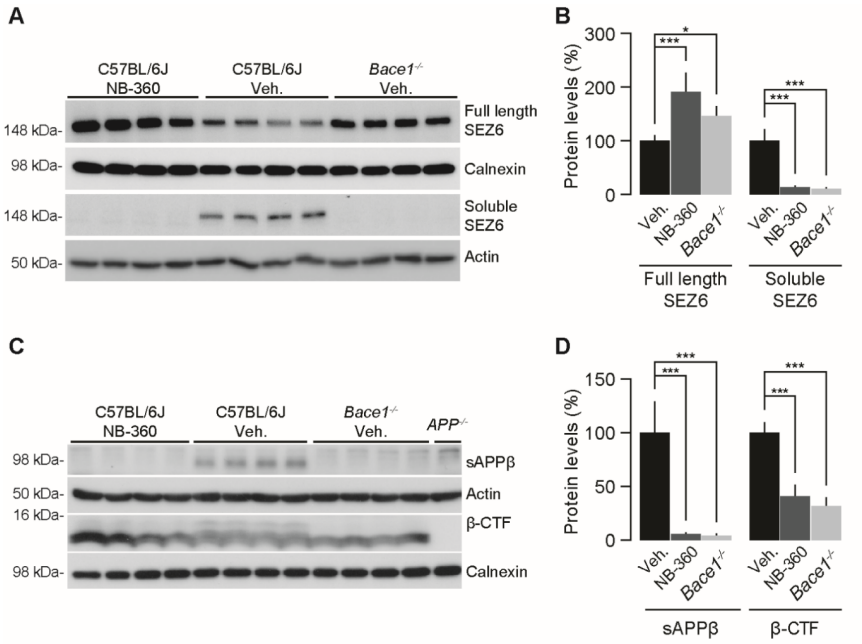

Figure 23: NB360 strongly inhibits BACE1 proteolytic activity

C57BL/6J mice were applied with food pellets which contains 0.25g/kg of NB-360 or vehicle for 21 days. *Bace1*$^{-/-}$ and *APP*$^{-/-}$ mice were applied vehicle food pellets 21 days. Mice whole brain homogenates were separated to soluble fractions and membrane extracts for immunoblotting. Actin and Calnexin were used as loading controls. Animals per group: n=4. (A) Both membrane extracts and soluble fractions were probed by anti-Sez6 antibody. Base on different fractions, full length membrane attached SEZ6 and soluble SEZ6 were separated. (B) Quantitative analysis of the signal intensity of full length and soluble SEZ6. One-way ANOVA, full length Sez6: $F(2,9)=15.70$ $p<0.01$, soluble Sez6: $F(2,9)=67.86$ $p<0.001$. Both membrane extracts and soluble fractions were probed by anti-sAPPβ (18957, IBL) and anti-β-CTF (Y188, Abcam) antibodies. APP-/- mice was used to antibody validation. (D) Quantitative analysis of the signal intensity of sAPPβ and β-CTF. One-way ANOVA, sAPPβ: $F(2,9)=44,62$ $p<0.001$, APP β-CTF: $F(2,9)=44.05$ $p<0.001$. Bonferroni's test was used for post-hoc analysis. $p<0.05$(*), $p<0.001$(***). Error bars represent S.E.M.

2. BACE1 inhibition affects dendritic spine plasticity via SEZ6

2.1. Effect of BACE1 inhibition in *Sez6*$^{-/-}$ mice

Previously, Filser and colleagues demonstrated that strong BACE1 inhibition by two structurally different inhibitors, SCH1682496 (Merck & Co) and LY2811376 (Eli Lilly and Company), impairs dendritic spine plasticity (Filser et al., 2015). Here, we verified whether NB-360 has similar impacts on spine plasticity. Using chronic *in vivo* two-photon microscopy, we imaged layer I dendritic tufts of cortical layer V pyramidal neurons in inhibitor treated WT control (*Sez6*$^{+/+}$*:GFP-M*) mice (Figure 24A upper line). The mice were repeatedly imaged every 7 days. The first two timepoints were considered as baseline recordings, and then NB-360 was applied to mice from day 8 till day 28 (3 weeks) as highlighted in grey (Figure 24). We also recorded three more timepoints as post treatment recovery period. In line with previous data, NB-360 administration reduced total spine density in control mice (Figure 24B, upper filled circles). Then we set the total dendritic spine density of two pre-treatment time-points as 100% for each animal, and normalized the rest of timepoints in ordered to emphasize the effects of inhibitor treatment (Figure 24B, lower). Our data also showed that NB-360 reduced the density of the persistent spines (present for ≥ 7 days), as well as newly gained spines in control mice (Figure 24C-D). Shortly after withdrawing NB-360, the deficits were gradually recovered. Since all three different BACE1 inhibitors (SCH1682496, LY2811376 and NB-360) impair spine density, it is likely an on-target side effect.

As a protease, BACE1 most likely regulates dendritic spine plasticity via it substrates. *Sez6*$^{-/-}$ mice showed similar deficit as BACE1 inhibitor-treated mice, like reduced dendritic spine density and spatial memory deficit. Therefore, we hypothesized that BACE1-inhibition influences spine dynamic may via SEZ6 protein. To investigate this hypothesis, we applied NB-360 to *Sez6*$^{-/-}$*:GFP-M* mice and traced the spine density and dynamic as described in control mice (Figure 24A lower line). During base line condition, the dendritic spine density in *Sez6*$^{-/-}$*:GFP-M* mice were 15.9 ± 9.4% lower compared to control mice. In contrast to control mice, NB-360 did not affect total spine density in *Sez6*$^{-/-}$*:GFP-M* mice (Figure 24B, open circles). It is noteworthy that, NB-360 administration decreased the total dendritic spine density by 15.6 ± 8.9% in control mice, reaching a similar density as in *Sez6*$^{-/-}$*:GFP-M* mice (Figure 24B). The spine dynamic was also analyzed in *Sez6*$^{-/-}$*:GFP-M* mice. The results showed that the structural plasticity is not affected by BACE1 inhibitor treatment (Figure 24C-E). In summary, NB-360 alters spine density and plasticity in control mice but not in *Sez6*$^{-/-}$*:GFP-M* mice, suggesting BACE1 mediated shedding of SEZ6 plays an important role in maintaining dendritic spine density under physiological conditions.

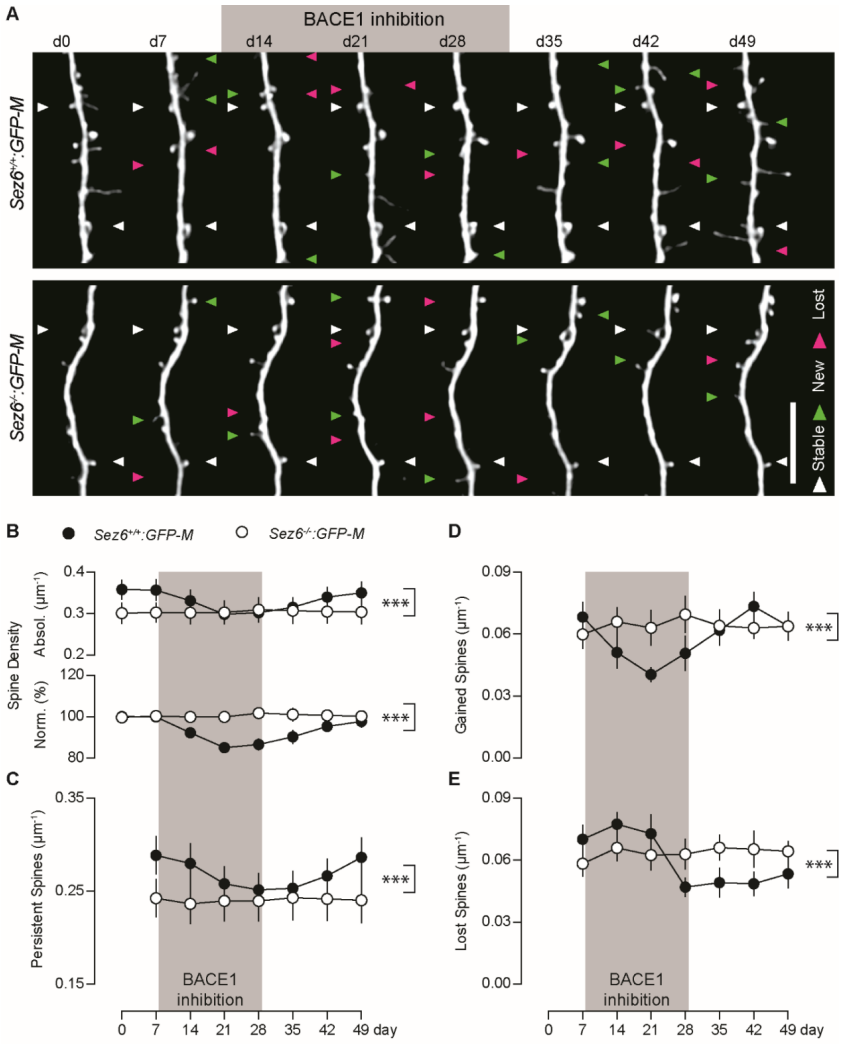

Figure 24: NB-360 alters dendritic spine plasticity via SEZ6

(A) Images of apical dendrites of layer 5 neurons in layer 1 cerebral cortex. These apical dendrites were labelled by eGFP. The same dendrites were imaged every 7 days using in vivo 2-photon microscopy. BACE1 inhibitor (NB-360) treatment was applied from day 8 till day 29. The treatment period is highlighted in gray. Vehicle was given to mice before and after NB-360 treatment period. Persistent spines (present ≥ 7 days): white arrowheads. Gained spines: green arrowheads. Lost spines: red arrowheads. Scale bar: 10µm. (B-E) Quantitative analysis of the denticity of total spine (B), persistent spines (C), gained spines (D) lost spines (E) from *Sez6$^{+/+}$:GFP-M* and *Sez6$^{-/-}$:GFP-M* mice. (B Top) Absolut value, Two-way ANOVA $F(7,77)=15.16$, interaction $p<0.001$. (B Bottom) The normalized value relative to the average of the first two times points. Two-way ANOVA $F(7,77)=12.28$, interaction $p<0.001$. (C) Two-way ANOVA $F(6,66)=13.75$, interaction $p<0.001$. (D) Two-way ANOVA $F(6,66)=4.75$, interaction $p<0.001$. (E) Two-way ANOVA $F(6,66)=6.74$, interaction $p<0.001$. Animals per group: n=6-7. $p<0.001$(***). Error bars represent S.E.M.

2.2. Effect of BACE1 inhibition in *Sez6*$^{cKO/cKO}$ mice

We have demonstrated that knockout *Sez6* at adult stage impairs dendritic spine density. The protein levels of both BACE1 and SEZ6 are highest during early postnatal period in mice (Kim et al., 2002; Osaki et al., 2011; Willem et al., 2006). This indicates that they have important function for neuronal development. Then we wonder whether NB-360 does not influence dendritic spine density and plasticity in *Sez6*$^{-/-}$ mice is due to developmental deficit or compensate effect occurred during development stage. To investigate this hypothesis, we again employed the *Sez6*$^{cKO/cKO}$*:SlickV* mice. In this experiment, Tamoxifen was applied to 3-month-old mice for 5 consecutive days. Then, 9 days was given to mice for recovery (as highlighted in purple) (Figure 25). Same method was performed to *Sez6*$^{cKO/cKO}$*:SlickV* mice which is repeatedly imaging the layer I dendritic tufts of cortical layer V pyramidal neurons (Figure 25A). *Sez6*$^{LoxP/LoxP}$*:SlickV* mice, which is without Tamoxifen treatment, served as control. After baseline recordings, NB-360 was applied to mice from day 8 till day 28 (3 weeks) as highlighted in grey (Figure 25), follow by recording of post treatment recovery period.

Similar to GFP-M mice, BACE1 inhibitor administration impaired total spine density in control (*Sez6*$^{LoxP/LoxP}$*:SlickV*) mice (Figure 25B, upper, filled circles). Then we set the total dendritic spine density of two pre-treatment time-points as 100% for each mouse, and normalized the rest of timepoints in order to emphasize the effects of inhibitor treatment (Figure 25B, lower, filled circles). NB-360 also affected spine dynamic, like reducing the density of the persistent spines (present for ≥ 7 days) (Figure 25C filled circles) and newly

gained spines (Figure 25D), as well as increasing lost spines (Figure 25E filled circles). Shortly after withdrawal NB-360, the deficits were gradually recovered. Similar as *Sez6*$^{-/-}$ mice, BACE1 inhibition did not alter total spine density and spine dynamic (fraction of persistent, new gained and lost spines) in *Sez6*^{cKO} neurons (Figure 25B-E, open circles). Since *SlickV* mice have a very sparse and weak eYFP labeling, the total number of analyzed dendrites is lower compared to GFP-M mice (2-6 vs 8-10, respectively), resulting a high statistical variation. Therefore, a trend of reduced fraction of new gained spines did not reach statistical significance (p=0.19). Nevertheless, NB-360 treatment impairs the impaired total spine density and dynamic in both control mice (*Sez6*$^{+/+}$*:GFP-M* and *Sez6*$^{LoxP/LoxP}$*:SlickV*). NB-360 treatment does not alter spine density and dynamic in both constitutive and conditional *Sez6* knockout mice (*Sez6*$^{-/-}$*:GFP-M* and *Sez6*$^{cKO/cKO}$*:SlickV*). These data further support the hypothesis that SEZ6 mediates BACE1-inhibition-induced spine alterations.

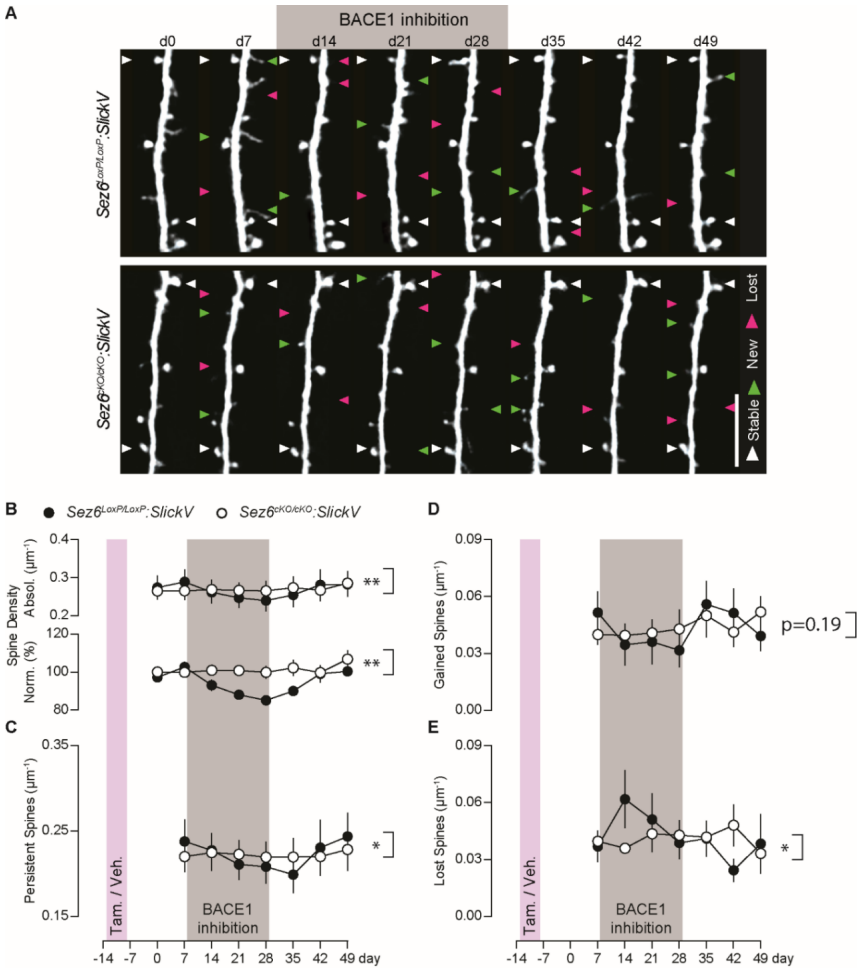

Figure 25: NB-360 does not alter dendritic spine plasticity in Sez6$^{cKO/cKO}$ neurons

(A) Images of apical dendrites of layer 5 neurons in layer 1 cerebral cortex. These apical dendrites were labeled by eYFP. The same dendrites were imaged every 7 days using in vivo 2-photon microscopy. Tamoxifen was applied to *Sez6$^{LoxP/LoxP}$:SlickV* and *Sez6$^{cKO/cKO}$:SlickV* mice from day -12 till day -8. Tamoxifen treatment period is highlighted in purple. BACE1 inhibitor (NB-360) treatment was applied from day 8 till day 29. NB-360 treatment period is highlighted in gray. Vehicle was given to mice before and after NB-360 treatment period. Persistent spines (present ≥ 7 days): white arrowheads. Gained spines: green arrowheads. Lost spines: red arrowheads. Scale bar: 10µm. (B-E) Quantitative analysis of the denticity of total spine (B), persistent spines (C), gained spines (D) lost spines (E) from *Sez6$^{LoxP/LoxP}$:SlickV* and *Sez6$^{cKO/cKO}$:SlickV* mice. (B Top) Absolut value, Two-way ANOVA $F(7,70)=3.58$, interaction $p<0.01$. (B Bottom) The normalized value relative to the average of the first two times points. Two-way ANOVA $F(7,63)=4.16$, interaction $p<0.01$. (C) Two-way ANOVA $F(6,60)=2.71$, interaction $p<0.05$. (D) Two-way ANOVA $F(6,60)=1.52$, interaction $p=0.19$. (E) Two-way ANOVA $F(6,60)=2.73$, interaction $p<0.05$. Animals per group: n=6. $p<0.05$(*), $p<0.01$(**). Error bars represent S.E.M.

3. Chronic application of NB-360 does not alter synaptic plasticity *Sez6*$^{-/-}$ mice

Structural alterations of synapses are usually considered as an indicator for functional changes. We have demonstrated that NB-360 interferes spine plasticity via SEZ6. To investigate whether NB-360 impairs synaptic plasticity and whether it involves SEZ6 too, the WT mice (C57BL/6J) and *Sez6*$^{-/-}$ mice were applied with NB-360 or vehicle for 3 weeks. At the last day of treatment, the mice were sacrificed, their brains were harvest and acutely sliced in 350 μm thick hippocampal slices for field recordings. The synaptic plasticity was test in hippocampus Schaffer collateral - CA1 pathway. After 20 min of baseline recordings, high frequency stimulation (HFS; 100 pulses/s) was used to induce hippocampal long-term potentiation (LTP) in *Sez6*$^{-/-}$ mice and WT mice, followed by 60 min of continuous recording (Figure 26 A-B). HFS caused a notable post-tetanic potentiation in vehicle-treated WT mice. We also showed that NB-360 impairs LTP in WT mice (Figure 26C). Although the LTP is low in the CA1 synapse of *Sez6*$^{-/-}$ mice, NB-360 treatment did not alter LTP (Figure 26C). Our results suggest that BACE1 inhibition induces synaptic plasticity deficits might involve SEZ6.

Additionally, we investigated whether NB-360 induced LTP impairment is due to pre-synaptic mechanisms. The pre-synaptic terminal is relatively normal in *Sez6*$^{-/-}$ mice, however BACE1 is enriched in pre-synaptic terminals. If NB-360 would induce pre-synaptic alteration, it might be evidence which against SEZ6 involve in BACE1 inhibition induces synaptic plasticity deficits. To test this hypothesis, we monitored paired-pulse facilitation (PPF) at Schaffer collateral - CA1 synapses using two different inter-stimulus

intervals (ISIs), 35 ms and 50 ms. The results show that NB-360 treatment did not affect PPF in either WT or *Sez6*$^{-/-}$ mice (Figure 26D). Our findings showed that there is no obvious pre-synaptic alteration, implying that the LTP changes are most likely due to post-synaptic alterations.

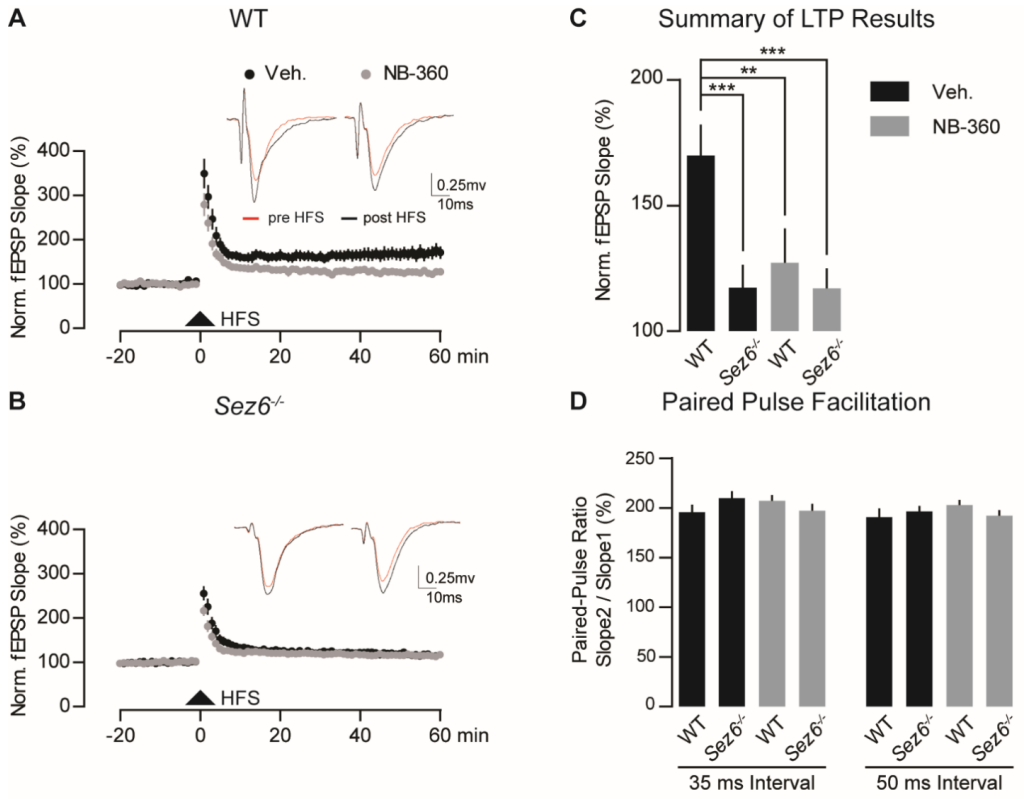

Figure 26: NB-360 does not alter LTP in *Sez6*$^{-/-}$ mice

(A) the LTP in WT brain slices was impaired by chronic treatment of NB-360. (B) Same treatment does influence LTP in *Sez6*$^{-/-}$ brain slices. Representative traces of evoked is shown respectively. Schaffer collaterals-CA1 pathway was tetanized using high-frequency stimulation (HFS). red lines: fEPSP before stimulation; black lines: fEPSP after stimulation. (C) Quantitative analysis of the LTP magnitudes which is averaged from 50 - 60 min. Two-way ANOVA $F(1,24)=9.57$, interaction $p<0.01$. Bonferroni's post hoc test: $p<0.01$**, $p<0.001$***). Animals per group: n=7. (D) The paired-pulse facilitation was analyzed using 2 different intervals (35ms and 50ms) in NB-360 or vehicle treated WT and Sez6-/- mice. 35 ms: Two-way ANOVA $F(1,23)=3.753$, interaction $p=0.07$. 50 ms: Two-way ANOVA $F(1,23)=1.917$, interaction $p=0.18$. Animals per group: n=5-8. Error bars represent S.E.M.

DISCUSSION

1. SEZ6 regulates dendritic spine density and plasticity

Previous studies show that SEZ6 involves in many neuronal activities, including regulation of neurite development, dendritic spine density (Gunnersen et al., 2007). SEZ6 is also proposed to be involved in the etiology of several neurodevelopmental disorders (Ambalavanan et al., 2016; Gilissen et al., 2014; Mulley et al., 2011; Yu et al., 2007). Here we confirmed that the dendritic spine density is decreased in conventional *Sez6* knockout (*Sez6*$^{-/-}$) mice. Then we show that SEZ6 regulates spine density in a dose depend manner, it means that the expression level is critical for the function of SEZ6. It also indicates that the proteinase (BACE1) which regulating the cell surface level of SEZ6, might influence spine density or dynamic via SEZ6 (Munro et al., 2016; Pigoni et al., 2016).

Sez6$^{-/-}$ mice show alterations in neurite branching during the development. Moreover, *Sez6* knockdown in neurons caused altered calcium activity (Anderson et al., 2012; Gunnersen et al., 2007). The SEZ6 expression level is high during early postnatal stage (Kim et al., 2002; Osaki et al., 2011). To rule out developmental deficits, we used conditional knockout (*Sez6*$^{cKO/cKO}$) mice, in which *Sez6* gene deletion occurred only in the small subset of eYFP/CreERT2 positive neurons in adulthood. In these neurons, dendritic spine density is reduced similar to the situation in constitutive *Sez6*$^{-/-}$ neurons, indicating that SEZ6 is not only critical for neuronal development but also important for maintaining

the normal dendritic spine density in adult mice. In *Sez6*$^{cKO/cKO}$ mice, the spine density reduction in cortical neuron was smaller than that seen in *Sez6*$^{-/-}$ mice, which may be attributed to a general increase of the dendritic spine stability in adulthood (Grutzendler et al., 2002; Zuo et al., 2005). Using *Sez6*$^{cKO/cKO}$ mice, we can further pinpoint which SEZ6 proteolytic fragments are involved. As mention before, SEZ6 is cut by BACE1, and the sSEZ6 is secreted to extracellular matrix. In *Sez6*$^{cKO/cKO}$ mice, the small subset eYFP positive *Sez6*^{cKO} neurons lack cell-autonomous Sez6. These neurons were exposed to a relatively normal extracellular environment, since the proportion of *Sez6*^{cKO} neurons is really low (Young et al., 2008). The soluble Sez6 levels is normal in the surrounding neuropil. In this context, the sSEZ6 is not actively involved in dendritic spine density regulation. Since the SEZ6-CTF will be further processed by γ-secretase (Pigoni et al., 2016), it is not yet clear whether flSEZ6 or SEZ6-ICD is the critical player of regulating dendritic spine density.

We classified the dendritic protrusions base on their morphology (Figure 27) (Risher et al., 2014). The difference in spine shape may represent the different maturation states (Berry and Nedivi, 2017). Mushroom shaped spines and thin spines have similar shape. Both of them have large bulbous head, but Mushroom spines have relative narrow neck and thin spines have a long neck. Stubby spines are lack a distinctive head and neck configuration. Filopodia are the smallest hair-like structures protruding from dendrites, often described as immature spines (Berry and Nedivi, 2017). However, whether spines with different sizes serve distinct functions is not yet clear. In *Sez6*$^{-/-}$ mice, the densities

of stubby, thin and mushroom spines decrease. However, filopodia do not show changes. It might be indicated that the maturation of new spines is not impaired.

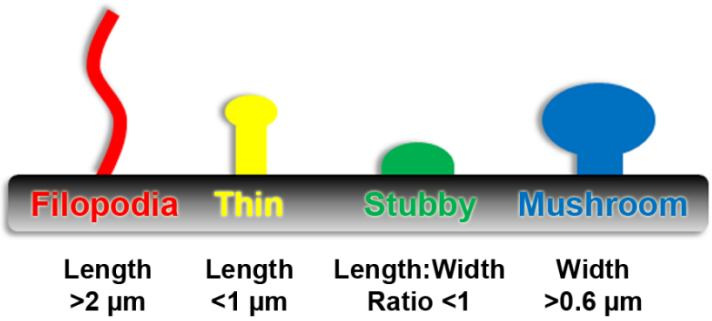

Figure 27: Schematic diagram of spine morphological categories

Base on their morphology, dendritic protrusions has been group into 4 types. Mushroom shaped spine has a large bulbous head and a relative narrow neck. Thin spines have similar shape, but smaller head and long neck. Stubby spine is lack of a distinctive head and neck. Filopodia are the thinnest hair-like structures (Risher et al., 2014).

Then we tested whether SEZ6 involved into regulating spine plasticity. It is also known as structural plasticity which is the consequence of structural changes in the number and shape of dendritic spines (Fu and Zuo, 2011). New spine formation is the structural base of memory consolidation (van der Zee, 2015) and reduced spine density is commonly seen in neurodegenerative diseases (Berry and Nedivi, 2017; Bittner et al., 2012; Hoffmann et al., 2013; Zou et al., 2016). To our surprised in standard housing condition, the fractions of new gained and lost spines do not show any changes compared to WT control. Then the enriched environmental (EE) condition was applied to *Sez6*$^{-/-}$ mice. EE

is an experimental setting in which is housing in an environment with complex of cognitive, motor and social stimulation. It is commonly used to boost dendritic spine turnover. Some spine density reduction and synaptic functional deficits were about to be recused by EE (Morelli et al., 2014). Consistent with our previous finding, the dendritic spine density increased in control mice shortly after entering EE cages (Jung and Herms, 2014). Since the expression of SEZ6 is highly dependent on the neuronal activity and *Sez6* mRNA level significantly increased in neuronal cortex and naïve mouse after EE (Anderson et al., 2012; Rampon et al., 2000), indicating that any activity induced alteration might affected. Indeed, *Sez6*$^{-/-}$ mice started to show impaired dendritic spine plasticity in EE condition which is the spine density and new gained spine do not increase as control mice.

Dendritic spines are the excitatory postsynaptic compartments, which receive and integrate information from pre-synaptic inputs (Yuste and Bonhoeffer, 2001). To correlate the intravital microscopic findings with electrophysiological functional properties, we performed hippocampal field recordings using age-matched WT and *Sez6*$^{-/-}$ mice, as well as EE stimulated *Sez6*$^{-/-}$ mice and controls. We tested the Schaffer collateral-CA1 pathway. Since SEZ6 is mainly located in the somatodendritic compartment of neurons, which is in line with our findings that pre-synaptic function was not affected by the lack of SEZ6. But *Sez6*$^{-/-}$ mice showed impaired synaptic transmission, which might be the consequence of reduced dendritic spine density. Deceased LTP is also shown in *Sez6*$^{-/-}$ mice, which is consistent with defects in hippocampus-dependent memory (Gunnersen et al., 2007). EE improves a variety of hippocampal-dependent functions compared to

standard housing. We observed that LTP is significantly increased in WT control mice, but not in *Sez6*$^{-/-}$ mice after EE stimulation. Since hippocampal dendrites undergo spinogenesis after LTP induction (Nägerl et al., 2004, 2007), the observed LTP deficit in *Sez6*$^{-/-}$ mice may due to an impaired activity dependent dendritic spine plasticity. In addition, SEZ6 involves into neuronal activity in an NMDA-receptor dependent manner (Havik et al., 2007; Shimizu-Nishikawa et al., 1995a), which may also explain that SEZ6 is functionally involved in LTP maintenance.

In summary, we provide several new insights into the physiological roles of SEZ6 in the adult brain in this study. 1) we showed that SEZ6 involved into regulating dendritic spine density in a dose dependent manner; 2) SEZ6 involved into regulating the maturation of new spines; 3) SEZ6 involved into regulating synaptic functional plasticity; 4) SEZ6 involved in regulating dendritic spine plasticity in complex stimulation condition.

2. BACE1 inhibition impairs synaptic structure and function via SEZ6

As the most common form of senile dementia, AD is a significant challenge to healthcare systems worldwide. Currently, the promising potential therapeutic strategies are: 1) prevention of Aβ production by inhibiting or modulating the amyloid cascade enzymes, BACE1 and γ-secretase complex with small molecules (Huang and Mucke, 2012; Neumann et al., 2015; Yuan et al., 2013); 2) enhancing clearance of Aβ or amyloid plaques by immunotherapies (Doody et al., 2014; Salloway et al., 2014); 3) prevention of Aβ aggregation (Ryan et al., 2015). Unfortunately, the outcomes of γ-secretase inhibitor trials were disappointing because too many important signaling cascades, including

Notch signaling, are affected by chronic inhibition of the γ-secretase complex (Bittner et al., 2009; De Strooper, 2014). Immunotherapy studies have shown only marginal disease modification, although it has been reported that Aβ antibody treatment benefits a subset of patients in the early stages of disease progression (Reardon, 2015). BACE1 is another very attractive therapeutic target, mainly because 1) it initiates the amyloidogenic cascade (Lin et al., 2000), 2) *Bace1* knockout mice are viable and fertile (Cai et al., 2001), 3) the pathological hallmarks of AD, such as high Aβ load, plaque deposition and electrophysiological dysfunction, are largely prevented in BACE1 null APP transgenic mice (Luo et al., 2001; Ohno et al., 2004), and 4) BACE1 activity can be blocked by small molecules (May et al., 2011; Neumann et al., 2015; Stamford et al., 2012). Several BACE1 inhibitors are currently in AD clinical trials (Godyń et al., 2016; May et al., 2011). However, BACE1 inhibition interferes structural and functional synaptic plasticity in mice (Filser et al., 2015). This may be due to inhibition of BACE1 processing of several its physiological substrates, which would then lead to on-target side effects.

Although BACE1 has many substrates, We hypothesized that BACE1-inhibition-induced structural and functional synaptic alterations could be due to disruption of the SEZ6 function for the following reasons: SEZ6 is predominantly processed by BACE1 (Kuhn et al., 2012) and *Sez6* null mice display certain similar deficits compared to BACE1 inhibited (Filser et al., 2015) or knockout mice (Laird et al., 2005), including reduced cortical neuron dendritic spine density and diminished performance in hippocampal-dependent behavioral tests (Gunnersen et al., 2007).

We used chronic intravital microscopy and electrophysiological field recordings to study NB-360 treated WT and *Sez6* knockout mice. NB-360 blocked BACE1 activity almost completely, similar to the effects of high-doses of BACE1 inhibitors SCH1682496 and LY2811376 (Filser et al., 2015; May et al., 2011; Stamford et al., 2012). We also observed that NB-360 interfered with structural and functional synaptic plasticity in WT mice. Since three structurally different BACE1 inhibitors (NB-360, SCH1682496 and LY2811376) influenced dendritic spine plasticity and hippocampal LTP in a similar way, off-target effects are rather unlikely (Filser et al., 2015; Killick et al., 2015). Unlike in WT mice, both dendritic spine density and plasticity were not affected by chronic NB-360 treatment suggesting that SEZ6 is involved in BACE1-inhibition-induced spine alterations. However, *Sez6*$^{-/-}$ mice show developmental deficits like neurite branching alterations during development and *Sez6* knockdown neurons show altered calcium activity (Anderson et al., 2012; Gunnersen et al., 2007). To rule out developmental deficits, we applied NB-360 to conditional knockout (*Sez6*$^{cKO/cKO}$) mice. NB-360 treatment did not alter dendritic spine plasticity in *Sez6*^{cKO} neurons. Thus, we conclude that cell autonomous membrane-bound SEZ6 protein contributes to this structural synaptic alteration. Taken together, these data indicate that BACE1-inhibition-induced structural plasticity is via SEZ6.

BACE1 is a negative regulator of SEZ6 cell surface level (Pigoni et al., 2016). The detail mechanism of accumulated SEZ6 affects dendritic spine density and plasticity is not yet clear. SEZ6 contains 7 protein-protein interaction domains: 5 short consensus repeat (SCR) domains and 2 complement subcomponent C1r, C1s/sea urchin embryonic growth factor Uegf/bone morphogenetic protein 1 (CUB) domains (Gunnersen et al., 2007). Both

of SCR and CUB domains are considered to associate with complement proteins (Bork and Beckmann, 1993; Mizukami et al., 2016). It is known that complement signal cascaded is an important inducer for synaptic pruning in both physiological condition and AD cases (151-153). Full-length SEZ6 accumulated at the cell membrane of post-synaptic compartment upon BACE1 inhibition (Gunnersen et al., 2007; Zhu et al., 2018). It is interesting to study whether accumulated SEZ6 would induce synaptic pruning by recruiting complement protein to synapses.

Dendritic spines are the excitatory postsynaptic compartments, which receive and integrate information from pre-synaptic inputs (Yuste and Bonhoeffer, 2001). In order to correlate the intravital microscopic findings with electrophysiological functional properties, we performed hippocampal field recordings using brain slices from 3-week NB-360 treated age-matched WT and *Sez6*$^{-/-}$ mice, as well as vehicle treated controls. *Sez6*$^{-/-}$ mice showed impaired Schaffer collateral-CA1 LTP, which is consistent with previous data. Chronic BACE1 inhibition does not attenuate this further, indicating that SEZ6 is involved in BACE1-inhibition-induced reduction in synaptic plasticity. Since hippocampal dendrites undergo spinogenesis after LTP induction (Nägerl et al., 2004, 2007), the observed LTP attenuation may be due to an impaired dendritic spine plasticity, consistent with the overall decrease in spine density, smaller EPSCs seen in *Sez6*$^{-/-}$ mice (Gunnersen et al., 2007) and the reduced spine density observed in BACE1 inhibitor-treated WT mice. In addition, *Sez6* mRNA levels are increased after strong neuronal activity (Shimizu-Nishikawa et al., 1995a) and this was shown to occur in an NMDA-receptor dependent manner (Havik et al., 2007), which may imply that SEZ6 is

functionally involved in LTP maintenance. SEZ6 is mainly located in the dendritic and somatic compartment of neurons (Gunnersen et al., 2007), which is in line with our findings that pre-synaptic function was not affected by the lack of SEZ6. Surprisingly, pre-synaptic deficits were not observed in NB-360 treated WT mice, although BACE1 accumulates in pre-synaptic terminals (Hitt et al., 2012; Kandalepas et al., 2013) and *Bace1* knockout mouse neurons display a severe pre-synaptic dysfunction at the mossy fiber terminals (Wang et al., 2008, 2014). This may due to differences in the developmental trajectory of gene knockout-induced phenotypes compared to inhibitor treatment of adult mice and/or due to the different brain regions studied.

Other indirect consequences of BACE1 inhibition on synaptic plasticity have to be considered. Willem and colleagues reported a novel APP cleavage pathway, which involved MT-MMP to generate Aη-α/β. After BACE1 inhibition, the Aη-α significantly elevated due to more MT-MMP cleavage products go through the anti-amyloidogenic pathway. By acutely applying Aη-α in bath they observed a significant attenuation of hippocampal LTP, as well as reduced neuronal activity (Willem et al., 2015). However, another APP metabolites soluble APP alpha (sAPPα) also accumulates upon BACE1 inhibition (Fukumoto et al., 2010; Neumann et al., 2015), sAPPα has considerable neuroprotective and neurotrophic functions, including rescuing LTP deficits in the AD mouse (Fol et al., 2015). The precise mechanism of how sAPPα and Aη-α influences synaptic plasticity is not yet clear. Further studies are needed to clarify how APP cleavage products affect functional synaptic plasticity in physiological levels, and under pharmacological BACE1 inhibition.

BACE1 inhibitors prevent amyloid plaque formation AD models which strongly support the notion that BACE1 inhibitor treatments can be considered as a promising therapeutic approach for AD. But synaptic deficits which are observed upon strong BACE1 inhibition in WT mice may limit the usage of BACE1 inhibitors as a therapeutic approach for AD. It does not mean that we need to move on from BACE1 inhibition treatment. BACE1 inhibition induced synaptic deficits are only observed in condition of strongly suppressed the BACE1 proteolytic activity (Filser et al., 2015; Savonenko et al., 2008; Wang et al., 2014). Therefore, identifying the optimal dosage, which could balance BACE1 inhibition, induced synaptic deficits and Aβ induced impairments, is urgent. Establishing a reliable and appropriate method such identifying a few reliable biomarkers might be the most feasible approach. BACE1 CSF levels has been showed strong correlations to Aβ level, and it has been considered as biomarker for AD (Ewers et al., 2008, 2011; Holsinger et al., 2004; Pera et al., 2013; Shen et al., 2017; Timmers et al., 2017). But it may not represent whether the fundamental synaptic function is impaired by inhibitor treatment.

Ore data suggested that the optimal dosing in order to avoid synaptic side effects could be potentially achieved by monitoring the levels of SEZ6 cleavage products in the CSF on an individual basis, because 1) BACE1 derived SEZ6 cleavage products can be measured in body fluids (Khoonsari et al., 2016; Maccarrone et al., 2013; Pigoni et al., 2016), 2) SEZ6 is closely related to the structure and function of synapses and 3) BACE1-inhibition induced synaptic impairment is via altered process of SEZ6. Future studies are expected to provide more knowledge regarding the biological functions of BACE1 and safety of BACE1 inhibition approach in mouse models and AD patients.

Bibliography

Ambalavanan, A., Girard, S.L., Ahn, K., Zhou, S., Dionne-Laporte, A., Spiegelman, D., Bourassa, C. V, Gauthier, J., Hamdan, F.F., Xiong, L., et al. (2016). De novo variants in sporadic cases of childhood onset schizophrenia. Eur. J. Hum. Genet. *24*, 944–948.

Anderson, G.R., Galfin, T., Xu, W., Aoto, J., Malenka, R.C., and Südhof, T.C. (2012). Candidate autism gene screen identifies critical role for cell-adhesion molecule CASPR2 in dendritic arborization and spine development. Proc. Natl. Acad. Sci. U. S. A. *109*, 18120–18125.

Barão, S., Gärtner, A., Leyva-Díaz, E., Demyanenko, G., Munck, S., Vanhoutvin, T., Zhou, L., Schachner, M., López-Bendito, G., Maness, P.F., et al. (2015). Antagonistic Effects of BACE1 and APH1B-γ-Secretase Control Axonal Guidance by Regulating Growth Cone Collapse. Cell Rep. *12*, 1367–1376.

Barnea, A., and Nottebohm, F. (1994). Seasonal recruitment of hippocampal neurons in adult free-ranging black-capped chickadees. Proc. Natl. Acad. Sci. U. S. A. *91*, 11217–11221.

Berry, K.P., and Nedivi, E. (2017). Spine Dynamics: Are They All the Same? Neuron *96*, 43–55.

Bialas, A.R., and Stevens, B. (2013). TGF-β signaling regulates neuronal C1q expression and developmental synaptic refinement. Nat. Neurosci. *16*, 1773–1782.

Bittner, T., Fuhrmann, M., Burgold, S., Jung, C.K., Volbracht, C., Steiner, H., Mitteregger, G., Kretzschmar, H.A., Haass, C., and Herms, J. (2009). Gamma-secretase inhibition reduces spine density in vivo via an amyloid precursor protein-dependent pathway. J Neurosci *29*, 10405–10409.

Bittner, T., Burgold, S., Dorostkar, M.M., Fuhrmann, M., Wegenast-Braun, B.M., Schmidt, B., Kretzschmar, H., and Herms, J. (2012). Amyloid plaque formation precedes dendritic spine loss. Acta Neuropathol *124*, 797–807.

Blazquez-Llorca, L., Valero-Freitag, S., Rodrigues, E.F., Merchán-Pérez, Á., Rodríguez, J.R., Dorostkar, M.M., DeFelipe, J., and Herms, J. (2017). High plasticity of axonal pathology in Alzheimer's disease mouse models. Acta Neuropathol. Commun. *5*, 14.

Bork, P., and Beckmann, G. (1993). The CUB domain. A widespread module in developmentally regulated proteins. J. Mol. Biol. *231*, 539–545.

Buggia-Prévot, V., Fernandez, C.G., Riordan, S., Vetrivel, K.S., Roseman, J., Waters, J., Bindokas, V.P., Vassar, R., and Thinakaran, G. (2014). Axonal BACE1 dynamics and targeting in hippocampal neurons: a role for Rab11 GTPase. Mol. Neurodegener. *9*, 1.

Cai, H., Wang, Y., McCarthy, D., Wen, H., Borchelt, D.R., Price, D.L., and Wong, P.C. (2001). BACE1 is the major beta-secretase for generation of Abeta peptides by neurons. Nat. Neurosci. *4*, 233–234.

Cao, L., Rickenbacher, G.T., Rodriguez, S., Moulia, T.W., and Albers, M.W. (2012). The precision of axon targeting of mouse olfactory sensory neurons requires the BACE1 protease. Sci. Rep. *2*, 231.

Carrodus, N.L., Teng, K.S.-L., Munro, K.M., Kennedy, M.J., and Gunnersen, J.M. (2014). Differential labeling of cell-surface and internalized proteins after antibody feeding of live cultured neurons. J. Vis. Exp. e51139.

Caselli, R.J., Beach, T.G., Yaari, R., and Reiman, E.M. (2006). Alzheimer's disease a century later. J. Clin. Psychiatry *67*, 1784–1800.

Cheret, C., Willem, M., Fricker, F.R., Wende, H., Wulf-Goldenberg, A., Tahirovic, S., Nave, K.-A., Saftig, P., Haass, C., Garratt, A.N., et al. (2013). Bace1 and Neuregulin-1 cooperate to control formation and maintenance of muscle spindles. EMBO J. *32*, 2015–2028.

Chong, S.A., Benilova, I., Shaban, H., De Strooper, B., Devijver, H., Moechars, D., Eberle, W., Bartic, C., Van Leuven, F., and Callewaert, G. (2011). Synaptic dysfunction in hippocampus of transgenic mouse models of Alzheimer's disease: A multi-electrode array study. Neurobiol. Dis. *44*, 284–291.

Cui, M., Yang, Y., Yang, J., Zhang, J., Han, H., Ma, W., Li, H., Mao, R., Xu, L., Hao, W., et al. (2006). Enriched environment experience overcomes the memory deficits and depressive-like behavior induced by early life stress. Neurosci. Lett. *404*, 208–212.

Das, U., Wang, L., Ganguly, A., Saikia, J.M., Wagner, S.L., Koo, E.H., and Roy, S. (2016). Visualizing APP and BACE-1 approximation in neurons yields insight into the amyloidogenic pathway. Nat. Neurosci. *19*, 55–64.

Davis, K.E., Fox, S., and Gigg, J. (2014). Increased hippocampal excitability in the 3xTgAD mouse model for Alzheimer's disease in vivo. PLoS One *9*, e91203.

Devi, L., and Ohno, M. (2015). Effects of BACE1 haploinsufficiency on APP processing and Aβ concentrations in male and female 5XFAD Alzheimer mice at different disease stages. Neuroscience *307*, 128–137.

Dislich, B., Wohlrab, F., Bachhuber, T., Müller, S.A., Kuhn, P.-H., Hogl, S., Meyer-Luehmann, M., and Lichtenthaler, S.F. (2015). Label-free Quantitative Proteomics of Mouse Cerebrospinal Fluid Detects β-Site APP Cleaving Enzyme (BACE1) Protease Substrates In Vivo. Mol. Cell. Proteomics *14*, 2550–2563.

Dominguez, D., Tournoy, J., Hartmann, D., Huth, T., Cryns, K., Deforce, S., Serneels, L., Camacho, I.E., Marjaux, E., Craessaerts, K., et al. (2005). Phenotypic and biochemical analyses of BACE1- and BACE2-deficient mice. J. Biol. Chem. *280*, 30797–30806.

Doody, R.S., Thomas, R.G., Farlow, M., Iwatsubo, T., Vellas, B., Joffe, S., Kieburtz, K., Raman, R., Sun, X., Aisen, P.S., et al. (2014). Phase 3 trials of solanezumab for mild-to-moderate Alzheimer's disease. N. Engl. J. Med. *370*, 311–321.

Dorostkar, M.M., Burgold, S., Filser, S., Barghorn, S., Schmidt, B., Anumala, U.R., Hillen, H., Klein, C., and Herms, J. (2014). Immunotherapy alleviates amyloid-associated synaptic pathology in an Alzheimer's disease mouse model. Brain *137*, 3319–3326.

Durham, T.B., and Shepherd, T.A. (2006). Progress toward the discovery and development of efficacious BACE inhibitors. Curr. Opin. Drug Discov. Devel. *9*, 776–791.

Ewers, M., Zhong, Z., Bürger, K., Wallin, A., Blennow, K., Teipel, S.J., Shen, Y., and Hampel, H. (2008). Increased CSF-BACE 1 activity is associated with ApoE-

epsilon 4 genotype in subjects with mild cognitive impairment and Alzheimer's disease. Brain *131*, 1252–1258.
Ewers, M., Cheng, X., Zhong, Z., Nural, H.F., Walsh, C., Meindl, T., Teipel, S.J., Buerger, K., He, P., Shen, Y., et al. (2011). Increased CSF-BACE1 activity associated with decreased hippocampus volume in Alzheimer's disease. J. Alzheimers. Dis. *25*, 373–381.
Feil, S., Valtcheva, N., and Feil, R. (2009). Inducible Cre mice. Methods Mol. Biol. *530*, 343–363.
Feng, G., Mellor, R.H., Bernstein, M., Keller-Peck, C., Nguyen, Q.T., Wallace, M., Nerbonne, J.M., Lichtman, J.W., and Sanes, J.R. (2000). Imaging Neuronal Subsets in Transgenic Mice Expressing Multiple Spectral Variants of GFP. Neuron *28*, 41–51.
Fiala, J.C., Feinberg, M., Popov, V., and Harris, K.M. (1998). Synaptogenesis via dendritic filopodia in developing hippocampal area CA1. J. Neurosci. *18*, 8900–8911.
Filser, S., Ovsepian, S. V., Masana, M., Blazquez-Llorca, L., Brandt Elvang, A., Volbracht, C., Müller, M.B., Jung, C.K.E., and Herms, J. (2015). Pharmacological inhibition of BACE1 impairs synaptic plasticity and cognitive functions. Biol. Psychiatry *77*, 729–739.
Fol, R., Braudeau, J., Ludewig, S., Abel, T., Weyer, S.W., Roederer, J.-P., Brod, F., Audrain, M., Bemelmans, A.-P., Buchholz, C.J., et al. (2015). Viral gene transfer of APPsα rescues synaptic failure in an Alzheimer's disease mouse model. Acta Neuropathol.
Fu, M., and Zuo, Y. (2011). Experience-dependent structural plasticity in the cortex. Trends Neurosci. *34*, 177–187.
Fuhrmann, M., Mitteregger, G., Kretzschmar, H., and Herms, J. (2007). Dendritic pathology in prion disease starts at the synaptic spine. J Neurosci *27*, 6224–6233.
Fukumoto, H., Takahashi, H., Tarui, N., Matsui, J., Tomita, T., Hirode, M., Sagayama, M., Maeda, R., Kawamoto, M., Hirai, K., et al. (2010). A noncompetitive BACE1 inhibitor TAK-070 ameliorates Abeta pathology and behavioral deficits in a mouse model of Alzheimer's disease. J. Neurosci. *30*, 11157–11166.
Furley, A.J., Morton, S.B., Manalo, D., Karagogeos, D., Dodd, J., and Jessell, T.M. (1990). The axonal glycoprotein TAG-1 is an immunoglobulin superfamily member with neurite outgrowth-promoting activity. Cell *61*, 157–170.
Gautam, V., D'Avanzo, C., Hebisch, M., Kovacs, D.M., and Kim, D. (2014). BACE1 activity regulates cell surface contactin-2 levels. Mol. Neurodegener. *9*, 4.
Gengler, S., Hamilton, A., and Hölscher, C. (2010). Synaptic Plasticity in the Hippocampus of a APP/PS1 Mouse Model of Alzheimer's Disease Is Impaired in Old but Not Young Mice. PLoS One *5*, 1–10.
Ghosh, A.K., and Osswald, H.L. (2014). BACE1 (β-secretase) inhibitors for the treatment of Alzheimer's disease. Chem. Soc. Rev. *43*, 6765–6813.
Gilissen, C., Hehir-Kwa, J.Y., Thung, D.T., van de Vorst, M., van Bon, B.W.M., Willemsen, M.H., Kwint, M., Janssen, I.M., Hoischen, A., Schenck, A., et al. (2014). Genome sequencing identifies major causes of severe intellectual disability. Nature *511*, 344–347.

Giusti-Rodríguez, P., Gao, J., Gräff, J., Rei, D., Soda, T., and Tsai, L.-H. (2011). Synaptic deficits are rescued in the p25/Cdk5 model of neurodegeneration by the reduction of β-secretase (BACE1). J. Neurosci. *31*, 15751–15756.

Globus, A., Rosenzweig, M.R., Bennett, E.L., and Diamond, M.C. (1973). Effects of differential experience on dendritic spine counts in rat cerebral cortex. J. Comp. Physiol. Psychol. *82*, 175–181.

Godyń, J., Jończyk, J., Panek, D., and Malawska, B. (2016). Therapeutic strategies for Alzheimer's disease in clinical trials. Pharmacol. Rep. *68*, 127–138.

Götz, J., Chen, F., van Dorpe, J., and Nitsch, R.M. (2001). Formation of neurofibrillary tangles in P301l tau transgenic mice induced by Abeta 42 fibrils. Science *293*, 1491–1495.

Grutzendler, J., Kasthuri, N., and Gan, W.-B. (2002). Long-term dendritic spine stability in the adult cortex. Nature *420*, 812–816.

Gunnersen, J.M., Kim, M.H., Fuller, S.J., De Silva, M., Britto, J.M., Hammond, V.E., Davies, P.J., Petrou, S., Faber, E.S.L., Sah, P., et al. (2007). Sez-6 proteins affect dendritic arborization patterns and excitability of cortical pyramidal neurons. Neuron *56*, 621–639.

Haass, C. (2004). Take five--BACE and the gamma-secretase quartet conduct Alzheimer's amyloid beta-peptide generation. EMBO J. *23*, 483–488.

Haass, C., Koo, E.H., Mellon, A., Hung, A.Y., and Selkoe, D.J. (1992). Targeting of cell-surface beta-amyloid precursor protein to lysosomes: alternative processing into amyloid-bearing fragments. Nature *357*, 500–503.

Haass, C., Hung, A.Y., Schlossmacher, M.G., Oltersdorf, T., Teplow, D.B., and Selkoe, D.J. (1993). Normal cellular processing of the beta-amyloid precursor protein results in the secretion of the amyloid beta peptide and related molecules. Ann. N. Y. Acad. Sci. *695*, 109–116.

Hardy, J., and Allsop, D. (1991). Amyloid deposition as the central event in the aetiology of Alzheimer's disease. Trends Pharmacol. Sci. *12*, 383–388.

Hardy, J., and Selkoe, D.J. (2002). The amyloid hypothesis of Alzheimer's disease: progress and problems on the road to therapeutics. Science (80-.). *297*, 353–356.

Harris, K.M., and Kater, S.B. (1994). Dendritic spines: cellular specializations imparting both stability and flexibility to synaptic function. Annu. Rev. Neurosci. *17*, 341–371.

Harris, K.M., Jensen, F.E., and Tsao, B. (1992). Three-dimensional structure of dendritic spines and synapses in rat hippocampus (CA1) at postnatal day 15 and adult ages: implications for the maturation of synaptic physiology and long-term potentiation. J. Neurosci. *12*, 2685–2705.

Havik, B., Rokke, H., Dagyte, G., Stavrum, A.-K.K., Bramham, C.R.R., Steen, V.M.M., Håvik, B., Røkke, H., Dagyte, G., Stavrum, A.-K.K., et al. (2007). Synaptic activity-induced global gene expression patterns in the dentate gyrus of adult behaving rats: induction of immunity-linked genes. Neuroscience *148*, 925–936.

Hayashi, Y., and Majewska, A.K. (2005). Dendritic spine geometry: functional implication and regulation. Neuron *46*, 529–532.

Herms, J., and Dorostkar, M.M. (2016). Dendritic Spine Pathology in Neurodegenerative Diseases. Annu. Rev. Pathol. *11*, 221–250.

Hitt, B., Riordan, S.M., Kukreja, L., Eimer, W. a., Rajapaksha, T.W., and Vassar, R. (2012). β-Site amyloid precursor protein (APP)-cleaving enzyme 1 (BACE1)-deficient mice exhibit a close homolog of L1 (CHL1) loss-of-function phenotype involving axon guidance defects. J. Biol. Chem. *287*, 38408–38425.

Hitt, B.D., Jaramillo, T.C., Chetkovich, D.M., and Vassar, R. (2010). BACE1-/- mice exhibit seizure activity that does not correlate with sodium channel level or axonal localization. Mol. Neurodegener. *5*, 31.

Hoffmann, N.A., Dorostkar, M.M., Blumenstock, S., Goedert, M., and Herms, J. (2013). Impaired plasticity of cortical dendritic spines in P301S tau transgenic mice. Acta Neuropathol Commun *1*, 82.

Holsinger, R.M.D., McLean, C.A., Collins, S.J., Masters, C.L., and Evin, G. (2004). Increased beta-Secretase activity in cerebrospinal fluid of Alzheimer's disease subjects. Ann. Neurol. *55*, 898–899.

Holtmaat, A., Bonhoeffer, T., Chow, D.K., Chuckowree, J., De Paola, V., Hofer, S.B., Hubener, M., Keck, T., Knott, G., Lee, W.C., et al. (2009). Long-term, high-resolution imaging in the mouse neocortex through a chronic cranial window. Nat Protoc *4*, 1128–1144.

Hong, L., Turner, R.T., Koelsch, G., Shin, D., Ghosh, A.K., and Tang, J. (2002). Crystal structure of memapsin 2 (beta-secretase) in complex with an inhibitor OM00-3. Biochemistry *41*, 10963–10967.

Hong, S., Beja-Glasser, V.F., Nfonoyim, B.M., Frouin, A., Li, S., Ramakrishnan, S., Merry, K.M., Shi, Q., Rosenthal, A., Barres, B.A., et al. (2016a). Complement and microglia mediate early synapse loss in Alzheimer mouse models. Science *8373*, 1–10.

Hong, S., Dissing-Olesen, L., and Stevens, B. (2016b). New insights on the role of microglia in synaptic pruning in health and disease. Curr. Opin. Neurobiol. *36*, 128–134.

Hoon, M., Soykan, T., Falkenburger, B., Hammer, M., Patrizi, A., Schmidt, K.-F., Sassoe-Pognetto, M., Lowel, S., Moser, T., Taschenberger, H., et al. (2011). Neuroligin-4 is localized to glycinergic postsynapses and regulates inhibition in the retina. Proc. Natl. Acad. Sci. *108*, 3053–3058.

Hu, X., Hicks, C.W., He, W., Wong, P., Macklin, W.B., Trapp, B.D., and Yan, R. (2006). Bace1 modulates myelination in the central and peripheral nervous system. Nat. Neurosci. *9*, 1520–1525.

Hu, X., Zhou, X., He, W., Yang, J., Xiong, W., Wong, P., Wilson, C.G., and Yan, R. (2010). BACE1 deficiency causes altered neuronal activity and neurodegeneration. J. Neurosci. *30*, 8819–8829.

Hu, X., He, W., Luo, X., Tsubota, K.E., and Yan, R. (2013). BACE1 regulates hippocampal astrogenesis via the Jagged1-Notch pathway. Cell Rep. *4*, 40–49.

Hu, X., Hu, J., Dai, L., Trapp, B., and Yan, R. (2015). Axonal and Schwann Cell BACE1 Is Equally Required for Remyelination of Peripheral Nerves. J. Neurosci. *35*, 3806–3814.

Huang, Y., and Mucke, L. (2012). Alzheimer Mechanisms and Therapeutic Strategies. Cell *148*, 1204–1222.

Huang, F.L., Huang, K.-P., and Boucheron, C. (2007). Long-term enrichment enhances the cognitive behavior of the aging neurogranin null mice without affecting their hippocampal LTP. Learn. Mem. *14*, 512–519.
Iqbal, K., Liu, F., and Gong, C.-X. (2016). Tau and neurodegenerative disease: the story so far. Nat. Rev. Neurol. *12*, 15–27.
Jiang, M., Polepalli, J., Chen, L.Y., Zhang, B., Südhof, T.C., and Malenka, R.C. (2017). Conditional ablation of neuroligin-1 in CA1 pyramidal neurons blocks LTP by a cell-autonomous NMDA receptor-independent mechanism. Mol. Psychiatry *22*, 375–383.
Jonsson, T., Atwal, J.K., Steinberg, S., Snaedal, J., Jonsson, P. V., Bjornsson, S., Stefansson, H., Sulem, P., Gudbjartsson, D., Maloney, J., et al. (2012). A mutation in APP protects against Alzheimer's disease and age-related cognitive decline. Nature *488*, 96–99.
Jucker, M., Beyreuther, K., Haass, C., Nitsch, R.M., and Christen, Y. (2006). Alzheimer: 100 Years and Beyond (Berlin, Heidelberg: Springer Berlin Heidelberg).
Jung, C.K.E., and Herms, J. (2014). Structural dynamics of dendritic spines are influenced by an environmental enrichment: an in vivo imaging study. Cereb. Cortex *24*, 377–384.
Kalvodova, L., Kahya, N., Schwille, P., Ehehalt, R., Verkade, P., Drechsel, D., and Simons, K. (2005). Lipids as modulators of proteolytic activity of BACE: involvement of cholesterol, glycosphingolipids, and anionic phospholipids in vitro. J. Biol. Chem. *280*, 36815–36823.
Kamikubo, Y., Takasugi, N., Niisato, K., Hashimoto, Y., and Sakurai, T. (2017). Consecutive Analysis of BACE1 Function on Developing and Developed Neuronal Cells. J. Alzheimers. Dis. *56*, 641–653.
Kandalepas, P.C., and Vassar, R. (2014). The normal and pathologic roles of the Alzheimer's β-secretase, BACE1. Curr. Alzheimer Res. *11*, 441–449.
Kandalepas, P.C., Sadleir, K.R., Eimer, W.A., Zhao, J., Nicholson, D.A., and Vassar, R. (2013). The Alzheimer's beta-secretase BACE1 localizes to normal presynaptic terminals and to dystrophic presynaptic terminals surrounding amyloid plaques. Acta Neuropathol *126*, 329–352.
Karran, E., Mercken, M., and Strooper, B. De (2011). The amyloid cascade hypothesis for Alzheimer's disease: an appraisal for the development of therapeutics. Nat. Rev. Drug Discov. *10*, 698–712.
Kempermann, G., Kuhn, H.G., and Gage, F.H. (1997). More hippocampal neurons in adult mice living in an enriched environment. Nature *386*, 493–495.
Khoonsari, P.E., Häggmark, A., Lönnberg, M., Mikus, M., Kilander, L., Lannfelt, L., Bergquist, J., Ingelsson, M., Nilsson, P., Kultima, K., et al. (2016). Analysis of the Cerebrospinal Fluid Proteome in Alzheimer's Disease. PLoS One *11*, e0150672.
Killick, R., Hardy, J., and Simons, J.P. (2015). Reducing β-Amyloid by Inhibition of BACE1: How Low Should You Go? Biol. Psychiatry *77*, 683–684.
Kim, D.Y., Carey, B.W., Wang, H., Ingano, L. a M., Binshtok, A.M., Wertz, M.H., Pettingell, W.H., He, P., Lee, V.M.-Y., Woolf, C.J., et al. (2007). BACE1 regulates voltage-gated sodium channels and neuronal activity. Nat. Cell Biol. *9*, 755–764.

Kim, M.H., Gunnersen, J.M., and Tan, S.-S.S. (2002). Localized expression of the seizure-related gene SEZ-6 in developing and adult forebrains. Mech Dev *118*, 171–174.

Kimura, R., and Ohno, M. (2009). Impairments in remote memory stabilization precede hippocampal synaptic and cognitive failures in 5XFAD Alzheimer mouse model. Neurobiol. Dis. *33*, 229–235.

Kimura, R., Devi, L., and Ohno, M. (2010). Partial reduction of BACE1 improves synaptic plasticity, recent and remote memories in Alzheimer's disease transgenic mice. J. Neurochem. *113*, 248–261.

Kratzer, S., Mattusch, C., Kochs, E., Eder, M., Haseneder, R., and Rammes, G. (2012). Xenon attenuates hippocampal long-term potentiation by diminishing synaptic and extrasynaptic N-methyl-D-aspartate receptor currents. Anesthesiology *116*, 673–682.

Krishnan, V., Xu, Y., Macon, K., Volanakis, J.E., and Narayana, S.V.L. (2009). The structure of C2b, a fragment of complement component C2 produced during C3 convertase formation. Acta Crystallogr. D. Biol. Crystallogr. *65*, 266–274.

Kuhn, P.H., Koroniak, K., Hogl, S., Colombo, A., Zeitschel, U., Willem, M., Volbracht, C., Schepers, U., Imhof, A., Hoffmeister, A., et al. (2012). Secretome protein enrichment identifies physiological BACE1 protease substrates in neurons. EMBO J *31*, 3157–3168.

Laird, F.M., Cai, H., Savonenko, A. V, Farah, M.H., He, K., Melnikova, T., Wen, H., Chiang, H.-C., Xu, G., Koliatsos, V.E., et al. (2005). BACE1, a major determinant of selective vulnerability of the brain to amyloid-beta amyloidogenesis, is essential for cognitive, emotional, and synaptic functions. J. Neurosci. *25*, 11693–11709.

Lendvai, B., Stern, E.A., Chen, B., and Svoboda, K. (2000). Experience-dependent plasticity of dendritic spines in the developing rat barrel cortex in vivo. Nature *404*, 876–881.

Leuner, B., and Gould, E. (2010). Structural plasticity and hippocampal function. Annu. Rev. Psychol. *61*, 111–140, C1-3.

Lin, X., Koelsch, G., Wu, S., Downs, D., Dashti, A., and Tang, J. (2000). Human aspartic protease memapsin 2 cleaves the beta-secretase site of beta-amyloid precursor protein. Proc. Natl. Acad. Sci. U. S. A. *97*, 1456–1460.

Llinás, R., Lang, E.J., and Welsh, J.P. (1997). The cerebellum, LTD, and memory: alternative views. Learn. Mem. *3*, 445–455.

Luo, Y., Bolon, B., Kahn, S., Bennett, B.D., Babu-Khan, S., Denis, P., Fan, W., Kha, H., Zhang, J., Gong, Y., et al. (2001). Mice deficient in BACE1, the Alzheimer's β-secretase, have normal phenotype and abolished β-amyloid generation. Nat. Neurosci. *4*, 231–232.

Lynch, M.A. (2004). Long-term potentiation and memory. Physiol. Rev. *84*, 87–136.

Ma, R.-H., Zhang, Y., Hong, X.-Y., Zhang, J.-F., Wang, J.-Z., and Liu, G.-P. (2017). Role of microtubule-associated protein tau phosphorylation in Alzheimer's disease. J. Huazhong Univ. Sci. Technolog. Med. Sci. *37*, 307–312.

Ma, T., Trinh, M. a, Wexler, A.J., Bourbon, C., Gatti, E., Pierre, P., Cavener, D.R., and Klann, E. (2013). Suppression of eIF2α kinases alleviates Alzheimer's disease-related plasticity and memory deficits. Nat. Neurosci. *16*, 1299–1305.

Maccarrone, G., Ditzen, C., Yassouridis, A., Rewerts, C., Uhr, M., Uhlen, M., Holsboer, F., and Turck, C.W. (2013). Psychiatric patient stratification using biosignatures based on cerebrospinal fluid protein expression clusters. J Psychiatr Res *47*, 1572–1580.

Manabe, T., Wyllie, D.J., Perkel, D.J., and Nicoll, R.A. (1993). Modulation of synaptic transmission and long-term potentiation: effects on paired pulse facilitation and EPSC variance in the CA1 region of the hippocampus. J. Neurophysiol. *70*, 1451–1459.

May, P.C., Dean, R.A., Lowe, S.L., Martenyi, F., Sheehan, S.M., Boggs, L.N., Monk, S.A., Mathes, B.M., Mergott, D.J., Watson, B.M., et al. (2011). Robust central reduction of amyloid-β in humans with an orally available, non-peptidic β-secretase inhibitor. J. Neurosci. *31*, 16507–16516.

McConlogue, L., Buttini, M., Anderson, J.P., Brigham, E.F., Chen, K.S., Freedman, S.B., Games, D., Johnson-Wood, K., Lee, M., Zeller, M., et al. (2007). Partial reduction of BACE1 has dramatic effects on Alzheimer plaque and synaptic pathology in APP Transgenic Mice. J. Biol. Chem. *282*, 26326–26334.

McLaurin, J., Yang, D., Yip, C.M., and Fraser, P.E. (2000). Review: modulating factors in amyloid-beta fibril formation. J. Struct. Biol. *130*, 259–270.

Mitsui, S., Hidaka, C., Furihata, M., Osako, Y., and Yuri, K. (2013). A mental retardation gene, motopsin/prss12, modulates cell morphology by interaction with seizure-related gene 6. Biochem Biophys Res Commun *436*, 638–644.

Miyamoto, A., Wake, H., Moorhouse, A.J., and Nabekura, J. (2013). Microglia and synapse interactions: fine tuning neural circuits and candidate molecules. Front Cell Neurosci *7*, 70.

Mizukami, T., Kohno, T., and Hattori, M. (2016). CUB and Sushi multiple domains 3 regulates dendrite development. Neurosci. Res. *110*, 11–17.

Morelli, E., Ghiglieri, V., Pendolino, V., Bagetta, V., Pignataro, A., Fejtova, A., Costa, C., Ammassari-Teule, M., Gundelfinger, E.D., Picconi, B., et al. (2014). Environmental enrichment restores CA1 hippocampal LTP and reduces severity of seizures in epileptic mice. Exp. Neurol. *261*, 320–327.

Mulley, J.C., Iona, X., Hodgson, B., Heron, S.E., Berkovic, S.F., Scheffer, I.E., and Dibbens, L.M. (2011). The Role of Seizure-Related SEZ6 as a Susceptibility Gene in Febrile Seizures. Neurol Res Int *2011*, 917565.

Munro, K.M., Nash, A., Pigoni, M., Lichtenthaler, S.F., and Gunnersen, J.M. (2016). Functions of the Alzheimer's Disease Protease BACE1 at the Synapse in the Central Nervous System. J. Mol. Neurosci. *60*, 305–315.

Nägerl, U.V., Eberhorn, N., Cambridge, S.B., and Bonhoeffer, T. (2004). Bidirectional activity-dependent morphological plasticity in hippocampal neurons. Neuron *44*, 759–767.

Nägerl, U.V., Köstinger, G., Anderson, J.C., Martin, K.A.C., and Bonhoeffer, T. (2007). Protracted Synaptogenesis after Activity-Dependent Spinogenesis in Hippocampal Neurons. *27*, 8149–8156.

Naus, S., Richter, M., Wildeboer, D., Moss, M., Schachner, M., and Bartsch, J.W. (2004). Ectodomain shedding of the neural recognition molecule CHL1 by the

metalloprotease-disintegrin ADAM8 promotes neurite outgrowth and suppresses neuronal cell death. J. Biol. Chem. *279*, 16083–16090.
Neumann, U., Rueeger, H., Machauer, R., Veenstra, S.J., Lueoend, R.M., Tintelnot-Blomley, M., Laue, G., Beltz, K., Vogg, B., Schmid, P., et al. (2015). A novel BACE inhibitor NB-360 shows a superior pharmacological profile and robust reduction of amyloid-β and neuroinflammation in APP transgenic mice. Mol. Neurodegener. *10*, 44.
Nguyen, Q.-A., Horn, M.E., and Nicoll, R.A. (2016). Distinct roles for extracellular and intracellular domains in neuroligin function at inhibitory synapses. Elife *5*, 1–21.
Nicoll, R.A. (2017). A Brief History of Long-Term Potentiation. Neuron *93*, 281–290.
Ochs, S.M., Dorostkar, M.M., Aramuni, G., Schön, C., Filser, S., Pöschl, J., Kremer, A., Van Leuven, F., Ovsepian, S. V, and Herms, J. (2015). Loss of neuronal GSK3β reduces dendritic spine stability and attenuates excitatory synaptic transmission via β-catenin. Mol. Psychiatry *20*, 482–489.
Oddo, S., Caccamo, A., Shepherd, J.D., Murphy, M.P., Golde, T.E., Kayed, R., Metherate, R., Mattson, M.P., Akbari, Y., and LaFerla, F.M. (2003). Triple-transgenic model of Alzheimer's disease with plaques and tangles: intracellular Abeta and synaptic dysfunction. Neuron *39*, 409–421.
Ohno, M., Sametsky, E.A., Younkin, L.H., Oakley, H., Younkin, S.G., Citron, M., Vassar, R., and Disterhoft, J.F. (2004). BACE1 deficiency rescues memory deficits and cholinergic dysfunction in a mouse model of Alzheimer's disease. Neuron *41*, 27–33.
Ohno, M., Cole, S.L., Yasvoina, M., Zhao, J., Citron, M., Berry, R., Disterhoft, J.F., and Vassar, R. (2007). BACE1 gene deletion prevents neuron loss and memory deficits in 5XFAD APP/PS1 transgenic mice. Neurobiol. Dis. *26*, 134–145.
Osaki, G., Mitsui, S., and Yuri, K. (2011). The distribution of the seizure-related gene 6 (Sez-6) protein during postnatal development of the mouse forebrain suggests multiple functions for this protein: an analysis using a new antibody. Brain Res *1386*, 58–69.
Papouin, T., Dunphy, J.M., Tolman, M., Dineley, K.T., and Haydon, P.G. (2017). Septal Cholinergic Neuromodulation Tunes the Astrocyte-Dependent Gating of Hippocampal NMDA Receptors to Wakefulness. Neuron *94*, 840–854.e7.
Pera, M., Alcolea, D., Sanchez-Valle, R., Guardia-Laguarta, C., Colom-Cadena, M., Badiola, N., Suarez-Calvet, M., Llado, A., Barrera-Ocampo, A.A., Sepulveda-Falla, D., et al. (2013). Distinct patterns of APP processing in the CNS in autosomal-dominant and sporadic Alzheimer disease. Acta Neuropathol *125*, 201–213.
Pigoni, M., Wanngren, J., Kuhn, P.-H., Munro, K.M., Gunnersen, J.M., Takeshima, H., Feederle, R., Voytyuk, I., De Strooper, B., Levasseur, M.D., et al. (2016). Seizure protein 6 and its homolog seizure 6-like protein are physiological substrates of BACE1 in neurons. Mol. Neurodegener. *11*, 67.
van Praag, H., Kempermann, G., and Gage, F.H. (2000). Neural consequences of environmental enrichment. Nat. Rev. Neurosci. *1*, 191–198.
Del Prete, D., Lombino, F., Liu, X., and D'Adamio, L. (2014). APP is cleaved by Bace1 in pre-synaptic vesicles and establishes a pre-synaptic interactome, via its

intracellular domain, with molecular complexes that regulate pre-synaptic vesicles functions. PLoS One *9*, e108576.
Prince, M., Wimo, A., Guerchet, M., Ali, G.-C., Wu, Y.-T., and Prina, M. (2015). World Alzheimer Report 2015: The Global Impact of Dementia (London).
Puzzo, D., Privitera, L., Leznik, E., Fà, M., Staniszewski, A., Palmeri, A., and Arancio, O. (2008). Picomolar amyloid-beta positively modulates synaptic plasticity and memory in hippocampus. J. Neurosci. *28*, 14537–14545.
Qi, Y., Klyubin, I., Harney, S.C., Hu, N., Cullen, W.K., Grant, M.K., Steffen, J., Wilson, E.N., Do Carmo, S., Remy, S., et al. (2014). Longitudinal testing of hippocampal plasticity reveals the onset and maintenance of endogenous human Aß-induced synaptic dysfunction in individual freely behaving pre-plaque transgenic rats: rapid reversal by anti-Aß agents. Acta Neuropathol. Commun. *2*, 175.
Rajapaksha, T.W., Eimer, W.A., Bozza, T.C., and Vassar, R. (2011). The Alzheimer's β-secretase enzyme BACE1 is required for accurate axon guidance of olfactory sensory neurons and normal glomerulus formation in the olfactory bulb. Mol. Neurodegener. *6*, 88.
Rammes, G., Mattusch, C., Wulff, M., Seeser, F., Kreuzer, M., Zhu, K., Deussing, J.M., Herms, J., and Parsons, C.G. (2017). Involvement of GluN2B subunit containing N-methyl-d-aspartate (NMDA) receptors in mediating the acute and chronic synaptotoxic effects of oligomeric amyloid-beta (Aβ) in murine models of Alzheimer's disease (AD). Neuropharmacology *123*, 100–115.
Rampon, C., Jiang, C.H., Dong, H., Tang, Y.P., Lockhart, D.J., Schultz, P.G., Tsien, J.Z., and Hu, Y. (2000). Effects of environmental enrichment on gene expression in the brain. Proc Natl Acad Sci U S A *97*, 12880–12884.
Reardon, S. (2015). Antibody drugs for Alzheimer's show glimmers of promise. Nature *523*, 509–510.
Reiman, E.M. (2006). A 100-year update on Alzheimer's disease and related disorders. J. Clin. Psychiatry *67*, 1782–1783.
Risher, W.C., Ustunkaya, T., Singh Alvarado, J., and Eroglu, C. (2014). Rapid Golgi analysis method for efficient and unbiased classification of dendritic spines. PLoS One *9*, e107591.
Roberds, S.L., Anderson, J., Basi, G., Bienkowski, M.J., Branstetter, D.G., Chen, K.S., Freedman, S.B., Frigon, N.L., Games, D., Hu, K., et al. (2001). BACE knockout mice are healthy despite lacking the primary beta-secretase activity in brain: implications for Alzheimer's disease therapeutics. Hum. Mol. Genet. *10*, 1317–1324.
Rochin, L., Hurbain, I., Serneels, L., Fort, C., Watt, B., Leblanc, P., Marks, M.S., De Strooper, B., Raposo, G., and van Niel, G. (2013). BACE2 processes PMEL to form the melanosome amyloid matrix in pigment cells. Proc. Natl. Acad. Sci. U. S. A. *110*, 10658–10663.
Roder, S., Danober, L., Pozza, M.F., Lingenhoehl, K., Wiederhold, K.-H., and Olpe, H.-R. (2003). Electrophysiological studies on the hippocampus and prefrontal cortex assessing the effects of amyloidosis in amyloid precursor protein 23 transgenic mice. Neuroscience *120*, 705–720.

Ryan, T.M., Roberts, B.R., McColl, G., Hare, D.J., Doble, P.A., Li, Q.-X., Lind, M., Roberts, A.M., Mertens, H.D.T., Kirby, N., et al. (2015). Stabilization of Nontoxic Aβ-Oligomers: Insights into the Mechanism of Action of Hydroxyquinolines in Alzheimer's Disease. J. Neurosci. *35*, 2871.

Sadleir, K.R., Eimer, W.A., Cole, S.L., and Vassar, R. (2015). Aβ reduction in BACE1 heterozygous null 5XFAD mice is associated with transgenic APP level. Mol. Neurodegener. *10*, 1.

Saito, T., Matsuba, Y., Mihira, N., Takano, J., Nilsson, P., Itohara, S., Iwata, N., and Saido, T.C. (2014). Single App knock-in mouse models of Alzheimer's disease. Nat. Neurosci. *17*, 661–663.

Salloway, S., Sperling, R., Fox, N.C., Blennow, K., Klunk, W., Raskind, M., Sabbagh, M., Honig, L.S., Porsteinsson, A.P., Ferris, S., et al. (2014). Two phase 3 trials of bapineuzumab in mild-to-moderate Alzheimer's disease. N. Engl. J. Med. *370*, 322–333.

Savonenko, A. V, Melnikova, T., Laird, F.M., Stewart, K.-A., Price, D.L., and Wong, P.C. (2008). Alteration of BACE1-dependent NRG1/ErbB4 signaling and schizophrenia-like phenotypes in BACE1-null mice. Proc. Natl. Acad. Sci. U. S. A. *105*, 5585–5590.

Schilling, S., Mehr, A., Ludewig, S., Stephan, J., Zimmermann, M., August, A., Strecker, P., Korte, M., Koo, E.H., Müller, U.C., et al. (2017). APLP1 Is a Synaptic Cell Adhesion Molecule, Supporting Maintenance of Dendritic Spines and Basal Synaptic Transmission. J. Neurosci. *37*, 5345–5365.

Selkoe, D.J. (2001). Alzheimer's disease: genes, proteins, and therapy. Physiol. Rev. *81*, 741–766.

Selkoe, D.J., and Hardy, J. (2016). The amyloid hypothesis of Alzheimer's disease at 25 years. EMBO Mol. Med. 1–14.

Serrano-Pozo, A., Frosch, M.P., Masliah, E., and Hyman, B.T. (2011). Neuropathological alterations in Alzheimer disease. Cold Spring Harb. Perspect. Med. *1*, a006189.

Shen, Y., Wang, H., Sun, Q., Yao, H., Keegan, A.P., Mullan, M., Wilson, J., Lista, S., Leyhe, T., Laske, C., et al. (2017). Increased Plasma Beta-Secretase 1 May Predict Conversion to Alzheimer's Disease Dementia in Individuals With Mild Cognitive Impairment. Biol. Psychiatry 1–9.

Shimizu-Nishikawa, K., Kajiwara, K., Kimura, M., Katsuki, M., and Sugaya, E. (1995a). Cloning and expression of SEZ-6, a brain-specific and seizure-related cDNA. Brain Res Mol Brain Res *28*, 201–210.

Shimizu-Nishikawa, K., Kajiwara, K., and Sugaya, E. (1995b). Cloning and characterization of seizure-related gene, SEZ-6. Biochem Biophys Res Commun *216*, 382–389.

Shimshek, D.R., Jacobson, L.H., Kolly, C., Zamurovic, N., Balavenkatraman, K.K., Morawiec, L., Kreutzer, R., Schelle, J., Jucker, M., Bertschi, B., et al. (2016). Pharmacological BACE1 and BACE2 inhibition induces hair depigmentation by inhibiting PMEL17 processing in mice. Sci. Rep. *6*, 21917.

Sinha, S., and Lieberburg, I. (1999). Cellular mechanisms of beta-amyloid production and secretion. Proc. Natl. Acad. Sci. U. S. A. *96*, 11049–11053.

Sinha, S., Anderson, J.P., Barbour, R., Basi, G.S., Caccavello, R., Davis, D., Doan, M., Dovey, H.F., Frigon, N., Hong, J., et al. (1999). Purification and cloning of amyloid precursor protein beta-secretase from human brain. Nature *402*, 537–540.

Song, J.-Y., Ichtchenko, K., Sudhof, T.C., and Brose, N. (1999). Neuroligin 1 is a postsynaptic cell-adhesion molecule of excitatory synapses. Proc. Natl. Acad. Sci. *96*, 1100–1105.

Stachel, S.J., Coburn, C.A., Steele, T.G., Jones, K.G., Loutzenhiser, E.F., Gregro, A.R., Rajapakse, H.A., Lai, M.-T., Crouthamel, M.-C., Xu, M., et al. (2004). Structure-based design of potent and selective cell-permeable inhibitors of human beta-secretase (BACE-1). J. Med. Chem. *47*, 6447–6450.

Stamford, A.W., Scott, J.D., Li, S.W., Babu, S., Tadesse, D., Hunter, R., Wu, Y., Misiaszek, J., Cumming, J.N., Gilbert, E.J., et al. (2012). Discovery of an Orally Available, Brain Penetrant BACE1 Inhibitor that Affords Robust CNS Aβ Reduction. ACS Med. Chem. Lett. *3*, 897–902.

Steuble, M., Diep, T.-M., Schätzle, P., Ludwig, A., Tagaya, M., Kunz, B., and Sonderegger, P. (2012). Calsyntenin-1 shelters APP from proteolytic processing during anterograde axonal transport. Biol. Open *1*, 761–774.

De Strooper, B. (2014). Lessons from a failed γ-secretase Alzheimer trial. Cell *159*, 721–726.

Takahashi, R.H., Nagao, T., and Gouras, G.K. (2017). Plaque formation and the intraneuronal accumulation of β-amyloid in Alzheimer's disease. Pathol. Int. *67*, 185–193.

Tarawneh, R., and Holtzman, D.M. (2012). The clinical problem of symptomatic Alzheimer disease and mild cognitive impairment. Cold Spring Harb. Perspect. Med. *2*, a006148.

Timmers, M., Barão, S., Van Broeck, B., Tesseur, I., Slemmon, J., De Waepenaert, K., Bogert, J., Shaw, L.M., Engelborghs, S., Moechars, D., et al. (2017). BACE1 Dynamics Upon Inhibition with a BACE Inhibitor and Correlation to Downstream Alzheimer's Disease Markers in Elderly Healthy Participants. J. Alzheimer's Dis. *56*, 1–13.

Vassar, R. (2014). BACE1 inhibitor drugs in clinical trials for Alzheimer's disease. Alzheimers. Res. Ther. *6*, 89.

Vassar, R. (2016). BACE1 inhibition as a therapeutic strategy for Alzheimer's disease. J. Sport Heal. Sci. *5*, 388–390.

Vassar, R., Bennett, B.D., Babu-Khan, S., Kahn, S., Mendiaz, E.A., Denis, P., Teplow, D.B., Ross, S., Amarante, P., Loeloff, R., et al. (1999). Beta-secretase cleavage of Alzheimer's amyloid precursor protein by the transmembrane aspartic protease BACE. Science *286*, 735–741.

Vassar, R., Kuhn, P.-H., Haass, C., Kennedy, M.E., Rajendran, L., Wong, P.C., and Lichtenthaler, S.F. (2014). Function, therapeutic potential and cell biology of BACE proteases: current status and future prospects. J. Neurochem. *130*, 4–28.

Viana da Silva, S., Haberl, M.G., Zhang, P., Bethge, P., Lemos, C., Gonçalves, N., Gorlewicz, A., Malezieux, M., Gonçalves, F.Q., Grosjean, N., et al. (2016). Early synaptic deficits in the APP/PS1 mouse model of Alzheimer's disease involve neuronal adenosine A2A receptors. Nat. Commun. *7*, 11915.

Volianskis, A., Køstner, R., Mølgaard, M., Hass, S., and Jensen, M.S. (2010). Episodic memory deficits are not related to altered glutamatergic synaptic transmission and plasticity in the CA1 hippocampus of the APPswe/PS1δE9-deleted transgenic mice model of ß-amyloidosis. Neurobiol. Aging *31*, 1173–1187.

Wang, C.-L., Tang, F.-L., Peng, Y., Shen, C.-Y., Mei, L., and Xiong, W.-C. (2012). VPS35 regulates developing mouse hippocampal neuronal morphogenesis by promoting retrograde trafficking of BACE1. Biol. Open *1*, 1248–1257.

Wang, H., Song, L., Laird, F., Wong, P.C., and Lee, H.K. (2008). BACE1 knock-outs display deficits in activity-dependent potentiation of synaptic transmission at mossy fiber to CA3 synapses in the hippocampus. J Neurosci *28*, 8677–8681.

Wang, H., Song, L., Lee, A., Laird, F., Wong, P.C., and Lee, H.-K. (2010). Mossy fiber long-term potentiation deficits in BACE1 knock-outs can be rescued by activation of alpha7 nicotinic acetylcholine receptors. J. Neurosci. *30*, 13808–13813.

Wang, H., Megill, A., Wong, P.C., Kirkwood, A., and Lee, H.-K.K. (2014). Postsynaptic Target Specific Synaptic Dysfunctions in the CA3 Area of BACE1 Knockout Mice. PLoS One *9*, e92279.

Weber, M., Wu, T., Meilandt, W.J., Dominguez, S.L., Solanoy, H.O., Maloney, J.A., Ngu, H., Baca, M., Kung, C., Lima, L., et al. (2017). BACE1 across species: a comparison of the in vivo consequences of BACE1 deletion in mice and rats. Sci. Rep. *7*, 44249.

Wetzel, R., Shivaprasad, S., and Williams, A.D. (2007). Plasticity of amyloid fibrils. Biochemistry *46*, 1–10.

Weyer, S.W., Zagrebelsky, M., Herrmann, U., Hick, M., Ganss, L., Gobbert, J., Gruber, M., Altmann, C., Korte, M., Deller, T., et al. (2014). Comparative analysis of single and combined APP/APLP knockouts reveals reduced spine density in APP-KO mice that is prevented by APPsα expression. Acta Neuropathol. Commun. *2*, 36.

Willem, M., Garratt, A.N., Novak, B., Citron, M., Kaufmann, S., Rittger, A., DeStrooper, B., Saftig, P., Birchmeier, C., and Haass, C. (2006). Control of peripheral nerve myelination by the beta-secretase BACE1. Science *314*, 664–666.

Willem, M., Tahirovic, S., Busche, M.A., Ovsepian, S. V., Chafai, M., Kootar, S., Hornburg, D., Evans, L.D.B., Moore, S., Daria, A., et al. (2015). η-Secretase processing of APP inhibits neuronal activity in the hippocampus. Nature *526*, 443–447.

Wong, H.-K., Sakurai, T., Oyama, F., Kaneko, K., Wada, K., Miyazaki, H., Kurosawa, M., De Strooper, B., Saftig, P., and Nukina, N. (2005). beta Subunits of voltage-gated sodium channels are novel substrates of beta-site amyloid precursor protein-cleaving enzyme (BACE1) and gamma-secretase. J. Biol. Chem. *280*, 23009–23017.

Yan, R., Bienkowski, M.J., Shuck, M.E., Miao, H., Tory, M.C., Pauley, A.M., Brashier, J.R., Stratman, N.C., Mathews, W.R., Buhl, a E., et al. (1999). Membrane-anchored aspartyl protease with Alzheimer's disease beta-secretase activity. Nature *402*, 533–537.

Yang, G., Pan, F., and Gan, W.-B. (2009). Stably maintained dendritic spines are associated with lifelong memories. Nature *462*, 920–924.

Young, P., Qiu, L., Wang, D., Zhao, S., Gross, J., and Feng, G. (2008). Single-neuron labeling with inducible Cre-mediated knockout in transgenic mice. Nat Neurosci *11*, 721–728.

Yu, Z.-L.L., Jiang, J.-M.J.-J.J.M., Wu, D.-H.H., Xie, H.-J.J., Jiang, J.-M.J.-J.J.M., Zhou, L., Peng, L., and Bao, G.-S.S. (2007). Febrile seizures are associated with mutation of seizure-related (SEZ) 6, a brain-specific gene. J Neurosci Res *85*, 166–172.

Yuan, J., Venkatraman, S., Zheng, Y., McKeever, B.M., Dillard, L.W., and Singh, S.B. (2013). Structure-based design of β-site APP cleaving enzyme 1 (BACE1) inhibitors for the treatment of Alzheimer's disease. J. Med. Chem. *56*, 4156–4180.

Yuste, R., and Bonhoeffer, T. (2001). Morphological changes in dendritic spines associated with long-term synaptic plasticity. Annu. Rev. Neurosci. *24*, 1071–1089.

van der Zee, E.A. (2015). Synapses, spines and kinases in mammalian learning and memory, and the impact of aging. Neurosci. Biobehav. Rev. *50*, 77–85.

Zheng, H., Jiang, M., Trumbauer, M.E., Sirinathsinghji, D.J., Hopkins, R., Smith, D.W., Heavens, R.P., Dawson, G.R., Boyce, S., Conner, M.W., et al. (1995). beta-Amyloid precursor protein-deficient mice show reactive gliosis and decreased locomotor activity. Cell *81*, 525–531.

Zhou, L.J., Barao, S., Laga, M., Bockstael, K., Borgers, M., Gijsen, H., Annaert, W., Moechars, D., Mercken, M., Gevaer, K., et al. (2012). The Neural Cell Adhesion Molecules L1 and CHL1 Are Cleaved by BACE1 Protease in Vivo. J. Biol. Chem. *287*, 25927–25940.

Zhu, K., Xiang, X., Filser, S., Marinković, P., Dorostkar, M.M., Crux, S., Neumann, U., Shimshek, D.R., Rammes, G., Haass, C., et al. (2018). Beta-Site Amyloid Precursor Protein Cleaving Enzyme 1 Inhibition Impairs Synaptic Plasticity via Seizure Protein 6. Biol. Psychiatry *83*, 428–437.

Zou, C., Shi, Y., Ohli, J., Schüller, U., Dorostkar, M.M., and Herms, J. (2016). Neuroinflammation impairs adaptive structural plasticity of dendritic spines in a preclinical model of Alzheimer's disease. Acta Neuropathol. *131*, 235–246.

Zuo, Y., Lin, A., Chang, P., and Gan, W.B. (2005). Development of long-term dendritic spine stability in diverse regions of cerebral cortex. Neuron *46*, 181–189.

Abbreviations

°C	degree celcius
µg	microgram
µl	microliter
µl	micrometer
Aβ	amyloid beta
AD	Alzheimer's disease
ANOVA	analysis of variance
APP	amyloid precurser protein
BACE1	Beta-site amyloid precursor protein cleaving enzyme 1
CA1	Cornu Ammonis 1
CA3	Cornu Ammonis 3
dpi	days post-injection
CNS	central nervous system
e.g.	lat. exempli gratia; for example
eGFP	enhanced greed
et al.	and others
ER	endoplasmatic reticulum
FAD	familial Alzheimer's disease
Fig.	Figure
g	gram
h	hour
Hz	Hertz
kDa	kilodalton
KO	knock out
LTD	long-term depression
LTP	long-term potentiation
M	molar
mg	milligram
min	minute
ml	milliliter
mm	millimeter
mM	millimolar
MW	molecular weight
NaCl	sodium chloride
$NaHCO_3$	sodium bicarbonate
NGS	normal goat serum
nm	nanometer
NMDA	N-methyl-D-aspartate
P	p-value
PBS	phosphate buffered saline
PCR	polymerase chain reaction
PFA	paraformaldehyde

ROI	region of interest
PSD	Post-synaptic density
rpm	revolutions per minute
s	second
SD	standard deviation
SEM	standard error of the mean
t	time
Ti:Sa	lasing medium; sapphire crystal, doped with titanium ions
Tab.	Table
tg	transgene
Thy1	thymus cell antigen 1
TOR	turnover ratio
WT	wild type
YFP	yellow fluorescence protein

List of publications

Zhu, K., Xiang, X., Filser, S., Marinković, P., Dorostkar, M.M., Crux, S., Neumann, U., Shimshek, D.R., Rammes, G., Haass, C., Lichtenthaler S.F., Gunnersen J.M., Herms J. (2018). Beta-Site Amyloid Precursor Protein Cleaving Enzyme 1 Inhibition Impairs Synaptic Plasticity via Seizure Protein 6. Biol. Psychiatry 83, 428–437.

Rammes, G., Mattusch, C., Wulff, M., Seeser, F., Kreuzer, M., **Zhu, K.**, Deussing, J.M., Herms, J., and Parsons, C.G. (2017). Involvement of GluN2B subunit containing N-methyl-d-aspartate (NMDA) receptors in mediating the acute and chronic synaptotoxic effects of oligomeric amyloid-beta (Aβ) in murine models of Alzheimer's disease (AD). Neuropharmacology 123, 100-115.

Zou, C., Crux, S., Marinesco, S., Montagna, E., Sgobio, C., Shi, Y., Shi, S., **Zhu, K.**, Dorostkar, M.M., Müller, U.C., Herms J. (2016). Amyloid precursor protein maintains constitutive and adaptive plasticity of dendritic spines in adult brain by regulating D-serine homeostasis. EMBO J. 35, 2213-2222.

Zhu K., Zhang J., Liu S. (2011) Progress in the Study of Yeast Gal4 Transcription Factor. China Biotechnology. 31(01): 81-85.

Zhu, K., Herms J. (2017). Consequences of Inhibiting BACE1 on Synaptic Structure and Function. Submitted to Biol. Psychiatry.

Schmid, S., Rammes, G., Blobner, M., Kellermann, K., Bratke, S., Fendl, D., **Zhu, K.**, Schneider, G., Jungwirth, B. (2017) Cognitive decline in Tg2576 mice shows gender-specific differences and correlates with cerebral amyloid-beta. Submitted to Neurobiol Aging.

Scientific poster presentations

Zhu, K., Xiang, X., Dorostkar, M.M., Filser, S., Crux, S., Marinković, P., Neumann, U., Shimshek, D.R., Rammes, G., Haass, C., Lichtenthaler S.F., Gunnersen J.M., Herms J. “BACE1 Inhibition Impairs Synaptic Plasticity via Seizure Protein 6.” SfN annual Neuroscience meeting, November 2016, San Diego, USA.

Zhu, K., Xiang, X., Dorostkar, M.M., Filser, S., Crux, S., Marinković, P., Neumann, U., Shimshek, D.R., Rammes, G., Haass, C., Lichtenthaler S.F., Gunnersen J.M., Herms J. “BACE1 Inhibition Impairs Synaptic Plasticity via Seizure Protein 6.” Kloster Seeon meeting on BACE proteases in health and disease, September 2016, Seeon-Seebruck, Bavaria, Germany.

Acknowledgments

I would like to express my gratitude to my supervisor, Prof. Dr. Jochen Herms for providing useful advices about my research project. I furthermore want to cordially thank PD Dr. Stylianos Michalakis, who readily agreed to represent this dissertation at the faculty of chemistry and pharmacy.

I would like to thank Dr. Severin Filser and Dr. Carmelo Sgobio for great help. I appreciate their vast knowledge and skill in many areas and assistance in writing reports. I must also acknowledge Dr. med. Mario Dorostkar, Sophie Crux, Elena Montagna, Finn Peters, Dr. Sonja Blumenstock, Yuan Shi, Tanja Blume, Hazal Salihoglu, Viktoria Korzhova, Fanfan Sun and Martina Pigoni for their valuable suggestions and useful discussion. Furthermore, acknowledge must give to the excellent technical support provided by Eric, Kathi, Sarah and Nadine.

Several collaborators have provided me with material or the possibility to share thoughts and learn. I want to highlight Prof. Dr. Gerhard Rammes, Dr. Ulf Neumann, Dr. Derya R. Shimshek, Prof. Dr. Stefan F. Lichtenthaler and Prof. Dr. Jenny M. Gunnersen, to whom I am very thankful. I furthermore want to acknowledge all second readers of this thesis for your time and interest in this work.

Last but not least, thanks to my family: my wife and my parents. Thanks for all the love and support coming from them.